

AFAPL-TR-71-7

AD725027

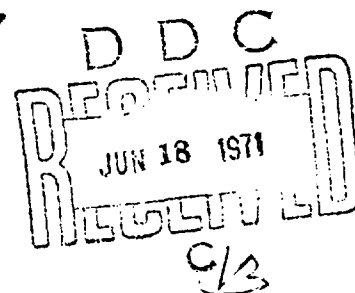
ANALYSIS OF AIRCRAFT FUEL TANK
FIRE AND EXPLOSION HAZARDS

THOMAS C. KOSVIC
LAURENCE B. ZUNG
MELVIN GERSTEIN

DYNAMIC SCIENCE
A DIVISION OF MARSHALL INDUSTRIES

TECHNICAL REPORT AFAPL-TR-71-7

MARCH 1971



This document is approved for public release ; distribution unlimited.

AIR FORCE AERO PROPULSION LABORATORY
AIR FORCE SYSTEMS COMMAND
WRIGHT-PATTERSON AIR FORCE BASE, OHIO 45433

NOTICE

When Government drawings, specifications, or other data are used for any purpose other than in connection with a definitely related Government operation, the United States Government thereby incurs no responsibility nor any obligation whatsoever; and the fact that the government may have formulated, furnished, or in any way supplied the said drawings, specifications, or other data, is not to be regarded by implication or otherwise as in any manner licensing the holder or any other person or corporation, or conveying any rights or permission to manufacture, use, or sell any patented invention that may in any way be related thereto.

ACCESSION FOR	
CFSTI	WHITE SECTION <input checked="" type="checkbox"/>
DDC	BUFF SECTION <input type="checkbox"/>
UNANNOUNCED	<input type="checkbox"/>
JUSTIFICATION	
BY	
DISTRIBUTION/AVAILABILITY CODES	
DIST.	AVAIL. and/or SPECIAL
A	

Copies of this report should not be returned unless return is required by security considerations, contractual obligations, or notice on a specific document.

Unclassified

Security Classification

DOCUMENT CONTROL DATA - R & D

(Security classification of title, body of abstract and indexing annotation must be entered when the overall report is classified)

1. ORIGINATING ACTIVITY (Corporate author) Dynamic Science, a Division of Marshall Industries 2400 Michelson Drive Irvine, California 92664		2a. REPORT SECURITY CLASSIFICATION Unclassified	
3. REPORT TITLE Analysis of Aircraft Fuel Tank Fire and Explosion Hazards		2b. GROUP	
4. DESCRIPTIVE NOTES (Type of report and inclusive dates) Final Report - July 1, 1969 - December 15, 1970			
5. AUTHOR(S) (First name, middle initial, last name) Thomas C. Kosvic Laurence B. Zung Melvin Gerstein			
6. REPORT DATE March 1971	7a. TOTAL NO. OF PAGES 75	7b. NO. OF PAGES 8	
8a. CONTRACT OR GRANT NO. F33615-69-C-1895	9a. ORIGINATOR'S REPORT NUMBER(S) SN-166-F		
b. PROJECT NO. 3048	9b. OTHER REPORT NO(S) (Any other numbers that may be assigned this report) AFAPL-TR-71-7		
10. DISTRIBUTION STATEMENT This document is subject to special export controls and each transmittal to foreign governments or foreign nationals may be made only with prior approval of Air Force Aero Propulsion Laboratory (AFAPL/SFH), Wright-Patterson Air Force Base, Ohio 45433			
11. SUPPLEMENTARY NOTES		12. SPONSORING MILITARY ACTIVITY Air Force Aero Propulsion Laboratory Wright-Patterson Air Force Base Ohio 45433	
13. ABSTRACT Under simulated flight environments, fuel/air ratios at various locations of the ullage space were determined using in-line gas chromatograph measurement. Using the shallow tank experimental data showed that during ascent and cruise portion of the flight profile, uniform fuel/air mixtures were found to exist within the entire ullage volume. Significant fuel/air gradients existed during the descent portion of the flight profile, with mainly air near the vent inlet. "Evaporative lag" was observed during ascent and level flight when liquid Jet A fuel was maintained at 80°F. When the liquid fuel temperature was increased to 120°F, evaporation rate was found to be rapid enough that the "evaporative lag" phenomena was no longer observed. By vibrating the fuel tank, it greatly increased the rate of off-gassing of dissolved air in the liquid fuel. This in turn significantly changed the fuel/air ratio in the ullage space. Two separate and complementary models were developed to predict fuel/air concentrations within the ullage. The well-stirred model describes situations when mixing of air and fuel vapors occurs very rapidly with no appreciable fuel/air gradients within the ullage volume. This model is particularly applicable to wing tank of aircraft and for tank configurations where the ratio of ullage volume to liquid fuel surface is small. For tank configurations where this is not true a second distributed F/A model was developed to describe such situations. Cool flame limits and transition between cool flame and normal flame ignition limits associated with supersonic flights were also investigated. No ignition was observed for Mach number below 2.7 and ignition was observed for Mach number equal to 3.0.			

DD FORM 1 NOV 63 1473

Unclassified

Security Classification

Security Classification

14		KEY WORDS		LINK A		LINK B		LINK C	
				ROLE	WT	ROLE	WT	ROLE	WT
		Aircraft Fuel Tanks							
		Combustibility							
		Flight Profiles							
		Inflight Hazards							
		F/A Ratio							
		Ullage Compositions							

Security Classification

ANALYSIS OF AIRCRAFT FUEL TANK
FIRE AND EXPLOSION HAZARDS

Thomas C. Kosvic
Laurence B. Zung
Melvin Gerstein

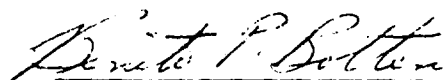
This document is approved for public release; distribution
unlimited.

FOREWORD

This study describes work performed under USAF Contract E33615-69-C-1895. The contract was initiated under Project Nr. 3048, "Fuels, Lubrication, and Hazards," Task Nr. 304807 "Aerospace Vehicle Hazard Protection" and was administered by the Air Force Aero Propulsion Laboratory, Wright-Patterson Air Force Base, Ohio, Capt. Edwin E. Ott (AFAPL/SFH), Project Engineer. This work was partially funded by FAA Agreement Nr. DOT-FA69NA-AP-42. Messrs, Charles M. Middlesworth and Eugene P. Klueg, representing the Federal Aviation Agency, contributed to the technical direction of the program. This report covers work performed during the period 1 July 1969 to 15 December 1970. It was submitted by the authors in January 1971. Dynamic Science, a Division of Marshall Industries, 2400 Michelson Drive, Irvine, California 92664, performed the study under the direction of Mr. Thomas C. Kosvic, Program Manager. Acknowledgment for technical assistance is given to the following engineers: Norman Helgeson, Jay Levine, Maurice Shaw, and W. R. Irwin for conducting the tests.

The contractor's report number is SN-166-F.

This technical report has been reviewed and is approved.



BENITO P. BOTTERI
Chief, Fire Protection Branch
Fuel and Lubrication Division

ABSTRACT

Under simulated flight environments, fuel/air ratios at various locations of the ullage space were determined using in-line gas chromatograph measurement. Using the shallow tank experimental data showed that during ascent and cruise portion of the flight profile, uniform fuel/air mixtures were found to exist within the entire ullage volume. Significant fuel/air gradients existed during the descent portion of the flight profile, with mainly air near the vent inlet. "Evaporative lag" was observed during ascent and level flight when liquid Jet A fuel was maintained at 80° F. When the liquid fuel temperature was increased to 120° F, evaporation rate was found to be rapid enough that the "evaporative lag" phenomena was no longer observed. By vibrating the fuel tank, it greatly increased the rate of offgassing of dissolved air in the liquid fuel. This in turn significantly changed the fuel/air ratio in the ullage space.

Two separate and complementary models were developed to predict fuel/air concentrations within the ullage. The well-stirred model describes situations when mixing of air and fuel vapors occurs very rapidly with no appreciable fuel/air gradients within the ullage volume. This model is particularly applicable to wing tanks of aircraft and for tank configurations where the ratio of ullage volume to liquid fuel surface is small. For tank configurations where this is not true a second distributed F/A model was developed to describe such situations. Cool flame limits and transition between cool flame and normal flame ignition limits associated with supersonic flights were also investigated. No ignition was observed for Mach number below 2.7 and ignition was observed for Mach number equal to 3.0.

TABLE OF CONTENTS

	<u>Page No.</u>
I. INTRODUCTION	1
II. DEFINITION OF THE HAZARD PROBLEM AND METHOD OF APPROACH	2
III. EXPERIMENTAL EQUIPMENT & TEST PROCEDURES	7
1. Temperature Controlled Experimental Fuel Tank	7
2. Tank Vibration System	7
3. Vent Air and Fuel Temperature Conditioning System	11
4. Tank Pressurization (Altitude) System	11
5. Sampling System	16
6. Recording Instrumentation	21
7. Test Procedure	22
IV. THEORETICAL MODELING OF AIRCRAFT FUEL TANK FIRE AND EXPLOSION HAZARDS	24
1. Well-Stirred Computer Model	24
2. Sample Results from Well-Stirred Computer Program	34
3. Distributed F/A Model	38
4. Sample Results of the Distributed O/F Model	41
V. EXPERIMENTAL RESULTS AND DISCUSSION	46
1. Fuel/Air Composition Measurements	46
2. Comparison Between Experimental and Analytical Results	57
3. Autoignition Characteristics	58
VI. CONCLUSIONS AND RECOMMENDATIONS	68
REFERENCES	70
APPENDIX A	
EXTENSION OF LEAN FLAMMABILITY LIMITS BY MISTS	71

FIGURES AND ILLUSTRATIONS

	<u>Page No.</u>
1. Logic Flow Chart for Assessment of Fuel Tank Hazard	4
2. Arrangement of Heaters and Cooling Coils on Cylindrical Portion of Unwetted Tank Walls	8
3. Vibration Adapter	9
4. Schematic of Vibration Generator in Place	10
5. Fuel Tank Vibration System	12
6. Overall View of Tank Monitor on Vibration Adapter	13
7. Test Tank with Descent Air Heater	14
8. Fuel Cooling System	15
9. Schematic Diagram of Pressure Control System	17
10. Gas Chromatograph for Fuel/Air Measurement	18
11. Automatic Sampling System	19
12. Sample Probe Selection Valve Installation	20
13. Fuel Tank Transport Processes	25
14. Fuel Tank and Flight Profiles Used for Sample Results	35
15. Variation of Fuel/Air Ratio During Ascent, Level, and Descent Flights for Jet-A Fuel	36
16. Variation of Fuel/Air Ratio for Jet A Fuel at 110°F	37
17. Diffusion/Convection Program Results for JP-4 at 46°F	42
18. Diffusion/Convection Program Results for JP-4 at 60°F	44
19. Diffusion/Convection Program Results for JP-4 at 107°F	45
20. Test Matrix for Fuel/Air Measurements	47
21. Probe Locations	48
22. JP4 Ascent Tests to 40,000 ft	49
23. Jet A Ascent Tests to 40,000 ft	51
24. JP4 Descent Tests from 40,000 ft	52
25. Jet A Descent Runs from 40,000 ft	53
26. JP4 Runs - Level Flight with Fuel Withdrawal	55
27. Jet A Runs Level Flight with Fuel Withdrawal	56
28. JP4 Ascent Tests to 40,000 ft	59
29. Mach 2.7 Flight Profile - Test Parameters	60
30. Mach 3.0 Flight Profile	61

FIGURES AND ILLUSTRATIONS (continued)

Page No.

31.	Mach 2.4 Flight Profile	62
32.	Flight Profile Test Results	63
33.	Autoignition Descent Tests	65
34.	Lower Ignition Limits for TFA/Air Mixtures at Various Simulated Altitudes	67
A-1	Extended Lean Flammability for JP-8	A-3
A-2	Extended Lean Flammability for JP-8	A-4
	Table A-1 - JP-8 Mist Ignition Calculations	A-5

SECTION I

INTRODUCTION

The degree of fire hazard associated with an aircraft fuel tank system is directly related to the nature of the fuel/air environment within the tank. As hydrocarbon fuel vapor and air mixtures burn only at fuel/air ratios existing between a rich and lean limit, it becomes necessary to assess the vulnerability hazard of an aircraft fuel tank in terms of those flight parameters causing mixtures of a combustible nature to exist. The existence of combustible fuel/air mixtures within the fuel tank ullage makes the fuel tanks susceptible to explosion or fire hazards if an ignition source is introduced.

Fuel/air concentration gradients have been found to exist within the fuel tanks (Ref. 1). One can define the degree of hazard by assuming that the larger the volume of combustible mixture, the more vulnerable or hazardous is the fuel tank. The work performed under this contract was to define the fuel tank geometry and flight profile histories that control mass transport and mixing processes leading to the presence of a large volume of combustible mixture within fuel tank ullage spaces. Analysis of fuel tank hazard phenomenon has proceeded along three lines. The first was an experimental study whereby an existing fuel tank test facility developed under previous Air Force support (Contract No. F33615-67-C-1553) was modified to allow for the simulation of the effects of aircraft vibrational environment, and equipped for direct sampling of the composition within the ullage spaces during simulated flight profiles. Gas chromatograph techniques were used to determine fuel/air concentrations at various locations within the ullage under simulated ascent, level and descent flight profiles. These experimental measurements provide a realistic assessment of fuel tank fire and explosion hazards due to external ignition sources. The second area of investigation was analytical modeling of mass transport processes occurring within the ullage space that control the formation of combustible mixtures. Two separate and complementary models were developed to predict fuel/air concentrations within the ullage. The well-stirred model describes situations when mixing of air and fuel vapors occurs very rapidly with no appreciable fuel/air gradients within the ullage volume. This model is particularly applicable to wing tanks of aircraft and for tank configurations where the ratio of ullage volume to liquid fuel surface is small. For tank configurations where this is not true a second distributed O/F model was developed to describe such situations. These two analytical models give us a powerful tool to predict fuel tank fire and explosion hazards and to correlate experimental data. The third area of investigation was concerned with cool flame limits and transition between cool flame and normal flame ignition limits associated with supersonic flights where liquid temperatures and fuel tank skin temperatures are typically very high. This portion of the study was conducted experimentally in terms of light emissions due to flame oxidation processes.

SECTION II

DEFINITION OF THE HAZARD PROBLEM AND METHOD OF APPROACH

A discussion of basic processes occurring within fuel tanks is useful in understanding the interpretation of the data and the development of the analytical model in later sections of the report. Generally after the filling process on the ground is completed, a uniform equilibrium fuel/air vapor mixture is found to exist within the ullage space. That is to say, the fuel partial pressure corresponds to the vapor pressure of the liquid fuel. During filling the degree of stirring and splashing is sufficient, such that this assumption is very good.

As the aircraft climbs to altitude free venting tanks capable of supporting only a low pressure differential vent a mixture overboard that consists of the initial fuel air mixture composition. If the evaporation rate of fuel vapors from the surface of the fuel is low, the fuel/air ratio within the ullage will be nearly uniform and the mixture vented out of the tank to the atmosphere, will essentially correspond to the initial values. As evaporation takes place the fuel/air ratio increases as the fuel vapor attempts to come to its equilibrium vapor pressure within the ullage. In other words, if we had a tank where a membrane was over the surface of the fuel and no evaporation could take place, the fuel to air ratio within the tank would be constant during the ascent stage of the flight. Because of evaporation, and depending upon the local rate of evaporation, the fuel/air ratio may remain relatively constant or may increase. A third phenomenon tending to complicate this rather simplified model is the fact that as the pressure decreases within the ullage, air previously dissolved within the fuel, comes out of the solution and contributes to the oxygen content in the ullage space. Rate of evolution of dissolved air has generally been conceded as controlled by the rate of ascent and vibration and slosh levels existing within the fuel tank. Previous investigators (Ref. 2) have defined safe flight envelopes of aircraft fuels as a function of altitude and liquid temperature. Fuel vapor compositions were assumed to exist at all times at their equilibrium or vapor pressure values within the ullage space. Transport processes such as evaporation and outgassing occurring in the tank determine the degree to which this is true. In other words, tanks considered safe based on equilibrium conditions may be highly vulnerable due to "evaporative lag" whereby the fuel partial pressure in the ullage space cannot maintain its equilibrium value corresponding to the liquid temperature.

At level flight or cruise at constant altitude, fuel is generally removed from the tank. It may be transferred from tank to tank for control of center of gravity or for engine usage. Because the volume in the fuel tank is constantly changing, a small amount of air must be continuously vented into the tank to provide for pressure equalization with the outside ambient air. It has been shown in previous work (Ref. 1) that rather substantial concentration gradients may exist in a deep tank for fuel withdrawal rates as low as one gallon per minute (diffusion time and diffusion distance is small compared to vent velocities). For wing tanks (shallow tanks) this may not be the case as diffusion time, because of small diffusion distances, may be very fast compared with vent velocities, leading to a more uniform mixture. Effects occurring during ascent such as air evolution, and mechanical injection of liquid fuel particles due to vibration may also continue during the level flight portion.

During the descent portion of the flight, a large quantity of air is vented into the fuel tank with a large amount of turbulence and stirring developed within the ullage space. Large concentration gradients must necessarily exist during this portion of the flight as the air entering the tank is essentially or entirely free of fuel vapors and somewhere within the fuel tank, fuel vapors do exist at near equilibrium concentrations. The tank may, however, exist at nearly uniform mixture composition except in the near region of the vent. An additional phenomenon can occur during descent as a result of particular vent configurations and fuel tank geometries. As diffusional processes are slow as compared to velocities occurring during descent, (10 to 15 ft/sec jet velocities), it is feasible that fuel vapors could essentially congregate in regions where they can exist at values higher than that corresponding to their equilibrium vapor pressure. In this case the condensation of the fuel vapors back into the liquid may occur. Although it is felt that three-dimensional flow effects are such that this condition may not exist to any significant extent in deep tanks, the possibility does exist for this phenomenon to occur in a long narrow wing tank with the vent located at one end.

Other basic transport processes occurring during the entire flight profile are those associated with heat transfer through the tank skin to the ullage space. During ascent as the ullage vapors expand and cool down, the misting phenomenon noted in previous studies (Ref. 2) is observed as a result of fuel condensation. The degree of heating associated with hot inner-structures may, however, raise the temperature of the ullage gas sufficiently by heat transfer to remove the ullage gas from this "dew point" or saturation condition. Supersonic flight may permit fuel tank skin temperatures to reach 500 to 550°F. These temperatures are sufficient that low level oxidation may occur within the ullage. These oxidations are essentially chain breaking of the large hydrocarbon molecules and give rise to the characteristic "cool flame" noted for these type of conditions (Ref. 3). There is little energy associated with these reactions and the primary evidence of their existence is in terms of their light emission.

Hazard Assessment

Figure 1 details the input requirements and flow logic for the overall model of the assessment of the fuel tank fire hazard associated with the flight of a particular aircraft. The basic philosophy is to define the time and spatial dependence of fuel/air mixture ratios within the ullage of a particular tank for the flight profile being investigated. This requires detailed calculation of the transport processes occurring within the tank supplemented by experimental data gathered using the fuel tank simulation facility to determine unknown constants. Two models are formulated that together with the experimental data yield required fuel/air mixture gradients and values. The degree of hazard associated with a particular tank is then based on interpretation of the mixture profiles in terms of published ignition limit curves for the particular fuel being used and the expected strength of the ignition sources. The degree of hazard is then based on the percent of the ullage volume that is within combustible regions, the pressure rise associated with the combustion of this mixture (should it occur), and the maximum over pressure the tank structure can withstand. Figure 1 presents a flow chart for the processes of evaluating

Logic Flow Chart for Assessment of Fuel Tank Ullage Space Vulnerability Hazard

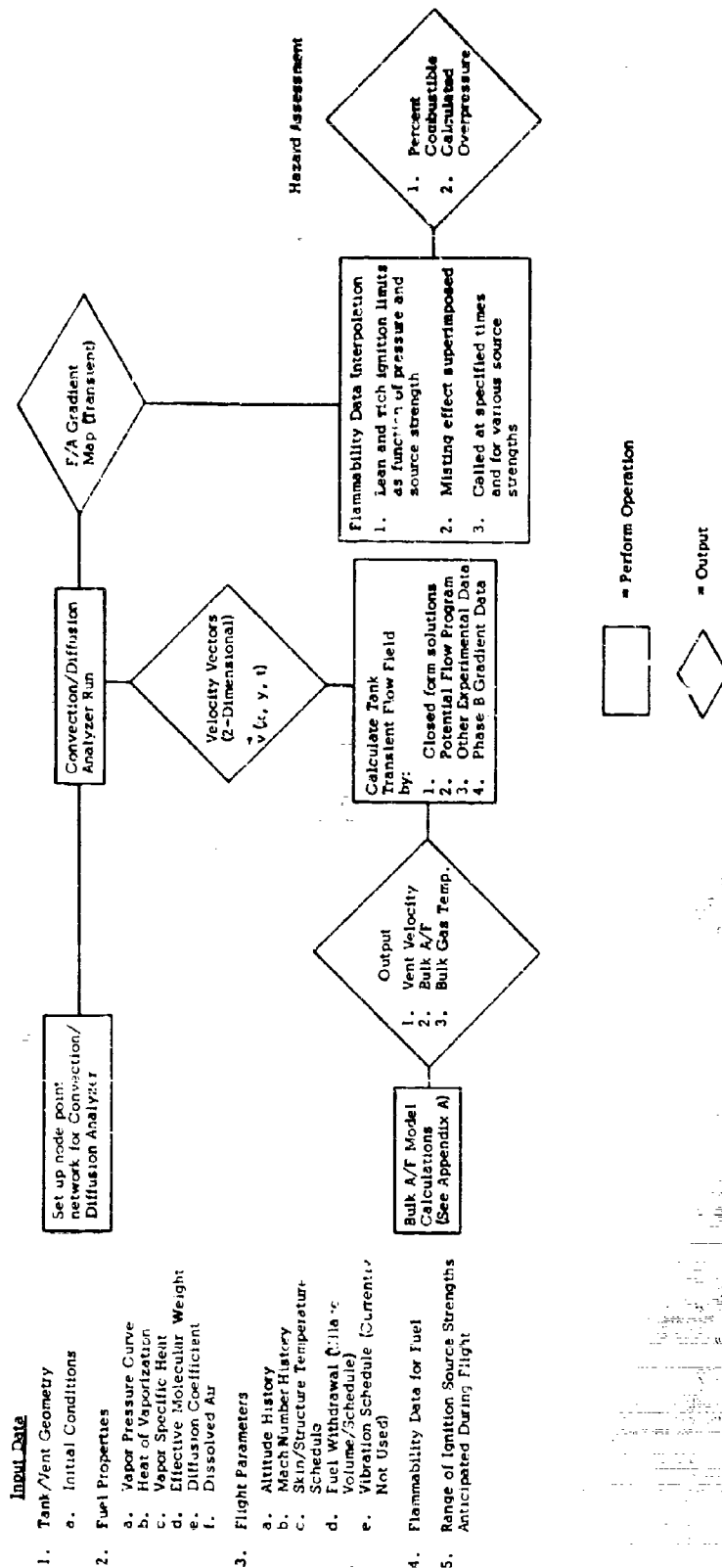


Figure 1. Logic Flow Chart for Assessment of Fuel Tank Hazard

the vulnerability hazard of a fuel tank. The left side of the figure shows the items required as input to the models. These may be broken down into five categories: first is the geometry and vent size location for the particular tank being investigated. Tank geometry is described in terms of a table of ullage volume versus fuel quantity. A set of initial conditions, temperature and volume used to start the calculations, complete the input data and define the initial equilibrium mixture composition.

A second series of input data are fuel properties. These include the vapor pressure and heat of evaporation versus liquid temperature of the particular fuel being examined. Other fuel properties required are the vapor specific heat, the molecular weight of the vapor, diffusion coefficient of the fuel vapors in air and the amount of dissolved air within the fuel.

A third set of controlling parameters are flight indicators such as the altitude history, the Mach number history, the skin and internal structure temperature, the fuel withdrawal rate, and vibration schedule associated with the particular aircraft fuel tank being studied.

A fourth required item is the flammability range for the particular fuel under study. These flammability limits exist within the literature and a study has shown they are relatively independent of the pressure but do depend upon strength of the ignition source.

A fifth item of required input data for the vulnerability model is the range of ignition source strength expected during a particular flight. Currently these are employed in terms of effective spark ignition energy.

Figure 1 demonstrates the logic behind the required input values and the method of utilization in determining the vulnerability of a particular fuel tank flight profile.

Proceeding through Figure 1 in a step-wise manner, the first operation is concerned with setting up the node mesh for the Distributed F/A Model. This involves the calculation of the equivalent resistors and capacitors for diffusion and convection employed by the program.

The second operation is to perform the bulk or well-stirred F/A calculation; the primary purpose of which is to define vent velocity and average gas F/A and temperature. These not only provide realistic bounds for the distributed F/A model but prescribe an essential input quantity in the vent velocity.

Based on the bulk F/A calculations above, the calculated vent velocity and tank geometry are used to determine the internal velocity field within the ullage. Four techniques are available for defining the velocity field. These include:

1. Closed form potential flow solutions,
2. Potential flow fields calculated numerically,
3. Experimental data of other investigators,
4. Experimental data estimated based on the test results of this program.

It appears, at this time, that definition of the velocity field is a major consideration in the development of the overall model. Calculations done using a plug flow velocity model for a specialized geometry have been successful. Indications are based on an initial literature search and test data that a significant amount of recirculation and turbulence can be generated even at low venting rates and the ullage will tend toward being well-stirred (Bulk F/A Model) except in the jet region of the vent.

Velocity vectors as defined by one of the techniques above are then input to the Distributed F/A Model for each mesh point previously defined.

The distributed F/A program is then run for the entire flight profile and concentration maps developed. At specified times during the calculation interpolation in the ignition limit curves for the source strength specified will determine the hazard rating for that time.

The assessment of the hazard can then be made based on the product of four quantities, shown below:

$$\text{Hazard} = P_A \cdot P_{F.T.} \cdot P_{IGN} \cdot \frac{\Delta P_{ad}}{\Delta P_{ref}}$$

The first is the probability of an aircraft hit, the second is the probability that the hit will be in the fuel tank, the third is the probability that the tank will ignite, and the fourth quantity is the pressure rise due to combustion divided by reference pressure rise, such as the tank structural limit. The third and fourth quantities are assessed by the above model while the first and second must be prescribed by the user.

The quantity P_{IGN} relates the strength and location of the ignition source to the flammability map of the ullage. Three assumptions in estimating this quantity are used prior to the incorporation of any additional data. The first is rounds entering the ullage in a noncombustible region will not cause an ignition (no stirring of ullage mixture and no air entrapment by round). The second is that the ignition source can be characterized by an equivalent "spark" energy. The third is that published ignition limits and relations between ignition limits and ignition source energies are applicable. It can be seen then that the above quantity relates the strength of the ignition source and the location at which the round enters the tank to ignition potential.

The fourth quantity $\Delta P_{ad}/\Delta P_{ref}$ is a calculated pressure rise due to adiabatic combustion within the ullage divided by a reference pressure such as the fuel tank structural limit, that is input to the model. The pressure rise due to combustion is calculated based on a determination of the percent of the ullage mixture that is flammable. A standard chemical equilibrium combustion program (ODE available through CPIA) is used to determine the pressure rise. These calculations are currently performed externally to the computer programs. The required input is enthalpy (determined by F/A) of a particular combustible zone and the density. Output is the combustion pressure of this zone. By summation of the pressure rise of each zone, over all zones that are combustible the total pressure rise is estimated.

SECTION III

EXPERIMENTAL EQUIPMENT & TEST PROCEDURES

A fuel tank testing facility, capable of simulating supersonic flight profiles, and developed under previous Air Force support (Contract No. F33615-67-C-1553), was modified to permit sampling of the vapor mixture in the ullage space and to evaluate the effect of tank vibration. The entire test setup consists of the following six systems.

1. Temperature controlled experimental fuel tank.
2. Tank vibration system.
3. Vent air and fuel temperature conditioning system.
4. Tank pressurization (altitude) system.
5. Sampling System.
6. Recording instrumentation.

1. TEMPERATURE CONTROLLED EXPERIMENTAL FUEL TANK.

A stainless steel (304) experimental fuel tank, 2' in dia, 5' in length and 3/16" thick was used throughout the entire test program. Figure 2 shows the sketch of the experimental fuel tank. The tank capacity was approximately 110 gallon and was designed to withstand 120 psia internal pressure. Pyrex windows 8 1/2" in diameter were provided at both ends of the tank for observation. Specially designed port openings were provided for instrumentation mounting.

The wall temperature of the experimental fuel tank was controlled through the use of electrical resistance heaters and cooling coils using water as a coolant. The arrangement of resistance heaters and cooling coils is shown in Figure 2. The total heating capacity for the resistance heaters was 39 kw.

2. TANK VIBRATION SYSTEM.

In order to simulate the dynamic test conditions, the test stand was modified to incorporate a vibration adapter and a spring bar system. The details of the vibration adapter is shown in Figure 3. The adapter was connected to the spring bar by means of four shackles. Provisions were made to vary the positions of the shackles along the length of the adapter. The entire system (adapter and the spring bar) was installed over the test stand as shown in Figure 4.

Input force to achieve tank vibrations was generated by a mechanical vibration generator powered by a DC motor (one horsepower). The vibrator was connected to the motor with a flexible drive shaft. The vibrator was of the reaction type with counter rotating adjustable steel eccentric weights. The generator had two shafts which were geared together so that the

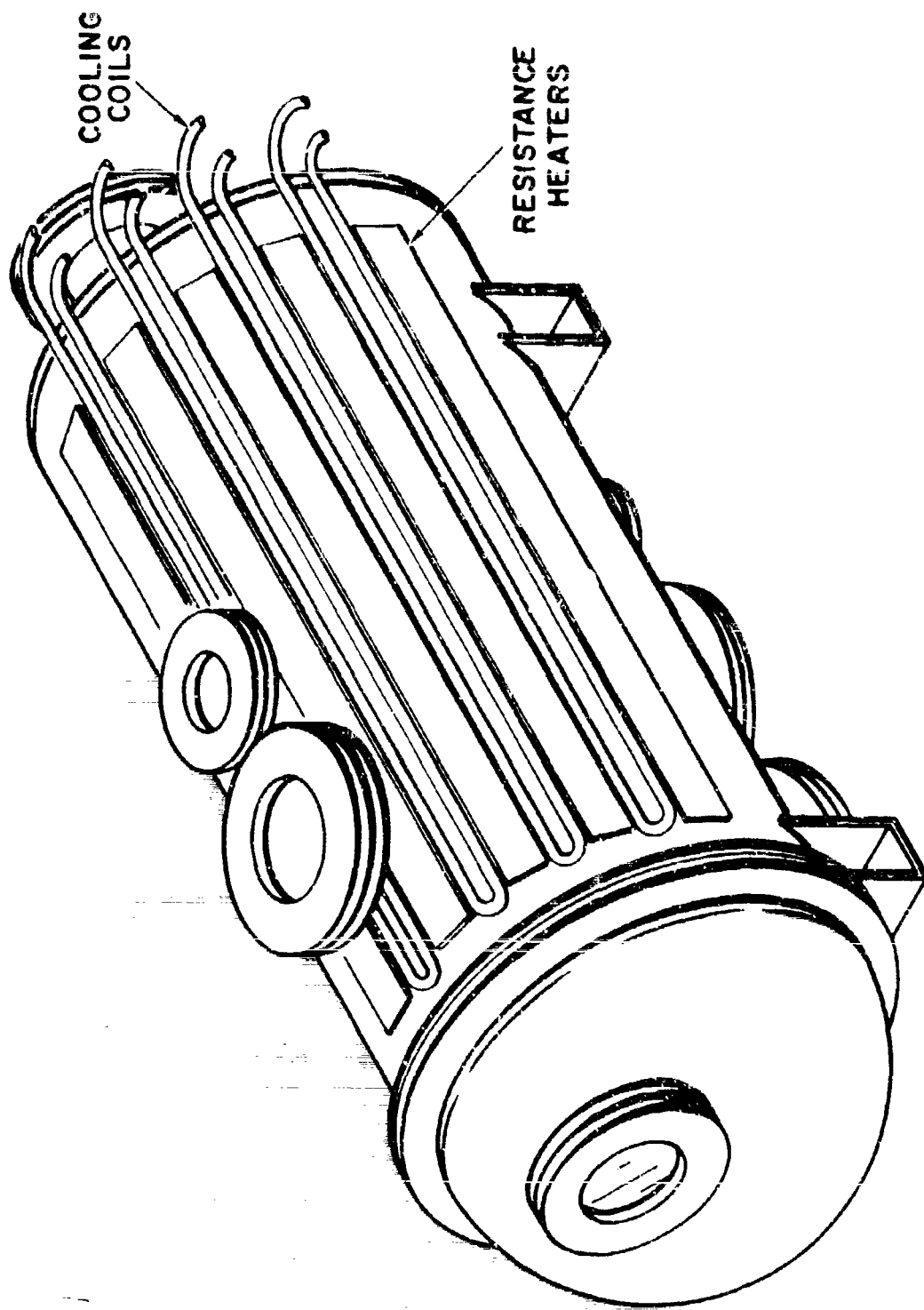
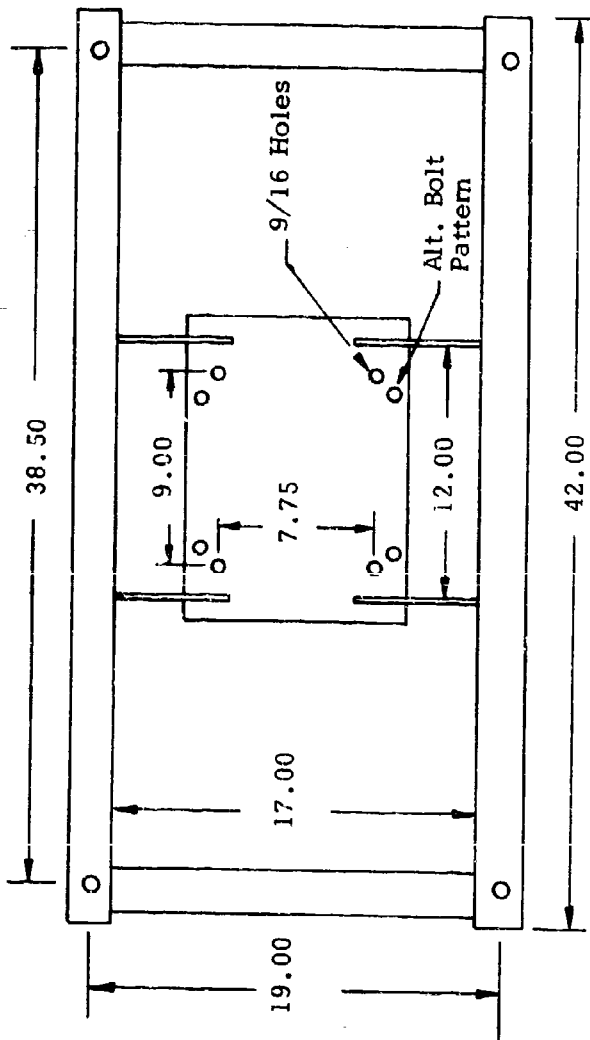
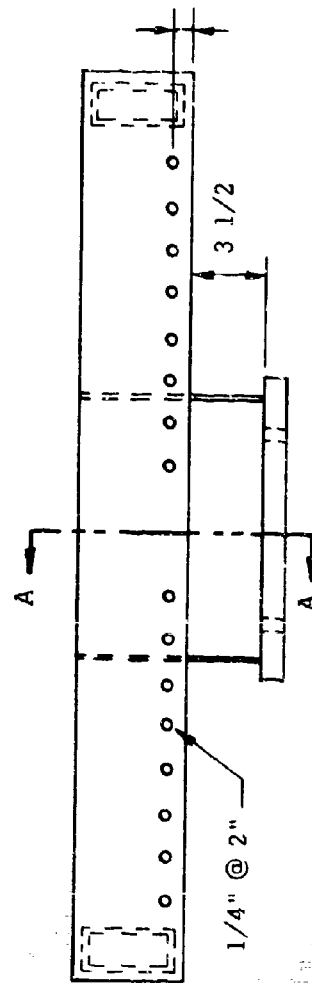


Figure 2. Arrangement of Heaters and Cooling Coils on Cylindrical Portion of Unwetted Tank Walls.

Top View



Side View



Section A-A

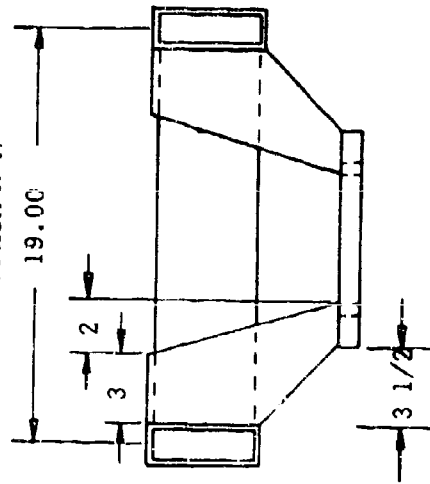


FIGURE 3. Vibration Adapter

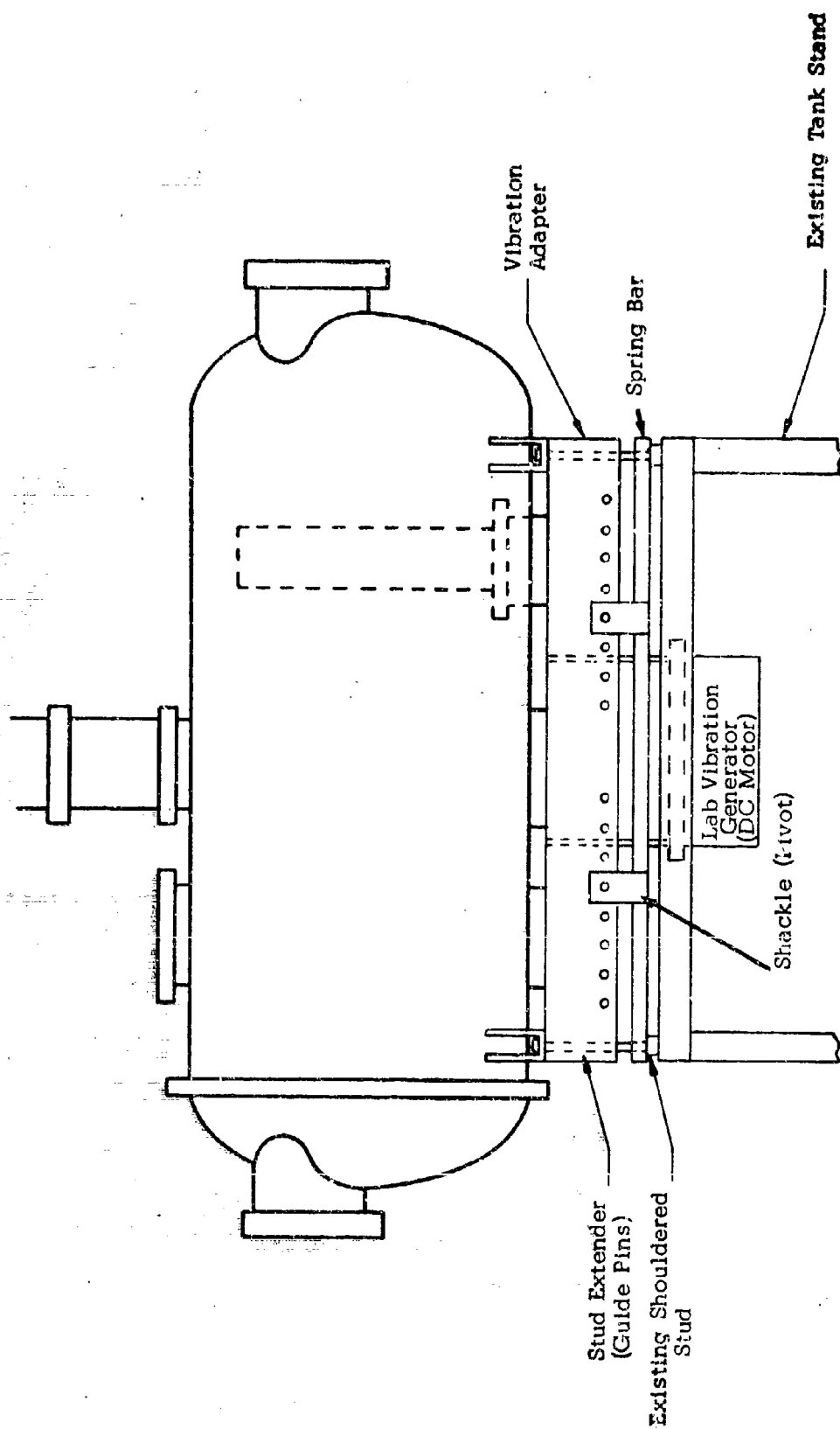


FIGURE 4. Schematic of Vibration Generator in Place

centrifugal force of the individual shaft was resolved into a rectilinear force normal to the plane of the shaft's axes. The generator was mounted onto the adaptor (shown in Figure 4) resulting in the experimental fuel tank vibrating in the vertical mode. Desired vibration levels were achieved when the input frequency was in resonance with the spring bar system. Resonance amplification factors as high as 15 were obtained. The natural vibration frequency of the spring bar was directly related to the distance between the shouldered stud and the shackles (see Figure 4). By varying the position of the shackles, different vibration frequencies could be achieved. Specified vibration frequencies and vibration levels encountered during typical flight environments were simulated by properly adjusting the positions of the shackles. Figure 5 is a close view of the test stand with the vibration generator mounted onto the adapter. An overall view of the experimental fuel tank is shown in Figure 6.

3. VENT AIR AND FUEL TEMPERATURE CONDITIONING SYSTEM.

To better simulate vent conditions at high flight speeds, a specially designed heat exchanger was used to control the vent air temperatures. This modification also had the added advantage of avoiding fuel condensation at the originally unheated vent. The heat exchanger consisted of two concentric copper tubes, with outer tubes $3/4$ " in diameter and inner tubes $1/2$ " in diameter. The entire heat exchanger was approximately 20 ft in length. Strip heaters were provided along the entire length of the heat exchanger. Vent air was allowed to flow through the inner tubes and the desired temperature of the vent air was easily achieved by varying the airflow rate between the concentric tubes and the heat output of the stripped heaters. Figure 7 shows the experimental fuel tank with the vent air heat exchanger. An additional valve was installed to prevent fuel vapor entering the heat exchanger during the ascent phase of the flight profile. A thermal insulator (asbestos) was installed to prevent possible flame propagation into the heat exchanger.

Immersion heaters and a separate heat sink bath were used to vary the liquid fuel temperatures. Immersion heaters were installed inside the experimental fuel tank. The total heating capacity of the immersion heaters was 26 kw. Liquid fuels at various higher temperatures were obtained by controlling the rate of heat output of the immersion heaters. To obtain liquid fuel at temperatures lower than the room temperature, a separate heat sink bath was used. Figure 8 shows the liquid fuel cooling system. A refrigeration compressor unit was used to condition the temperature of a water-glycol mixture within the heat sink bath. Lower liquid temperatures were achieved by circulating the fuel through the heat sink bath.

4. TANK PRESSURIZATION (ALTITUDE) SYSTEM.

The desired ascent rate of the flight profile was obtained by controlling the evacuation rate provided by a vacuum pump having a capacity of $15.2 \text{ ft}^3/\text{min}$. A throttle valve in the 2" evacuation line provided the control of the evacuation rate. A fine control was established by supplying bleed air to the vacuum line via the ascent throttle valve and ascent regulator. The descent rate was obtained

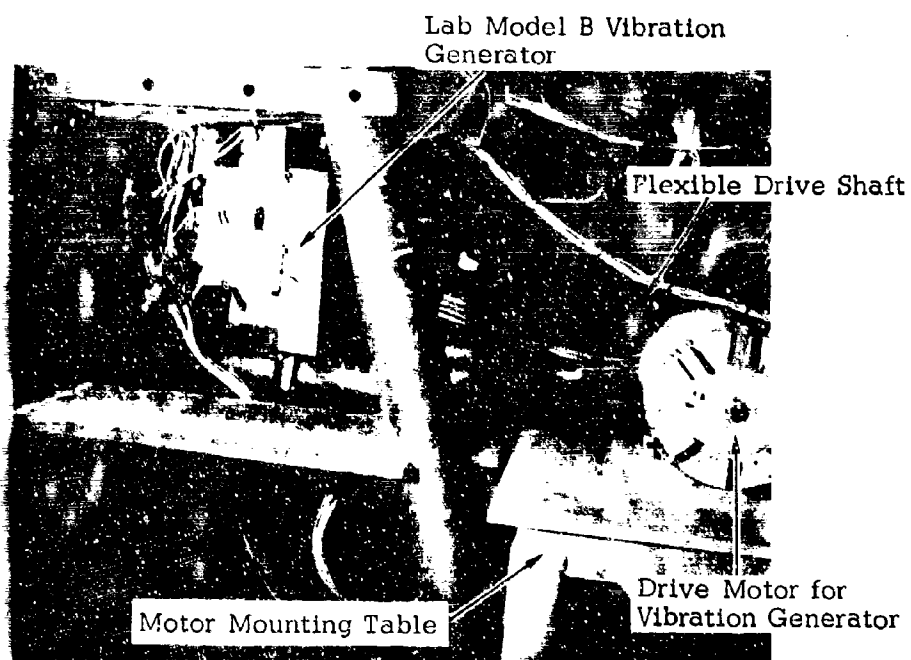


Figure 5. Fuel Tank Vibration System

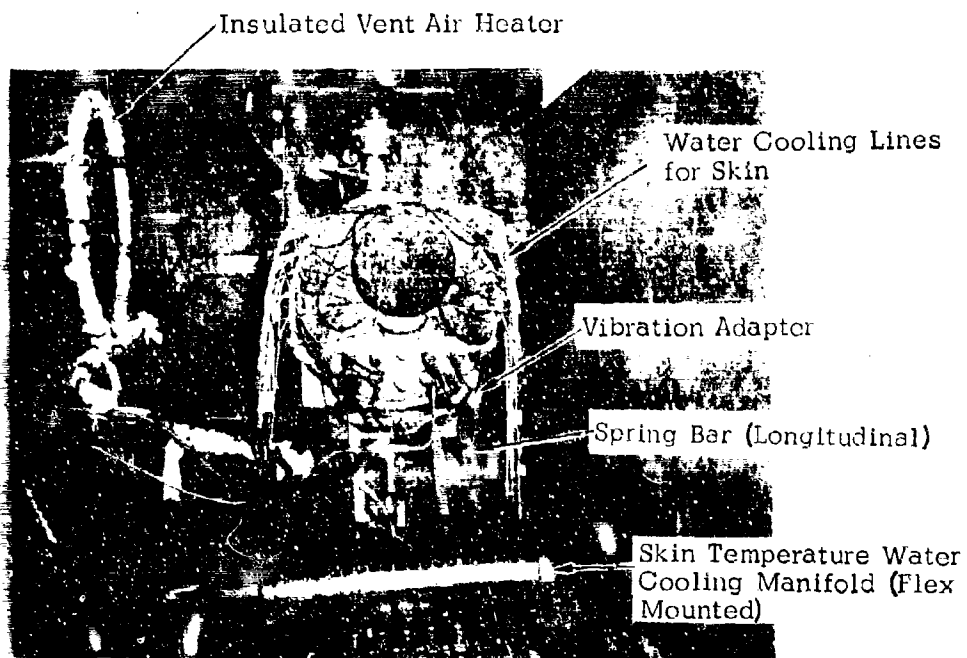


Figure 6. Overall View of Tank Monitor on Vibration Adapter

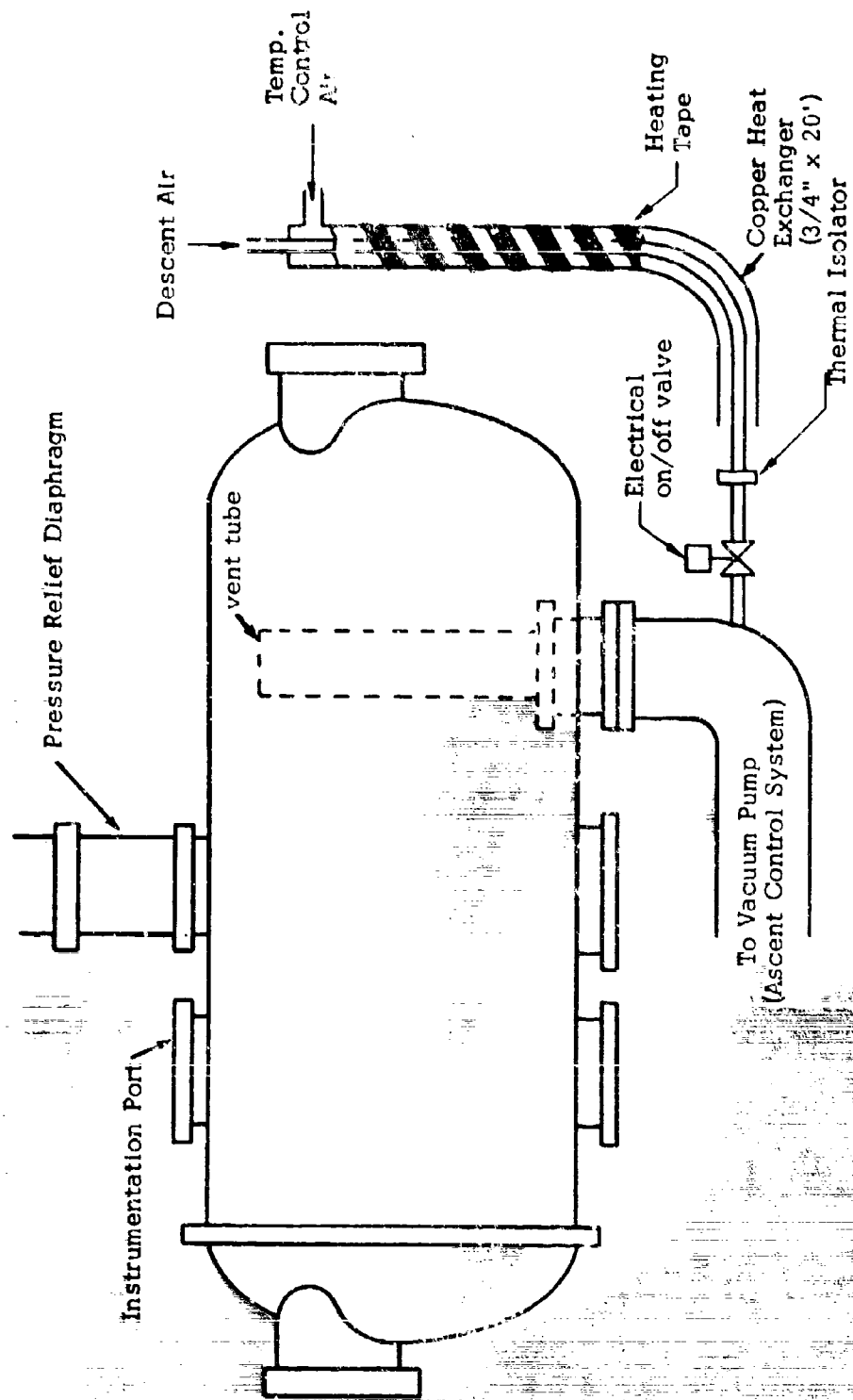


FIGURE 7. Test Tank With Descent Air Heater

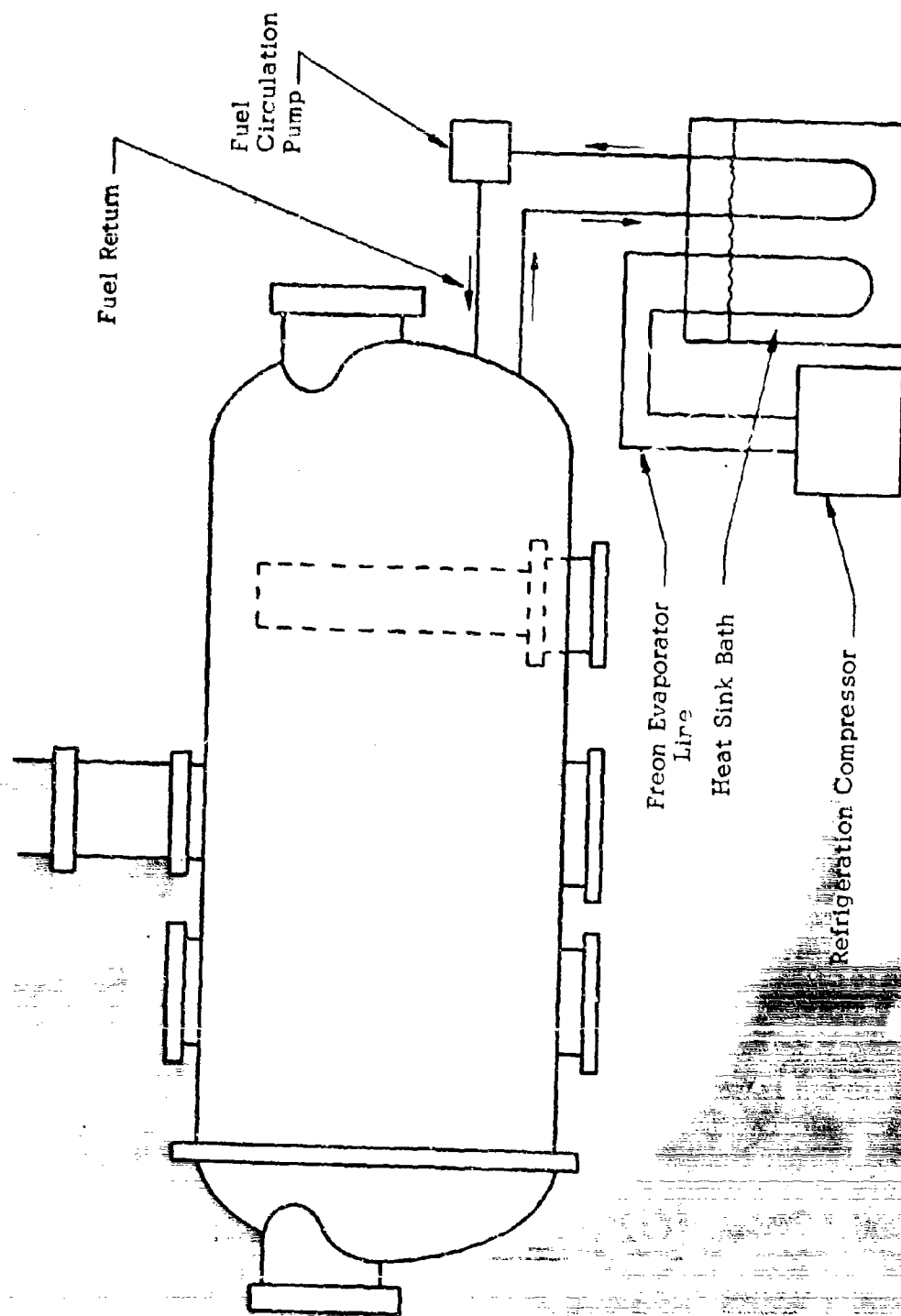


FIGURE 8 . Fuel Cooling System

by isolating the vacuum pump and by controlling the air bleed rate through the descent throttle and descent regulator. A nitrogen purge system was provided to minimize possible reactions within the tank. The pressure control system is schematically outlined in Figure 9.

5. SAMPLING SYSTEM.

Fuel air ratios of the ullage vapor mixture were determined using a portable gas chromatograph with a flame ionization detector. Several important criteria were used in choosing the appropriate instrument for measuring the fuel/air ratio of the vapor phase. These included data accuracy, capable of measuring a wide range of fuel/air ratios under variable total sampling pressures, rapid sampling rate, small sample size so as not to disturb the processes occurring within the tank, ease of data analysis, and data reduction. The portable gas chromatograph used in the program appeared to best meet these criteria. This instrument was equipped with two different separating columns. One of the columns was essentially a dummy column with no appreciable sample separation. This allowed rapid determination of total hydrocarbon (less than 30 seconds). Fuel/air ratios were deduced from these measurements. A second column was capable of separating gas components more extensively. It was therefore inherently more time consuming and was used only to analyze hydrocarbon components to determine effective molecular weight. Figure 10 is a picture of the gas chromatograph and the integrating recorder.

Figure 11 shows the schematic of the automatic fuel vapor mixture sampling system. The sampling probe was provided with five sample inlets. These sample inlets were located at various selected positions within the ullage space. Five electrically actuated sample selection valves, capable of operating under high temperature environments (400°F) were used to select the samples to be analyzed. Figure 12 shows the location of the selection valves. The sample line was directly connected to the portable gas chromatograph. The entire length of the sample line (from the electrically actuated valves to the g.c. inlet) was temperature conditioned to avoid condensation of fuel vapors within the line. Flexible strip heaters were used and wrapped around the sample line to raise the line to necessary temperatures in order to avoid fuel condensation.

An automatic sequencing unit was used to operate the entire sampling procedure. The sequence of operation was briefly summarized as follows:

Event 1. - One of the sample selection valves and the sample interrupt valve (solenoid valve immediately upstream of the vacuum pump) were first opened remotely.

Event 2. - Gas sample was allowed to flow for 30 seconds to flush out the samples previously retained in the line and at the same time to draw in the new sample.

Event 3. - The sample interrupt valve was then closed to allow the line pressure to equalize to that of the experimental fuel tank pressure (10 seconds).

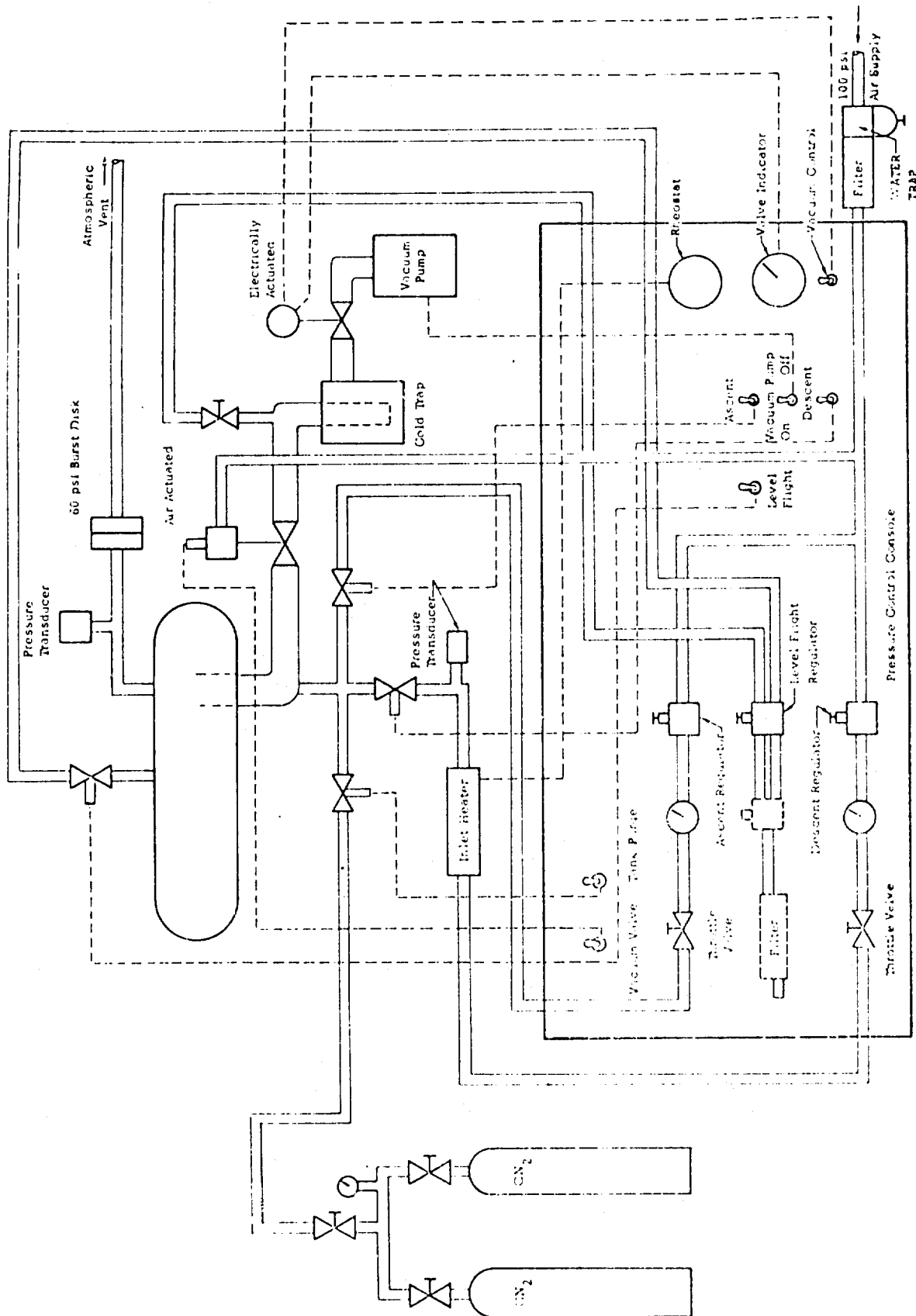


Figure 9. Schematic Diagram of Pressure Control System

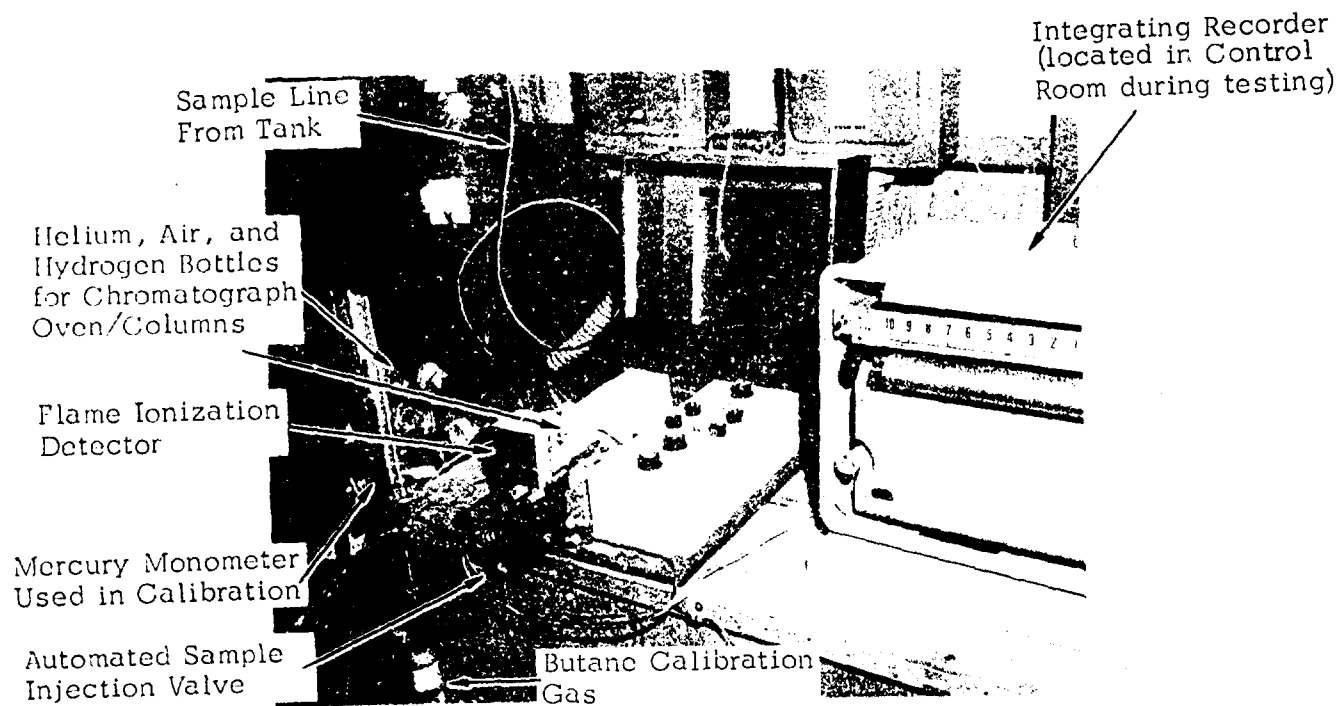


Figure 10. Gas Chromatograph for Fuel/Air Measurement.

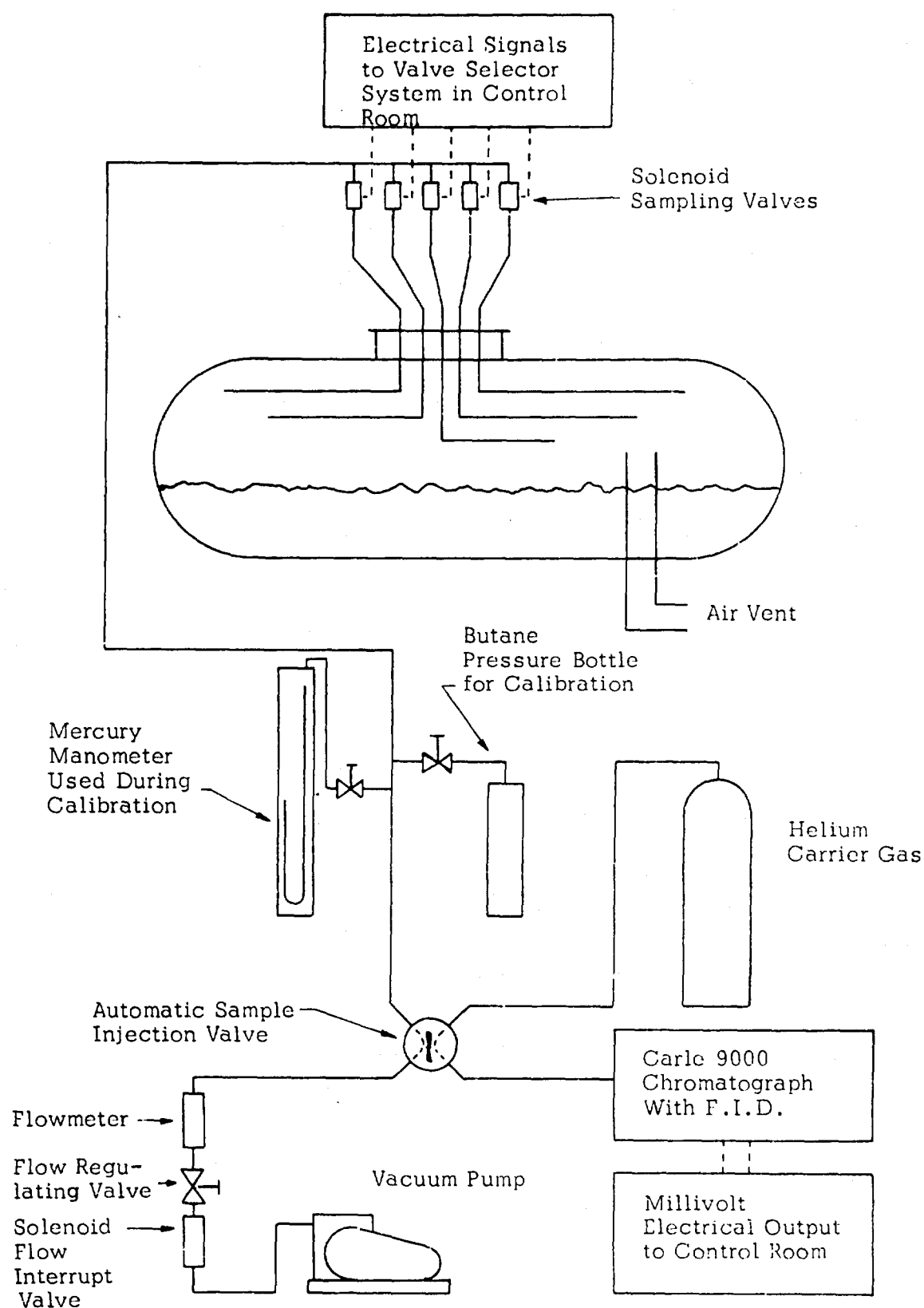


Figure 11. Automatic Sampling System

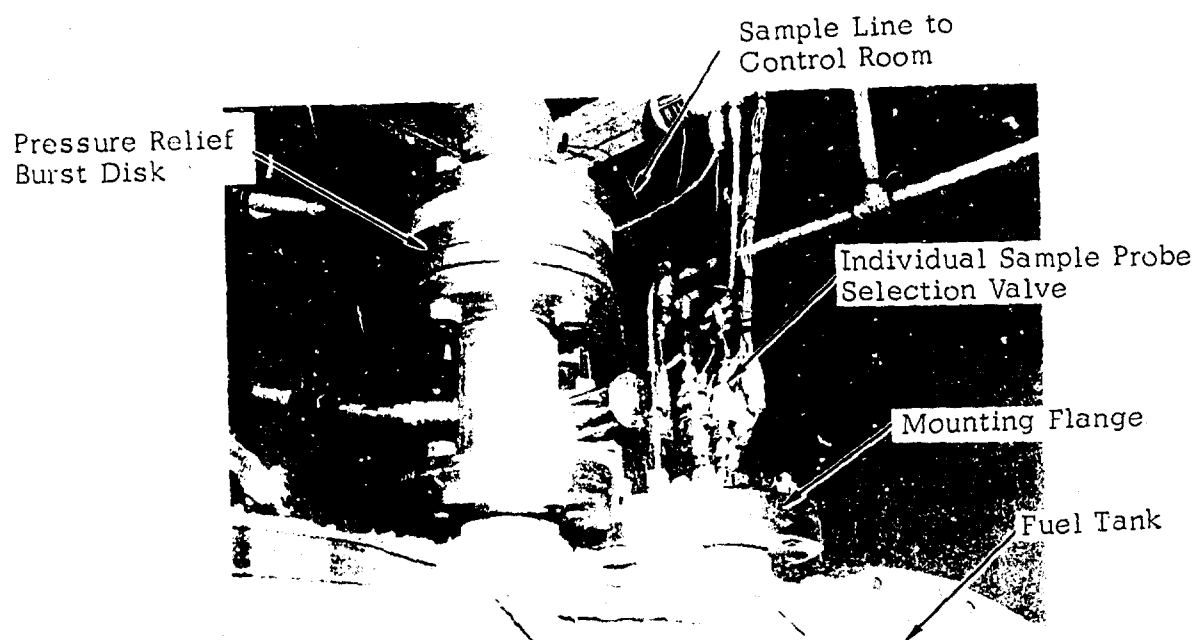


Figure 12. Sample Probe Selection Valve Installation

Event 4. - Helium gas was used to inject the sample into the chromatograph (sample injection valve actuated).

Event 5. - A second sample selection valve and the sample interrupt valve were opened to allow a new sample to flow for another 30 seconds.

Event 6. - Analysis of the previous sample occurred 30 seconds after the injection valve was actuated and the result was recorded remotely on an integrating recorder in the control room.

The sequencing unit automatically controlled the opening and closing of various valves and thus allowed analysis of the five gas samples in sequence. Pure butane gas was used for calibration.

6. RECORDING INSTRUMENTATION.

A total of seventeen thermocouples were provided for measuring temperatures at various internal positions of the tank. Exposed thermocouples were provided for monitoring the vapor phase temperature and remote junctions were used for thermocouples monitoring the liquid phase and the wall temperatures. The thermocouple leads were of various lengths and could be adjusted at the port where they entered the tank to reach different parts of the tank interior. Approximately 35 thermocouple clips were provided on the interior of the tank walls so that the thermocouples could be moved from one position to another. Two of the thermocouple outputs were used for input to two feedback controller systems which independently controlled the liquid temperature and the unwetted wall temperature. Twelve (12) of the remaining thermocouples were monitored on a 12 point strip chart recorder. An oscillograph was also available for recording the thermocouple outputs over short periods of time.

Two programmer-controller combination sets for independently controlling the liquid-phase temperature and the unwetted tank wall temperature were used. The system was adjusted to operate in the range of 0-500°F using iron-constant thermocouples. The electronic circuit of each controller utilized a firing circuit to control up to 100 amperes of current supplied at 460 volts.

Each controller operated in any of the three modes: manual, set-point, or programmer. Manual control permitted a linear increase in power supplied to the load with an increase in dial setting up to 100%. Set-point provided a means for dialing in a specific temperature to which it was desired the work be controlled and through the use of the programmer a variable temperature could be specified. Programming was easily accomplished by drawing the desired temperature-time profile on a card coated with a conductive film. When this card was inserted into the programmer a control signal was generated and transmitted to the controller as a control point.

A strain-gauge pressure transducer (0-50 psia) was used to continuously monitor the pressure of the experimental fuel tank. A strip chart recorder was used to record the pressure transducer output. Rate of ascent and descent as well as flight altitude were interpreted based on these measurements.

Any normal ignition that might occur within the experimental fuel tank would probably be indicated by abrupt changes of both pressure and temperature within the tank. Lower level luminous reactions often occurred, however, which would not be detected by either of the above parameters. To detect these low intensity reactions and also to confirm the occurrence of any normal ignition, a photomultiplier tube was installed outside the observation window at one end of the test tank. The observation window at the opposite end of the tank was optically shielded and a small test light was installed under this shield to serve as a check on the operability of the photomultiplier. The continuously monitored output from the photomultiplier tube was recorded on a strip-chart recorder.

Vibration level and frequency were measured using two accelerometers powered by charge amplifiers. Two units were used to check for the rocking mode by comparing base angle between output peaks. These units were calibrated at 1 g acceleration by dropping on a soft pad. Free flight acceleration level was 1 g. A multichannel oscillograph was used to record accelerometer output.

7. TEST PROCEDURE

Test parameters consisted of

- a. Altitude history
- b. Temperature history of fuel tank walls.
- c. Liquid fuel temperature.
- d. Vent air temperatures.
- e. Vibration level and frequency.
- f. Fuel fill level.
- g. Fuel withdraw rate.

The altitude history of the desired flight profile was achieved by first plotting the corresponding pressure history on the recording paper of the strip chart recorder. The pressure of the experimental fuel tank was varied by throttling various ascent and descent control valves such that the output of the strain-gauge transducer (which registered the tank pressure) followed closely the pressure history previously plotted on the recording paper. The temperature histories of the fuel tank walls and the liquid fuel were attained by drawing temperature control cards describing the desired temperature histories. These cards were inserted into the programmer-controller combination sets for automatic control of the prescribed temperature of the fuel tank walls and the liquid fuel within the tank. Prescribed vent air temperature was attained prior to each test using the co-axial heat exchanger. Vent air temperature could be easily adjusted by varying the air flow rate between the inner and outer tubings. By varying the position of the shackles, prescribed vibration frequency was obtained. The vibration level was also set to that prescribed

in the test plan. Prior to each test possible changes in the composition of the liquid fuel were monitored using a closed-cup flash point tester. The tank was filled to the prescribed fuel level and fuel withdrawal rate was set to that corresponding to the normal engine consumption.

Tests were conducted to (1) establish cool flame versus normal flame autoignition hazards and (2) experimentally determine fuel/air composition existing in the ullage of the fuel tank. Photomultiplier data was used to evaluate the flame autoignition hazards. Gas chromatograph was used to determine the fuel/air compositions. Gas chromatograph was properly calibrated before each test using samples of pure butane. A mercury monometer was used to accurately monitor the pressure of the butane gas. As the flame ionization detector essentially counted the total carbon atoms, the output signal of the calibration run gave a relative measure of a known number of carbon atoms. Fuel/air compositions were determined based on the calibrated valves with corrections for changes of tank pressures, and the ratio of molecular weight of butane and the fuel vapor. The entire sampling procedure was operated using the automatic sequencing unit.

After each test, the flash point of the lower volatility (Jet A, JP7) liquid fuels was again measured. When flash point deviations of 5°F were observed, a fresh batch of liquid fuel was substituted.

The effective molecular weight of the fuel vapors was measured. For JP4 the value used was 72. For Jet A and JP7 the value used was 144°F. The measurement was done by freezing the hydrocarbon vapors out of a sample drawn from over the surface of the fuel using liquid nitrogen. After thawing the pressure and weight of the hydrocarbon gas was measured and the molecular weight calculated from the gas law.

These numbers were used to treat the fuel vapors as a single component gas in both the reduction of experimental data and the computer program development. This molecular weight will change with both liquid temperature and percent fuel vaporized. Changes should, however, show up in the measured flash point. Thus, the flash point test used to determine when the fuel required changing was a measure of the shift in molecular weight of the fuel vapors (distillation of light ends).

SECTION IV

THEORETICAL MODELING OF AIRCRAFT FUEL TANK FIRE AND EXPLOSION HAZARDS

Figure 13 shows the basic transport processes occurring within the fuel tank ullage space. The main source of fuel vapor is by evaporation from the liquid surface. Fuel droplets are also present due to vibration and sloshing of the fuel tank. Air enters the tank ullage mainly through venting and the evolution of air originally dissolved in the liquid fuel. In addition, pressure variations, tank configurations, liquid temperature, fuel withdrawal rates, type of fuel, and heat transfer between the tank inner-structure and the ullage gas mixture often play very significant roles. To determine fire and explosion hazards of aircraft fuel tanks, each of these phenomena has to be properly assessed and described.

Two separate and complementary models have been developed to determine fuel/air concentrations within the ullage space in order to assess the fire and explosion hazards. The first model describes the situation when mixing of air and fuel vapor occurs very rapidly with no appreciable fuel/air gradients within the ullage volume. This well-stirred model is particularly applicable to describe the ascent and level flight portion of the flight profile of shallow tanks.

During cruise at constant altitude, significant fuel/air gradients can occur within the ullage volume. This phenomenon has also been experimentally observed (Ref. 1). A second model or distributed F/A model, was developed taking into account concentration gradients within the ullage. In this model, effect of fuel withdrawal is important and the volume of air vented into the tank is governed by the volume of liquid fuel consumed by the engine. This model properly accounts for the velocity field created by the vented air coupled with the effect of molecular diffusion. The Thermal Analyzer Computer Program for solution of complex heat transfer problems has been properly modified to include the effect of convective flow as well as diffusion of mass rather than thermal energy in order to solve the fuel/air concentration gradients within the ullage space. The following sections describe the analyses and the computer programs that have been developed to evaluate fuel tank fire hazards and to interpret the experimental work performed in this study.

1. WELL-STIRRED COMPUTER MODEL.

The well-stirred model assumes that the ullage space is filled with a homogeneous mixture of fuel vapor and air. The model properly accounts for the rates of mass and energy transport due to fuel evaporation, venting (in or out), heat transfer, and out-gassing. Provisions have also been made for droplet formations in the ullage space due to condensation and tank vibration and sloshing. Appropriate expressions describing the formation of droplets have yet to be developed and experimentally verified.

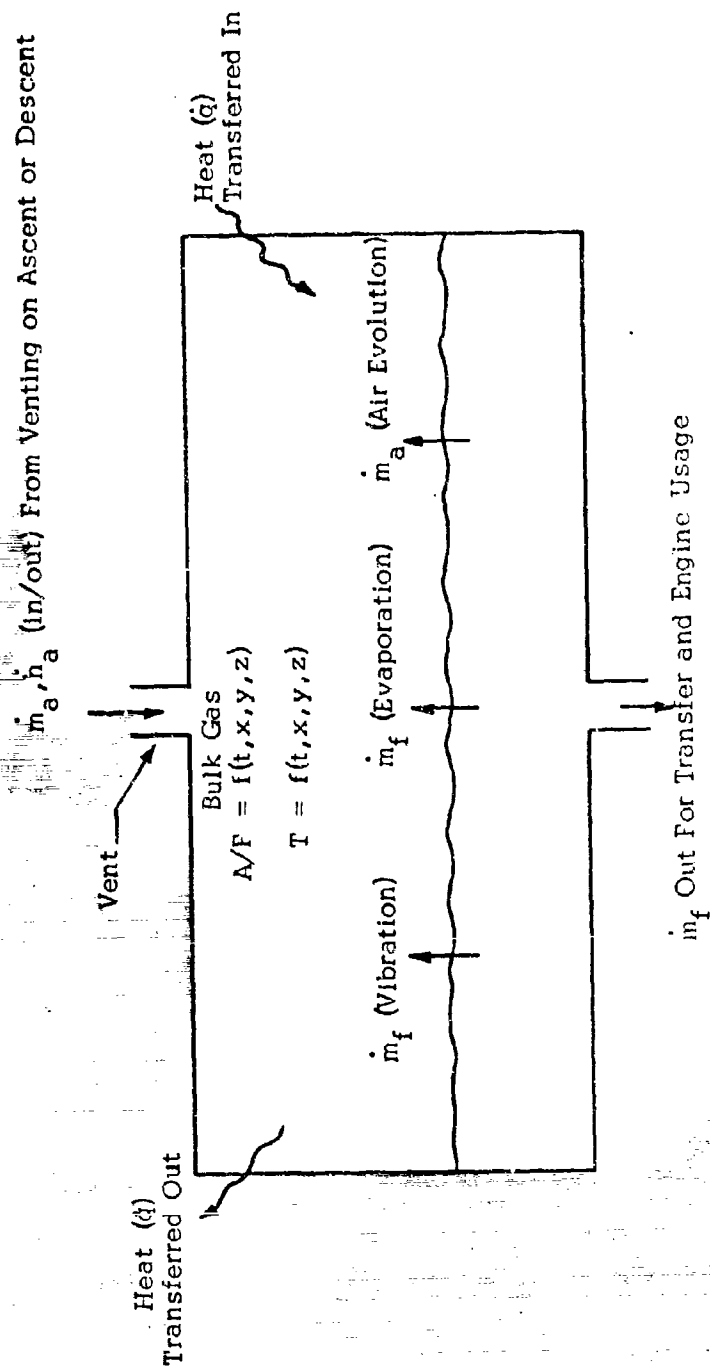


Figure 13. Fuel Tank Transport Processes.

The computer model requires the following variables as input:

- a. Altitude profile
- b. Liquid temperature history
- c. Skin and structure temperature history
- d. Vapor pressure relations of liquid fuels
- e. Fuel vapor effective molecular weight
- f. Ullage volume and exposed surface area schedule
- g. Vent size
- h. Estimates of internal heat transfer coefficients between ullage and tank structure.

Atmospheric properties (pressure, specific heat, and temperature) are included on a master tape of the Standard Atmosphere. The computer program calculates the fuel vapor and air concentrations, the corresponding vent velocity, and the bulk gas temperature.

The details of the well-stirred model are discussed below:

Basic Equations

The mass fraction of air in the ullage is defined as $z = m_a/m$ where m_a is the total mass of air and m is the total mass. The fuel vapor mass fraction is thus $1 - z$ and the F/A ratio is

$$F/A = \frac{1-z}{z} \quad (1)$$

The total mass is given by

$$m = \frac{PV\bar{M}}{RT} \quad (2)$$

where P , V , T are respectively the pressure, volume, and temperature of the ullage and \bar{M} is the average molecular weight defined as

$$\bar{M} = \left(\frac{z}{M_a} + \frac{1-z}{M_f} \right)^{-1} \quad (3)$$

The internal energy is given by

$$e = \frac{m\bar{c}_p T}{\bar{y}} \quad (4)$$

where \bar{c}_p is the average specific heat:

$$\bar{c}_p = (1-z) c_{p_f} + z c_{p_a} \quad (5)$$

and $\bar{\gamma}$ is the ratio of specific heats (\bar{c}_p/\bar{c}_v) or $\bar{\gamma} = \frac{1}{[1 - \frac{R}{\bar{M} \bar{c}_p}]}$ where

R is the universal gas constant.

The rate of change of m, e, and z are found by taking the derivatives of equations 2 and 4 and are

$$\frac{\dot{m}}{m} = \frac{\dot{P}}{P} + \frac{\dot{V}}{V} - \frac{\dot{T}}{T} - \bar{M}z \left(\frac{1}{M_a} - \frac{1}{M_f} \right) \quad (6)$$

$$\frac{\dot{e}}{e} = \frac{\dot{m}}{m} + \frac{\bar{\gamma}z}{\bar{c}_p} \left[(c_{p_a} - c_{p_f}) + R \left(\frac{1}{M_f} - \frac{1}{M_a} \right) \right] + \frac{\dot{T}}{T} \quad (7)$$

$$\frac{\dot{z}}{z} = \frac{\dot{m}_a}{m} - \frac{z\dot{m}}{m} \quad (8)$$

where \dot{m} , \dot{e} , \dot{z} denote dm/dt , de/dt , and dz/dt . The time rates of change of m, e, and m_a must be equal to the net flux of each into the ullage.

Mass Flux

The net mass flux is given by

$$\dot{m} = \dot{m}_v + \dot{m}_{ev} + \dot{m}_{og} - \dot{m}_{cond} + \dot{m}_{mist} \quad (9)$$

where the subscripts refer to the following:

- v = venting
- ev = evaporation of the liquid fuel
- og = outgassing from the liquid fuel or solution
- cond = condensing of fuel vapors
- mist = misting due to vibration

\dot{m}_{ev} , \dot{m}_{og} , \dot{m}_{cond} , and \dot{m}_{mist} can be calculated from the known conditions in the ullage, once suitable relations are prescribed. \dot{m}_v , however, depends on specific flight profiles and has to be solved simultaneously with other variables. Implicit in this formulation is that the tank pressure approaches to the local ambient pressure instantaneously. For tanks where

this is not true, the pressure history is that of the tank pressure.

The net flux of air into the ullage volume is the sum of air off-gassing $\dot{m}_{og} z_{og}$ and venting $\dot{m}_v z_v$.

$$\dot{m}_a = \dot{m}_{og} z_{og} + \dot{m}_v z_v \quad (10)$$

z_{og} denotes the fraction of air in the off-gassing mixture from the liquid fuel. z_v is introduced to distinguish the difference between air venting into the ullage volume as during descent and level flights and fuel/air mixtures venting into the atmosphere from the ullage volume as during ascent. In the former case where only air is entering the tank, $z_v = 1$. In the later case, z_v is equal to the calculated fraction of air in the ullage mixture.

Energy Flux

The first law of thermodynamics for an open system can be explained as

$$\dot{Q} + \sum \dot{m}_i h_i = \dot{e} + \dot{W} \quad (11)$$

where \dot{Q} is the rate of heat transfer to the system. $\sum \dot{m}_i h_i$ are the net energy flux associated with the mass entering and leaving the system. \dot{e} is the rate of change of the internal energy. The energy associated with the vapor mixtures entering and leaving the ullage volume can be expressed as follows:

$$\begin{aligned} \sum \dot{m}_i h_i = & \dot{m}_v c_{p_v} T_v + \dot{m}_{ev} c_{p_f} T_f + \dot{m}_{og} c_{p_{og}} T_f \\ & - \dot{m}_{cond} (c_{p_f} T - \Delta h_f) \end{aligned} \quad (12)$$

where $\dot{m}_v c_{p_v} T_v$ denotes the enthalpy flux due to venting. When the gas mixture is venting from the tank into the atmosphere, c_{p_v} , T_v , and \dot{m}_v are equal to the respective fuel/air mixture properties inside the ullage. In the case when air is entering the tank, $\dot{m}_v = \dot{m}_a$, $c_{p_v} = c_{p_a}$ and T_v is determined based on the local recovery air temperature associated with the supersonic flow of the aircraft. $\dot{m}_{ev} c_{p_f} T_f$ and $\dot{m}_{og} c_{p_{og}} T_f$ denote the enthalpy flux due to fuel vapor and off-gassing from the liquid fuel. The temperature of these gases are at the liquid fuel temperature T_f . The enthalpy loss due to vapor condensation in the ullage is denoted by $\dot{m}_{cond} (c_{p_f} T - \Delta h_f)$ where Δh_f is the latent heat of

vaporization of liquid fuels. The heat transfer to the ullage volume is

$$\dot{Q} = \sum_{j=1}^n h_j A_j (T_j - T) \quad (13)$$

where h_j is the heat transfer coefficient, the A_j is the exposed area of ullage interior surfaces and the T_j is the temperature of various tank surfaces. The enthalpy flux due to heat transfer is calculated by summing the contribution from each surface, including the liquid surface.

\dot{W} is negligible compared with \dot{Q} and $\sum h_i \dot{m}_i$ and is assumed equal to zero. Substituting equations (12) and (13) into equation (11), we obtain

$$\begin{aligned} \dot{e} = & \dot{m}_v c_{p_v} T_v + \dot{m}_{ev} c_{p_f} T_f + \dot{m}_{og} c_{p_{og}} T_f \\ & - \dot{m}_{cond} (c_{p_f} T - \Delta h_f) + \sum_{j=1}^n h_j A_j (T_j - T) \end{aligned} \quad (14)$$

Evaporation Rate (\dot{m}_{ev})

The rate of vapor evaporated from the liquid fuel to the ullage volume is directly proportional to the difference of the vapor pressure of the liquid fuel p_f^* and the partial fuel vapor pressure of the gas mixture in the ullage p_f . The mass transfer rate due to evaporation (Ref. 4) is thus

$$\dot{m}_{ev} \approx p_f^* - p_f = A k_g (p_f^* - p_f) M_f \quad (15)$$

A is the exposed liquid surface area. The mass transfer coefficient k_g (Ref. 4) is expressed as

$$k_g = \frac{D_v P}{RT \bar{p}_a \delta} \quad (16)$$

where D_v is the molecular diffusivity and δ is the characteristic transfer length. \bar{p}_a is the logarithmic mean partial pressure and is defined as

$$\bar{p}_a = \frac{p_f - p^*}{\ln(p_f/p^*)} \quad (17)$$

Equation (15) describes the rate of evaporation of the liquid fuel including the effect of vent air "blowing" over the liquid surface. This is accounted for by varying the characteristic transfer length δ which decreases with increasing velocity over the surface.

Off-gassing of Dissolved Air in Liquid Fuel (\dot{m}_{og})

Evolution of air (oxygen) into the ullage volume is described by Henry's Law relation, i.e., the mass of gas dissolved by a given volume of solvent, at a particular temperature, is proportional to the pressure of the gas in equilibrium with the solution. Likewise it may be derived that the rate of solution or evolution is related to the rate of change of pressure of the gas above the liquid. Mathematically this may be expressed as (Ref. 5).

$$\dot{m}_{og} = -K (m_d - m_e) \quad (18)$$

where \dot{m}_{og} represents the rate of gas evolution and or solution; K is an experimentally defined coefficient dependent on fuel tank geometry, vibration level, and fuel type and temperature. m_d is the current mass of gas dissolved in liquid fuel. m_e is the equilibrium concentration of solute gas in the liquid that would exist at that instant during the flight profile.

The quantities m_d and m_e bear further discussion. The solubility of gases in liquids is generally expressed in terms of the Bunsen coefficient (β) which is the volume of gas, at 0°C and one atmosphere pressure, dissolved in a unit volume of solvent (fuel) at a gas partial pressure of one atmosphere and at a particular temperature. The mass of gas dissolved in a liquid at one atmosphere partial pressure as represented by the Bunsen coefficient is then

$$\frac{\beta M}{0.797 \times 453} V_{li}$$

where the quantity .797 represents the volume (ft³) occupied by one mole of gas at these conditions, M is the molecular weight of the dissolved gas, and V_{li} is the total volume of liquid and 453 represents a conversion of units.

The initial mass of air m_{di} prior to aircraft ascent, dissolved in the liquid is then by Henry's law

$$m_{di} = \frac{\beta M}{0.797 \times 453} \left(\frac{p_{ai}}{14.7} \right) V_{li} \quad (19)$$

where $p_{ai}/14.7$ is the initial air partial pressure in atmospheres.

The equilibrium dissolved gas concentration that could exist at any time during the flight is then

$$m_l = \frac{\beta M}{0.797 \times 453} \left(\frac{p_a(t)}{14.7} \right) V_{li} \quad (20)$$

m_d , the current mass of gas dissolved in the liquid fuel, is the initial mass of air, m_{di} , minus the total off-gassing $\int_{t'=0}^t \dot{m}_{og} dt' = m_{og}$ and the

amount of the dissolved air removed due to fuel withdrawal $\int_{t'}^t \frac{m_d}{m_l} \dot{m}_l dt'$.

thus m_d can be expressed as

$$m_d = m_{di} - m_{og} - \int_{t'=0}^t \frac{m_d}{m_l} \dot{m}_l dt' \quad (21)$$

Substitute equation (20) and (21) into equation (18), the following equation describing the rate of air off-gassing is obtained.

$$\dot{m}_{og} = -K \left[\frac{\beta M}{0.797 \times 453} \left(\frac{p_{ai}}{14.7} \right) V_{li} - m_{og} - \int_{t'=0}^t \frac{m_d}{m_l} \dot{m}_l dt' \right. \\ \left. - \frac{\beta M}{0.797 \times 453} \frac{p_a(t)}{14.7} V_{li} \right] \quad (22)$$

Solution of equation (20) gives the rate of air off-gassing \dot{m}_{og} .

When gases dissolve from a mixture, such as air, instead of from a pure gas, the solubility of each component is proportional to its own partial pressure; in other words, Henry's Law applies to each gas independently of the others present in the mixture. In fact in aircraft fuels oxygen is more soluble than nitrogen. As the current program model treats only two species, air and fuel, differences in relative out-gassing of oxygen and nitrogen are lumped as one specie in terms of air.

Condensation (\dot{m}_{cond}) and Misting (\dot{m}_{mist})

Condensation of fuel vapors within the ullage into the liquid surface can occur because of two reasons: (1) venting and velocity effects may blow or congregate fuel vapors to a particular point where they exist at a concentration higher than that corresponding to the vapor pressure and (2) when the liquid fuel has a temperature lower than the saturation temperature, the fuel vapor condenses on the liquid surface. In the program under discussion (The Well Stirred Model) concentration gradients within the tank is negligible. Condensation may occur if the fuel is initially at an elevated temperature corresponding to a very high vapor pressure and due to flight phenomena the temperature of the liquid decreases rapidly. A condition may still exist where vapors are higher than that of the current vapor pressure corresponding to the liquid temperature. In this case condensation will also occur. The current model has provisions for the inclusion of condensation phenomena but as yet no relations describing at which it occurs are included.

Misting or the existence of two-phase mixture within the fuel tank ullage may occur because of two processes: The first is that a rapid ascent of the aircraft results in an expansion of the ullage gases thereby rapidly lowering the temperature. If the temperature is lowered to the dew point of the fuel vapors, two phase mixture will occur. The second method is by a mechanical injection of liquid particles into the ullage space, due to waves generated by vibration and sloshing characteristics associated with fuel tanks during normal flight environments. It is known that the formation of mist can significantly extend lean flammability limit but very little is known about the rate or quantity of mists that can exist within the fuel tank environment. The Well Stirred Computer Model has provision to describe the formation of misting but no specific relations have been developed to describe mass flux induced by misting in the ullage.

Governing Equations

\dot{m}_a can be eliminated using equation (10). Equation (8) thus takes the following form

$$\frac{z\dot{m}}{m} + \dot{z} - \frac{z_v}{m} \dot{m}_v = \frac{\dot{m}_{og} z_{og}}{m} \quad (23)$$

Using equation (14) to eliminate \dot{e} , equation (7) can be expressed as

$$\begin{aligned} \frac{\dot{m}}{m} + \frac{\bar{\gamma}\dot{z}}{\bar{c}_p} \left[(c_{p_a} - c_{p_f}) + R + \left(\frac{1}{M_f} + \frac{1}{M_a} \right) \right] - \frac{T}{T} \\ - \frac{\dot{m}_v c_{pv} T_v}{m \bar{c}_p T} \bar{\gamma} = \frac{\bar{\gamma}}{m \bar{c}_p T} \left[\dot{m}_{ev} c_{p_f} T_f + \dot{m}_{og} c_{p_{og}} T_f - \dot{m}_{cond} (c_{p_f} T - \Delta h_f) \right. \\ \left. + \sum_{j=1}^n h_j A_j (T_j - T) \right] \end{aligned} \quad (24)$$

where $\frac{m \bar{c}_p T}{\bar{\gamma}}$ has been substituted for the internal energy e . Reiterating equations (6) and (9)

$$\frac{\dot{m}}{m} + \frac{\dot{T}}{T} + \bar{M} \dot{z} \left(\frac{1}{M_a} - \frac{1}{M_f} \right) = \frac{\dot{P}}{P} + \frac{\dot{V}}{V} \quad (6)$$

$$\dot{m} - \dot{m}_v = \dot{m}_{ev} + \dot{m}_{og} - \dot{m}_{cond} \quad (9)$$

the governing equations, (23) and (24), equations (6) and (9) have been numerically integrated to solve the four following quantities: m , T , z , and m_v . Equations (18) and (22) are used to describe \dot{m}_{ev} and \dot{m}_{og} . The calculations performed to date, \dot{m}_{mist} and \dot{m}_{cond} are assumed negligible. The Well-Stirred Computer Program is capable of evaluating the effect of misting and condensation, once the appropriate expressions describing these phenomena are developed.

2. SAMPLE RESULTS FROM WELL-STIRRED COMPUTER PROGRAM.

A series of computer runs was made using the Well-Stirred Computer Program to demonstrate the effects of the various important phenomena that are described in the model formation. The tank configuration shown in Figure 14 was used for these sample cases. The tank dimensions were 15'x5'x2' with a total fuel capacity of approximately 1100 gallons. The tank was filled initially with Jet A fuel to 80% of its capacity (i.e., the depth of the fuel was 1.6 ft.)

The flight profile of the sample case consisted of a 20 minute ascent portion at 2000 ft/min ascent rate to 40,000 ft altitude, a 60 minute level flight at 40,000 ft altitude; a 40 minute descent portion at 1000 ft/min, descent rate. Figure 14 shows the altitude history of the sample case flight profile. The cruising speed at the level flight corresponded to 0.9 Mach number. The aircraft was assumed to accelerate linearly from zero velocity to 0.9 Mach number during the 20 minute ascent portion and decelerate linearly from Mach 0.9 to zero velocity during the 40 minute descent portion. The top and side walls of the tank were initially at 110°F. The sample calculation demonstrated the effects of different initial fuel temperatures (50°F and 110°F); fuel withdrawal rate (zero fuel withdrawal versus seven gallons/minute)

Figure 15 shows the fuel/air ratio variations throughout the complete flight profile for constant fuel temperature at 110°F and 50°F respectively without fuel withdrawal and without air outgassing. The solid lines are equilibrium fuel/air ratios, i.e., the fuel partial pressure corresponding to the vapor pressure at the liquid fuel temperature. The dotted curves show the calculated fuel/air ratios. It is seen that the calculated fuel/air ratios are significantly lower than that corresponding to the equilibrium fuel/air ratios. Even at the end of the one hour level flight, the calculated fuel/air ratios in the ullage volume approach to only approximately 80% of the equilibrium fuel/air ratios (see Fig. 15). This "lag phenomena" is a result of the low volatility of Jet A fuels. The rate of evaporation of liquid Jet A fuels is very slow in that it takes hours for the ullage mixture to reach equilibrium vapor concentrations (the solid line in Fig. 15) after a normal ascent. It is anticipated that this lag phenomena would be much less pronounced for high volatile fuels such as JP-4. During the descent portion of the flight profile, Figure 15 shows that the calculated F/A ratios follow closely to that of the equilibrium fuel/air concentrations.

Figure 16 shows the effect of fuel withdrawal at 7 gal/min (curve 3) and fuel withdrawal with air offgassing (curve 4). The liquid fuel temperature is at 110°F. Also shown on the figure are the equilibrium fuel/air ratios (curve 1) and calculated fuel/air ratios without fuel withdrawal and air offgassing for comparison. Fuel withdrawal is found to play a significant role in the ullage fuel/air ratios. The results show that as fuel is withdrawn from tank to simulate engine fuel consumption, the increased ullage volume is mostly filled with air vented into the tank. This greatly reduces the fuel/air ratios in the ullage. Figure 16 shows that the effect of fuel withdrawal is more important during level flight. For fuel withdrawal rate of 7 gal/min, the calculated fuel/air ratios in the ullage, after one hour level flight, is only about 50% of that without fuel withdrawal (compare curves 3 and 2). Fig. 16 The effect of fuel withdrawal also significantly lowers the ullage fuel/air

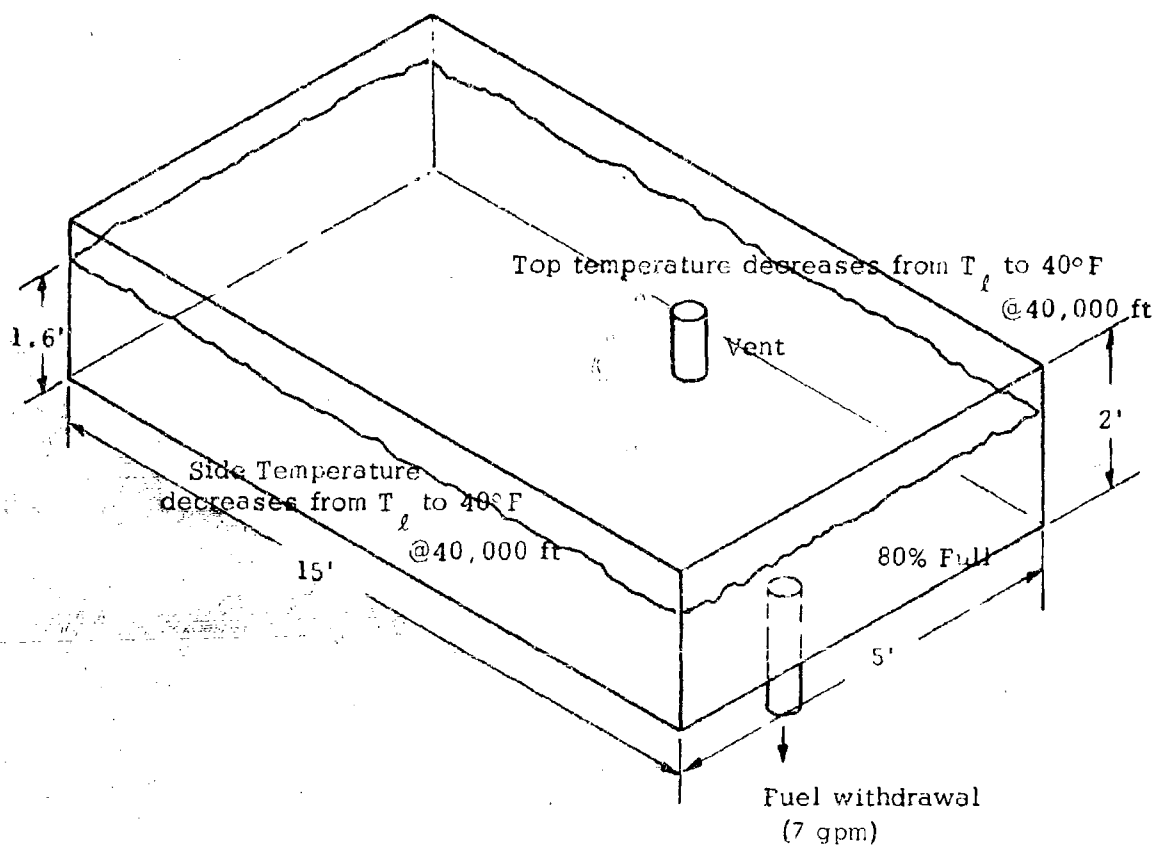
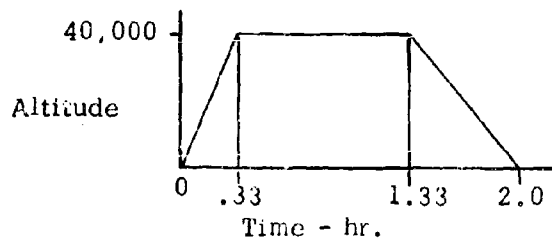
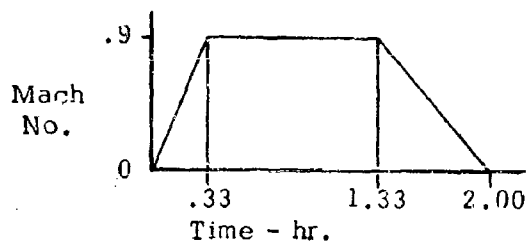


Figure 14. Fuel Tank and Flight Profiles Used for Sample Results.

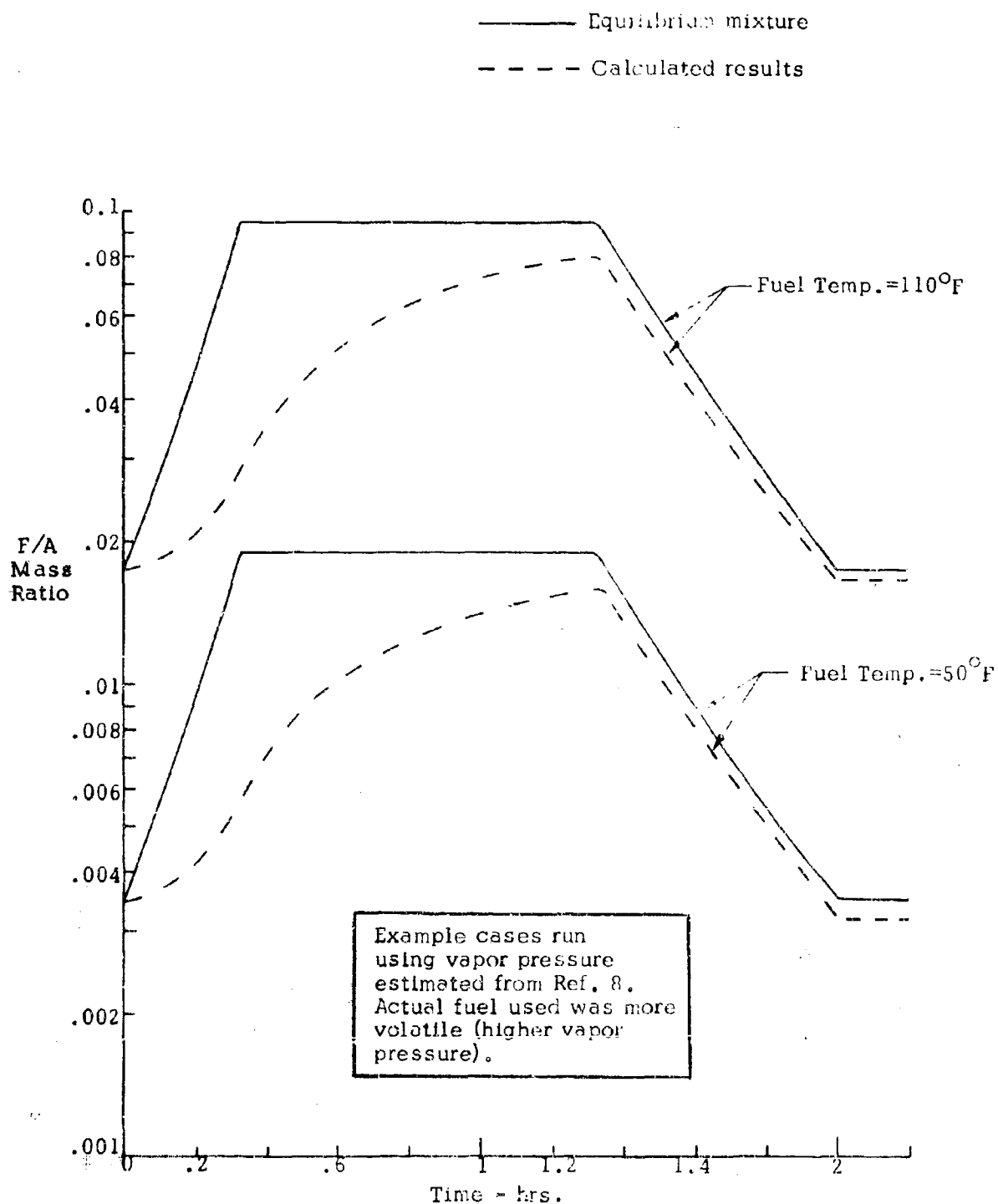


Figure 15. Variation of Fuel/Air Ratios During Ascent, Level, and Descent Flights for Jet A Fuel.

1. Equilibrium mixture
2. Calculated results without fuel withdrawal and offgassing
3. Calculated results including fuel withdrawal
4. Calculated results including fuel withdrawal and offgassing

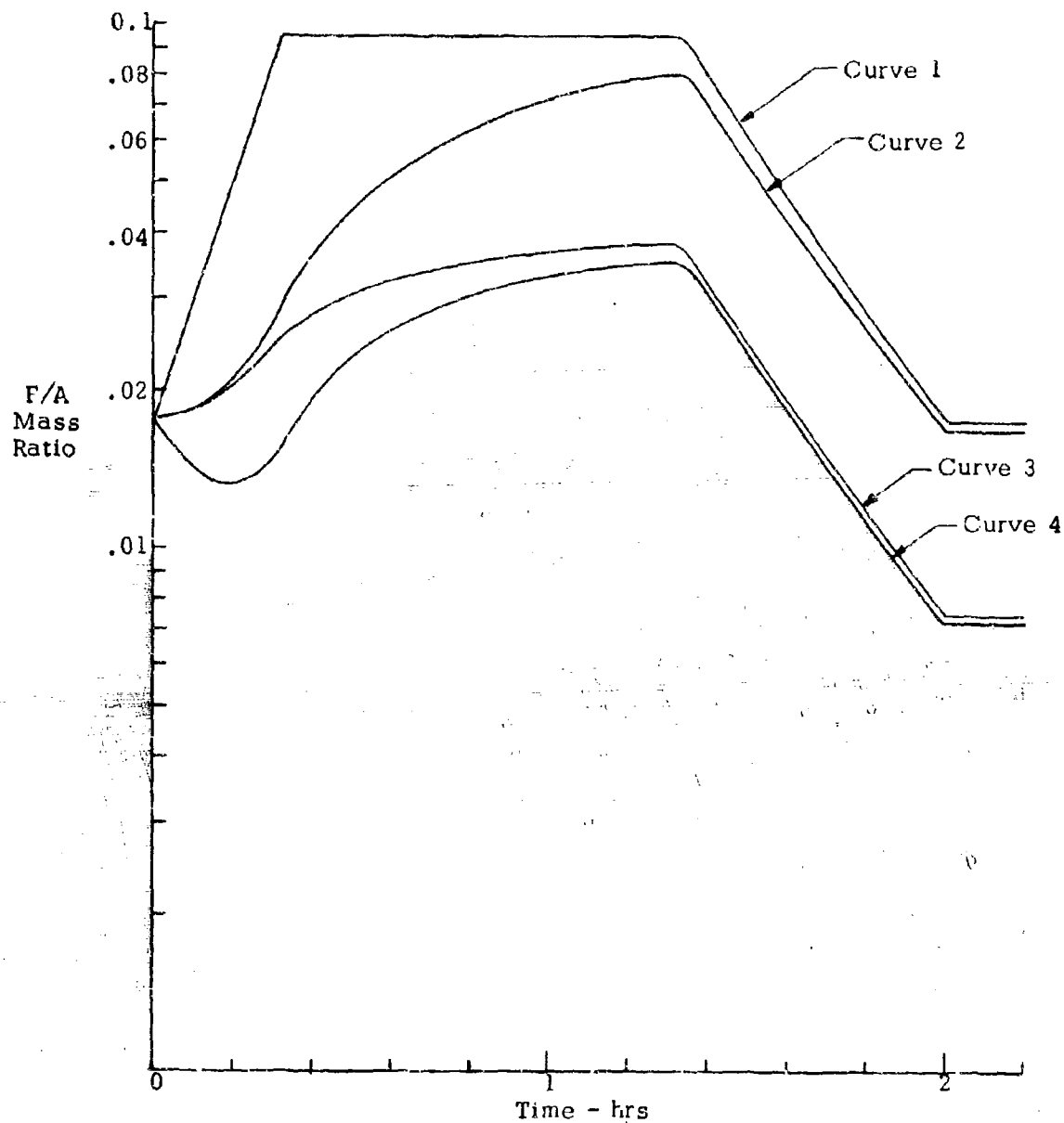


Figure 16. Variation of Fuel/Air Ratios for Jet A Fuel at 110°F.

ratios during the descent portion of the flight profile.

Curve 4 shows the fuel/air ratio variations within the ullage taking into account the effect of fuel withdrawal and offgassing of dissolved air in the liquid fuel. The effect of air offgassing is primarily noted during the ascent. This is to be expected since offgassing only occurs when there is a decrease in the ullage air partial pressure.

These sample runs were selected to demonstrate the effects of some of the important parameters discussed in the model. The results are applicable to wing tanks of an airplane flying under prescribed flight profiles. The results demonstrated the existence of lag phenomena due to slow fuel evaporation. Also demonstrated was the effect of increase in ullage volume due to fuel withdrawal and the effect of air addition into the ullage due to the evolution of dissolved air within the fuel. The values selected for the parameter which control each of these transport rate processes are the best available at the present time and the computer program can be used to predict the existence of combustible mixtures within aircraft fuel tanks.

3. DISTRIBUTED F/A MODEL.

During cruise at constant altitude, significant fuel air gradients can occur within the ullage volume. This is particularly true for certain tank configurations where the ratio of ullage volume to exposed liquid surface area is large. A separate model was developed to describe situations where concentration gradients in the ullage volume are significant.

Basic Equation

Consider the ullage volume V consisting of two gas species, fuel vapor and air. Define ρ as the density of the gas mixture and ρ_f and ρ_a as the densities of fuel vapor and air in the ullage volume. Thus

$$\rho_f + \rho_a = \rho \quad (25)$$

Define $C_f = \rho_f/\rho$ and $C_a = \rho_a/\rho$, thus

$$C_f + C_a = 1 \quad (26)$$

In terms of the notations used in the well-stirred model, $m_a = \rho_a V$, $m_f = \rho_f V$, and $m = \rho V$. The continuity equation, expressed in terms of C_f is

$$\rho \frac{\partial C_f}{\partial t} + \rho \bar{q} \cdot \nabla C_f = -(\rho D \nabla^2 C_f) \quad (27)$$

where D denotes the binary diffusion coefficient of fuel vapor and air and \bar{q} denotes the convective velocity within the ullage. \bar{q} is mainly introduced through air venting into the tank because liquid fuel is constantly being

withdrawn from the tank for engine consumption. \bar{q} is thus normally small and the pressure P of the gas mixture is assumed to be uniform. Thus P is a function of time t only: $P = P(t)$. Similarly, the temperature of the gas mixture T is also assumed to be a function of time t only: $T = T(t)$. Based on the equation of state, the gas density ρ is also a function of time t only, $\rho = \rho(t)$. Equation (27) can thus be simplified:

$$\frac{\partial C_f}{\partial t} + \bar{q} \cdot C_f = D \nabla^2 C_f \quad (28)$$

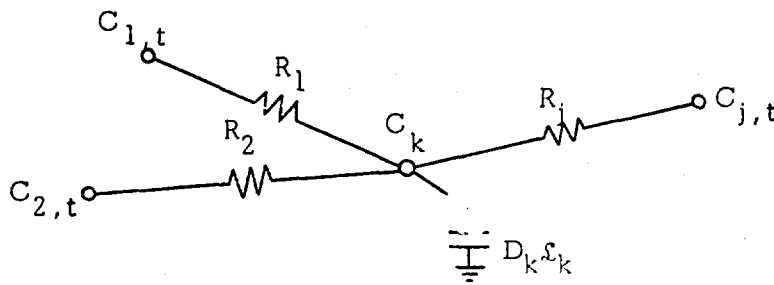
Equation (28) is numerically integrated for a prescribed pressure and temperature history $P(t)$ and $T(t)$, and a prescribed velocity flow field \bar{q} based on tank configuration and air venting into the tank.

Method of Solution for Equation (28)

The Thermal Analyzer Program (Ref. 6) has been previously developed to compute transient temperature distribution in configurations of arbitrary complexity. This program was modified to include the effect of convective flow \bar{q} and was used to solve equation (28) to determine fuel/air concentration gradients within the ullage. This program solves equations in finite difference form by means of a resistance-capacitance electrical analog finite difference method. The comparable variables in the mass transfer and electrical current flow systems may be noted as follows:

<u>MASS FLOW</u>	<u>ELECTRICAL</u>
Mass Concentration	Voltage
Mass Flux	Current
Resistance to Mass Flow $\approx 1/D$	Resistance
Characteristic Volume of Mass	Capacity

At a given node point k ,



the solution is obtained by applying Kirchhoff's Law at a point, or

$$\sum_j \frac{C_{j,t} - C_{k,t}}{R_j} = f_k \frac{dC_k}{dt} \quad (29)$$

where

- $C_{j,t}$ = Concentration at time t of any arbitrary node j connected to node k by a resistor R_j
- R_j = Resistor connecting nodes j and k , coupling diffusion & conv.
- $C_{k,t}$ = Concentration of node k at time t
- $C_{k,t+\Delta t}$ = Concentration of node k after time increment Δt
- f_k = Capacity of node k

By making the assumption that the surrounding concentration, C_j , remains constant over a time interval Δt , it is possible to integrate equation (29) directly. However, as a result of a comparison study, it was found that better results were obtained by using the equation which results from assuming

$$\frac{dC_k}{dt} \approx \frac{C_{k,t+\Delta t} - C_{k,t}}{\Delta t} \quad (30)$$

and solving for $C_{k,t+\Delta t}$ directly than by using the integrated equation. This comparison was made by running the same problem using both equations and varying the computing interval Δt . It was found that the linear equation, i.e., that obtained by using equation (30) was far less sensitive to Δt , and that the results obtained using the integrated equation approached the linear results as $\Delta t \rightarrow 0$. Although the integrated equation is "exact," it is suspected that the linear approximation, which "leads" the exact solution tends to anticipate the results. As a result, the equation used by the computer to solve the mass balance at a node was derived by combining equations (29) and (30) to obtain

$$C_{k,t+\Delta t} = \frac{\Delta t}{f_k} \left[\sum_j \frac{C_{j,t} - C_{k,t}}{R_j} \right] + C_{k,t} \quad (31)$$

If the value of capacity f_k is zero, e.g., in a steady state problem, $C_{k,t}$ in Equation (29) is replaced by $C_{k,t+\Delta t}$ to give

$$C_{k,t+\Delta t} = \frac{\sum_j \frac{C_{j,t}}{R_j}}{\sum_j \frac{1}{R_j}} \quad (32)$$

If no capacitor is attached to node k , i.e., R_k unspecified, mass balance is computed at node k and C_k remains unchanged.

It is to be noted that the new concentration at a node is based upon the concentration at the previous time point. To make the new concentration independent of the order in which they are computed, each node is provided with two concentration storages, one for the "old" concentration, $C_{k,t}$, and one for the "new" concentration, $C_{k,t+\Delta t}$. At the beginning of each cycle, the values in the two storages are identical. During the mass balance, the concentrations in the "C at t" block are used to compute new values which go into the "C at (t+Δt)" block, the old concentration values remaining unchanged. At the end of the mass balance, the concentrations in the "t" block are set equal to those in the "(t+Δt)" block and the process repeated.

4. SAMPLE RESULTS OF THE DISTRIBUTED F/A MODEL.

Consider a rectangular fuel tank (36"x36"x40") initially filled with liquid fuel to 80% of the tank capacity. As fuel is being withdrawn from the tank, fuel/air gradients appear due to air vented into the tank. Based on the tank configuration, it is seen that fuel/air gradients mainly exist in the direction normal to the liquid fuel surface. Based on this one-dimensional approximation, the distributed F/A model is used to determine the fuel/air gradients normal to the liquid surface. The ullage is initially assumed to consist of a uniform fuel/air mixture. The liquid surface is receding at a rate corresponding to the fuel withdrawal rate. The air is assumed to vent uniformly through the top of the tank.

Figure 17 shows the calculated fuel/air concentrations for liquid JP4 at 46°F, with fuel withdrawal rate maintained at 1/2 gal/min. The curves are presented in terms of fuel/air ratios as a function of distance from the top of the tank. At time $t=0$, the ullage mixture has a uniform concentration as shown by the horizontal curve. Once air is vented into the tank due to fuel withdrawal, significant fuel/air gradients appear as shown by curves at time $t=0.5$ hr, $t=1.0$ hr, and $t=1.5$ hr. Based on the calculations, it is seen that for liquid JP4 at 46°F the gas mixture in the entire ullage is within flammability limits.

Under separate Army support (Ref. 1) an experimental program was carried out to determine fuel/air concentrations of the ullage volume based on gas chromatograph measurements. The experimental data are also presented in Figure 17 for comparison. The calculated fuel/air ratios using distributed

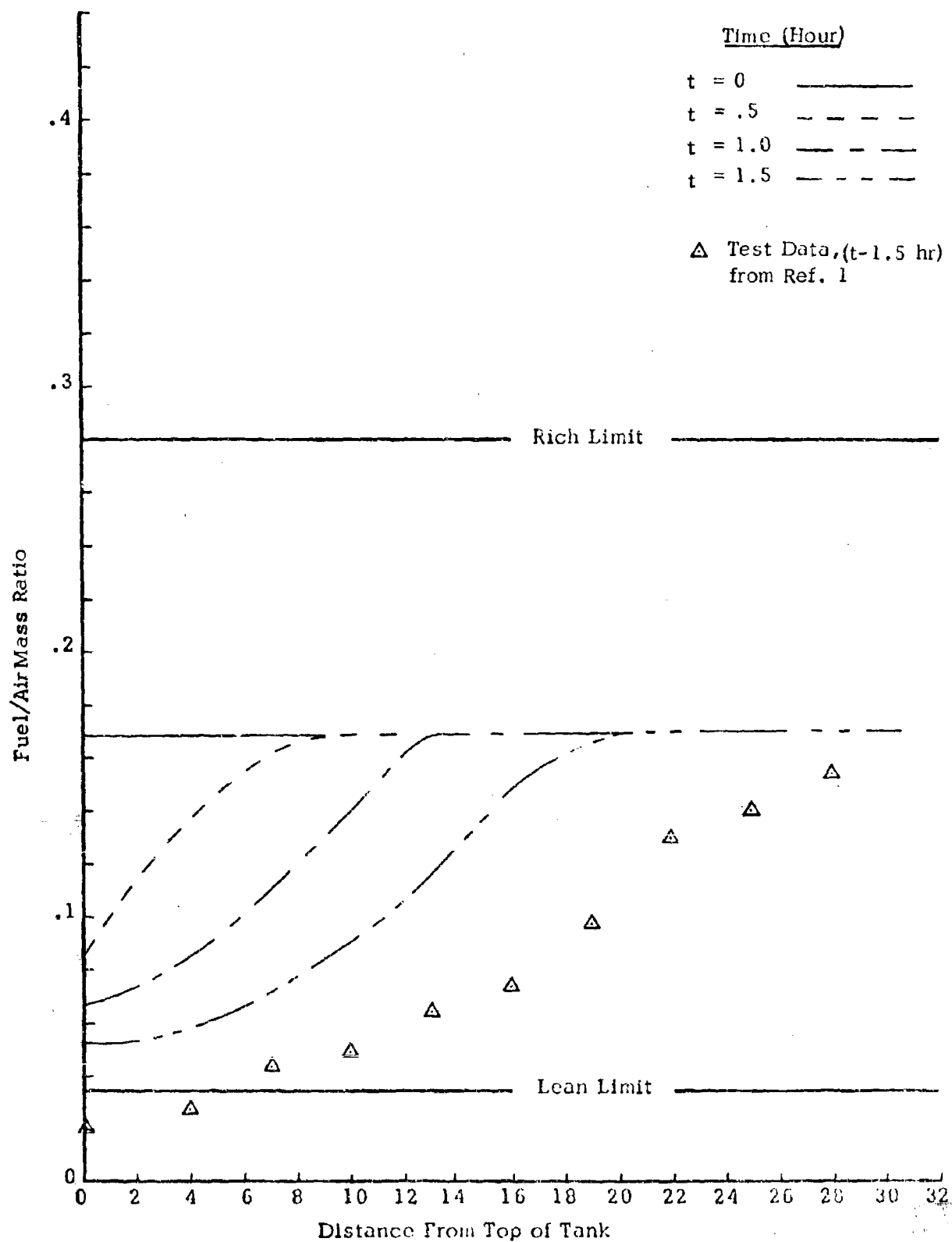


Figure 17. Diffusion/Convection Program Results for JP-4 at 46°F

F/A model show good agreement with experimental measurements. (compare curve for $t=1.5$ with experimental curve).

Similar results are also presented in Figures 18 and 19 for liquid JP4 at 60°F and 107°F. It is noteworthy that if the ullage were assumed to have uniform fuel/air mixtures, with fuel vapor concentrations corresponding to the vapor pressure of the liquid fuel, the vapor mixture in the entire ullage will be too fuel-rich to be combustible for liquid JP4 at 107°F. Based on the calculated results as shown in Figure 19, it is seen that because of the presence of fuel/air gradient, a significant portion of the ullage near the top of the tank contains combustible mixture even for liquid JP4 at 107°F. This observation is also verified by the experimental measurements as shown in Figure 19.

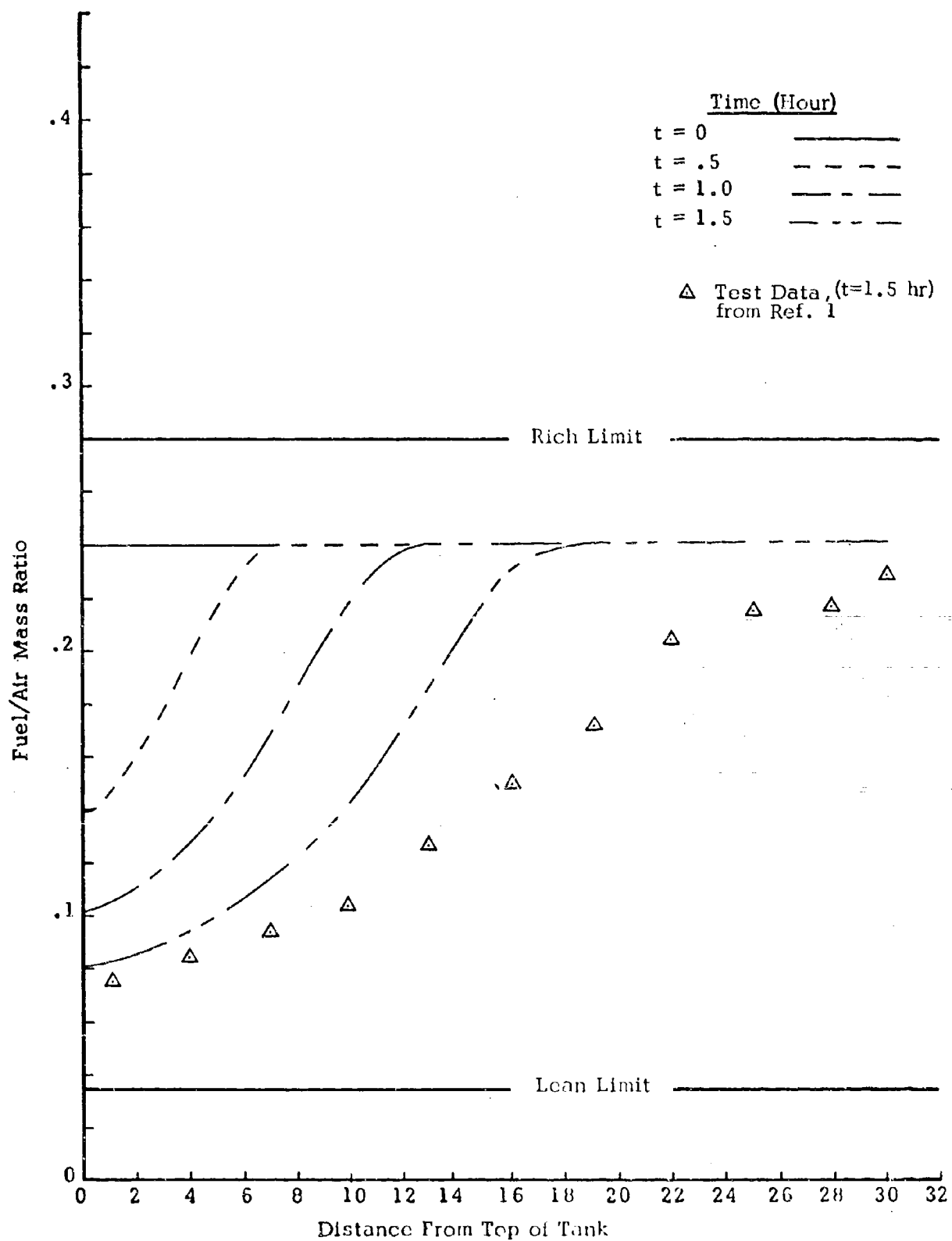


Figure 18. Diffusion/Convection Program Results for JP-4
at 60° F

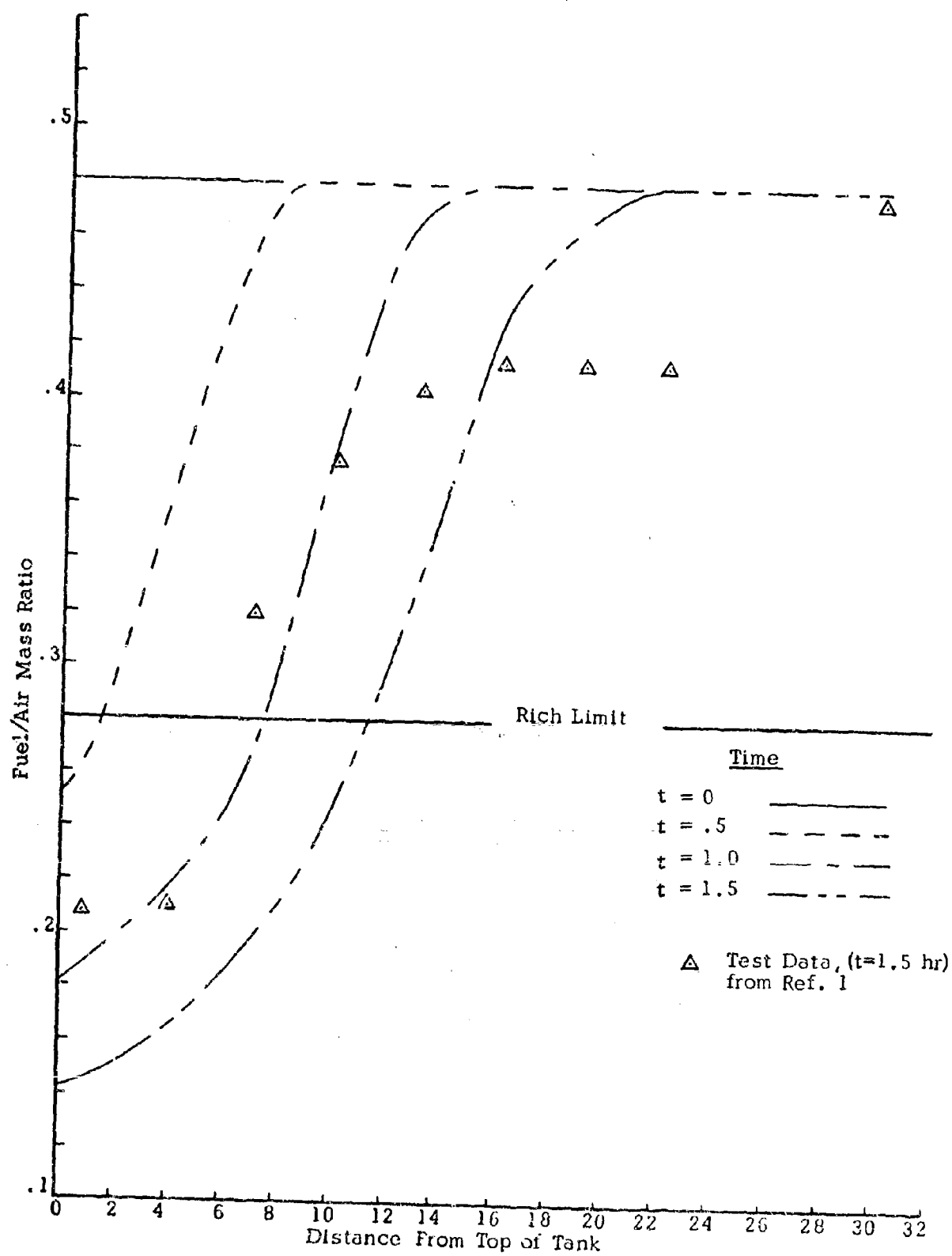


Figure 19. Diffusion/Convection Program Results for JP-4 at 107°F

SECTION V

EXPERIMENTAL RESULTS AND DISCUSSION

1. FUEL/AIR COMPOSITION MEASUREMENTS

Using the equipment and procedures outlined in Section II, a series of flight simulation tests were run to determine fuel/air composition maps as a function of flight profile. The importance of various transport phenomena such as the evaporation rate, evaporative lag, and air outgassing was also investigated. The flight simulations were constructed by dividing a flight profile into its three portions: ascent, level flight, and descent. For ascent and descent the flight variables varied between tests were fuel type (JP4 or Jet A), rate of pressure change (ascent/descent rate), and the existence or nonexistence of vibration. Vibration levels used were approximately 1/4 G at 10 cycles per second. Liquid temperature of 80 and 120, and 180°F were examined. For level flight the test variables were fuel type, altitude, liquid temperature, and the existence or nonexistence of vibration. All level flight profiles were run with the inclusion of fuel withdrawal at a rate of approximately .94 gal/min. A summary of the test variables is presented in Figure 20. Three sample probe locations were used. These are shown schematically in the following figure. (21) Probe 1 was located in the mouth of the inlet air vent. Probe 3 was at the same level as 1 but 6" axially from the vent. Probe 2 was 4" from the top of the tank and 27" axially from Probe 2. All tests were initiated with the tank half-filled (approximately 50 gal of fuel added) and the fuel at the prescribed test temperature. Skin temperatures were left at ambient conditions as was the inlet vent air temperature.

These variables cited above were selected to demonstrate the important phenomena that can occur because of various flight and fuel unloading conditions. Runs were selected where a fuel-rich mixture of JP4 could become combustible due to evaporative lag with high ascent rates. Similarly the Jet A runs were selected so that an initially combustible mixture could become too lean because of the same phenomena. A second purpose of the test series was to determine what flight regimes yield the largest mixture gradients within the ullage of the fuel tank and to determine the parameters which lead to extreme gradient conditions.

Ascent Flight Test Results.

Figure 22 presents the results of the ascent runs made with JP4 fuel. The following conditions were tested: 80°F fuel with no-vibration and 2000 ft/min ascent; 80°F fuel with vibration and 2000 ft/min ascent; and 120°F fuel with vibration and a high ascent rate of 6000 ft/min. The test results are coded to the particular test by individual symbols. The numbers associated with the data points refer to the probe location at which the sample was taken. Also plotted on the figure are equilibrium fuel/air ratios. These correspond to the case of infinite evaporation rate. By comparing the two runs at 80°F we see that the run with vibration lagged in fuel/air ratio behind the no-vibration run; and that the run without vibration was close to equilibrium at the beginning of ascent and departed near the end of ascent. Also it is noted that gradients within the tank at any particular time appeared to be rather small.

<u>Ascent to 40,000 ft</u>						
<u>Test No.</u>	1	2	3	4	5	6
<u>Fuel</u>						
JP4	X	X	X			
Jet A				X	X	X
<u>Rate ft/min</u>						
2000	X	X		X		X
6000			X		X	
<u>Liquid Temp.</u>						
80	X	X				
120			X	X	X	
180						X
<u>Vibration</u>						
0	X					
.25g@10cps		X	X	X	X	X

<u>Descent</u>					
<u>Test No.</u>	1	2	3	4	5
<u>Fuel</u>					
JP4	X	X			
Jet A			X	X	X
<u>Rate - ft/min</u>					
2000		X	X	X	
8000	X				X
<u>Liquid Temp.</u>					
80	X	X			
120			X	X	X
180					
<u>Vibration</u>					
0	X		X		
.25g@10cps		X		X	X

<u>Level Flight with Fuel Withdrawal</u>					
<u>Test No.</u>	1	2	3	4	5
<u>Fuel</u>					
JP4	X	X			
Jet A			X	X	X
<u>Altitude</u>					
20,000 ft	X	X			
40,000 ft			X	X	X
<u>Liquid Temp.</u>					
80	X	X			X
120			X	X	
<u>Vibration</u>					
0	X		X		
.25g@10cps		X		X	X

Figure 20. Test Matrix For Fuel/Air Measurements.

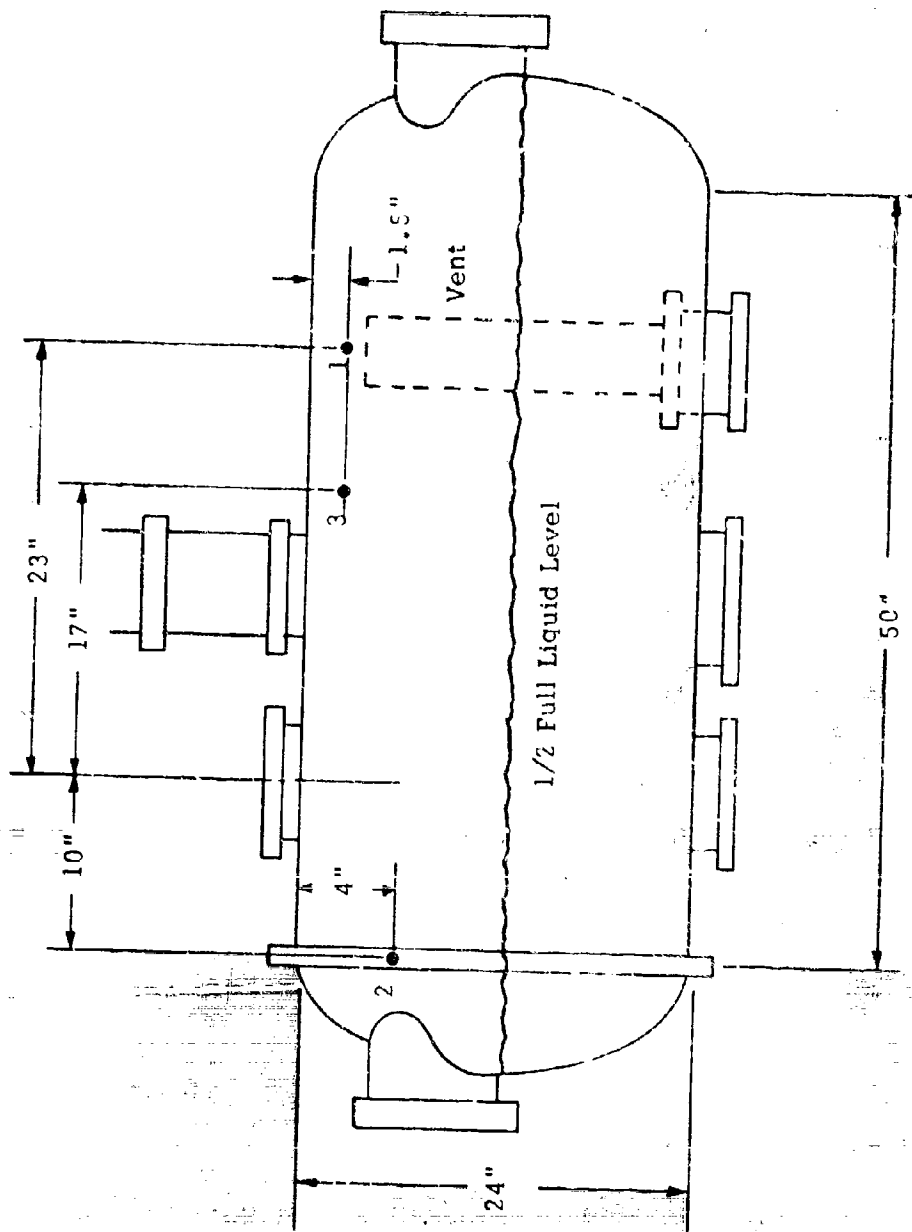


Figure 21. Probe Locations

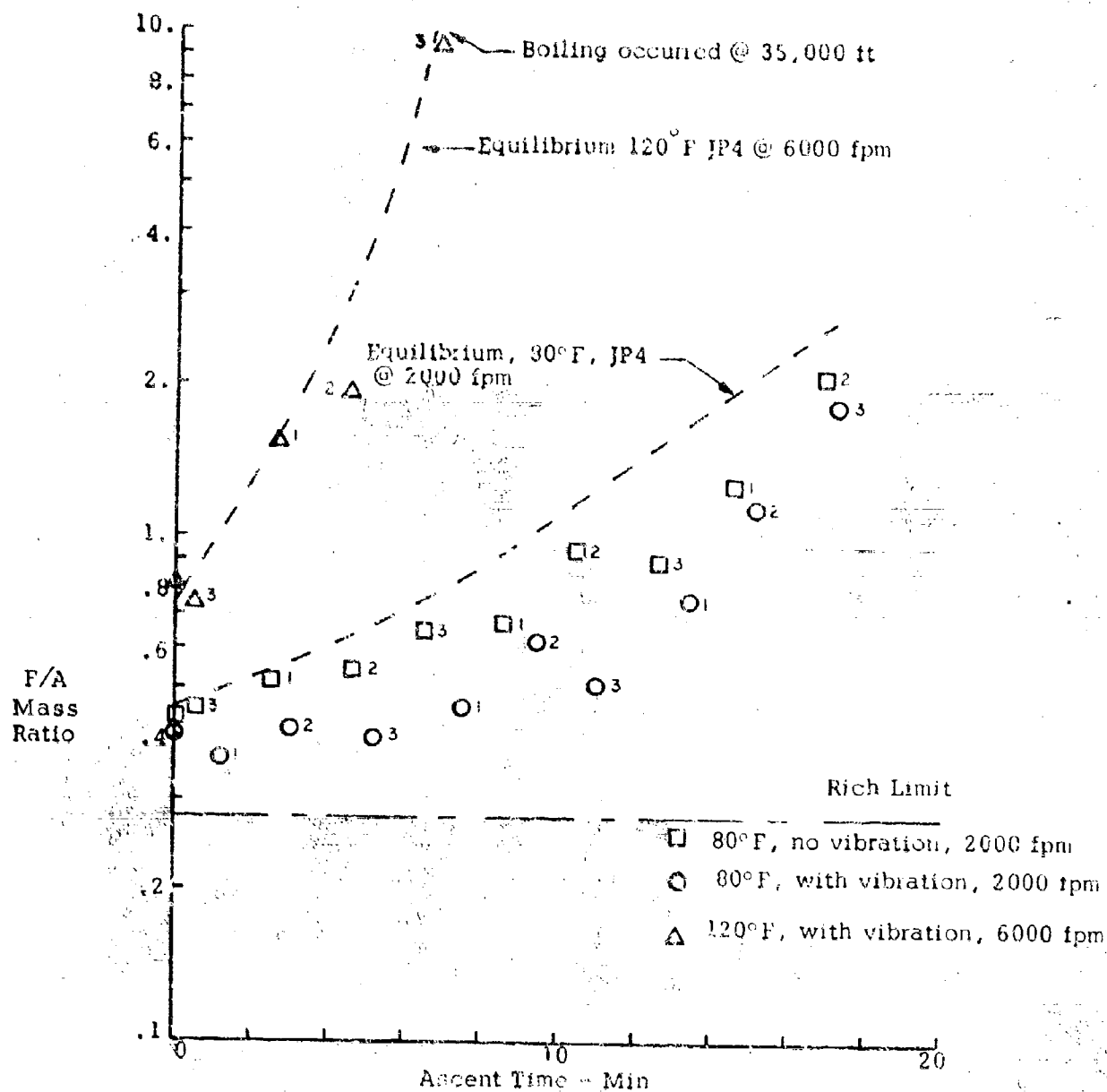


Figure 22. JP4 Ascent Tests to 40,000 ft - 1/2 Full Tank.

The difference in lag phenomena between these two runs may be attributed to a decrease in fuel/air ratio due to air outgassing from the fuel induced by the vibration. At 120°F and 6000 ft/min ascent rate the fuel could remain very close to equilibrium. That is the fuel pressure within the ullage remains close to its vapor pressure. For this run boiling of the fuel occurred at an altitude of 35,000 ft, thereby terminating the run. From these results it can be seen that even with a relatively volatile fuel an evaporative lag may exist at temperatures as high as 80°F. The lag at 80°F, however, was not sufficient to bring this mixture within combustible bounds. Figure 23 presents the test results from an ascent test conducted with Jet A. These tests were conducted at 120°F with vibration at ascent rates of 2000 and 6000 ft/min and 180°F with vibration at ascent rates of 2000 ft/min. Also plotted on these curves are the equilibrium fuel air mixture ratios. It can be seen that Jet A at temperatures of 120 and 180°F and ascent rates of 2000 ft/min nearly approaches the equilibrium vapor pressure. The lag measured is relatively minor. At 120°F with 6000 ft/min ascent rate, however, a lag of approximately 50% of fuel/air mixture was noted. It is seen then that evaporative lag is controlled by the temperature (vapor pressure) of the liquid and the rate of ascent of the fuel tank, with ascent rate appearing to be more important in the range of conditions investigated. It is noted that gradients within the tank at any time appear rather small.

Descent Test Results.

Figure 24 presents the results from descent tests conducted with JP4 fuel. These tests were initiated from an altitude of 40,000 ft with a one-half full fuel tank. The JP4 runs were conducted at 80°F liquid temperature, no vibration, 8000 ft/min descent rate; and 80°F liquid temperature with vibration, and 2000 ft/min descent rate. Also plotted on the curve are the equilibrium fuel/air mixtures. It is noted that the mixture tends to be below that of equilibrium. This is due to a net velocity of air into the vent essentially sweeping the fuel vapors toward the liquid surface. It can be seen from the figure that Probes 1 and 3 closest to the vent showed much lower fuel/air ratios at any particular time, than Probe 2 which is closer to the liquid and further away from the vent. Probe 2 is still some 8" above the liquid and also indicates a fuel/air ratio lower than equilibrium. Thus the fuel vapors are being redistributed by convection due to venting of air into the tank. If a sufficient number of probes were available the total mass of fuel vapors would be nearly the same as before the start of descent except for a small loss due to condensation. It is possible in redistribution of fuel vapors for the vapor pressure at the liquid surface to be exceeded and condensation of fuel vapors into the liquid to occur to some extent. The rather limited number of data points acquired at 8000 ft/min descent rate does not give one a complete picture of what is occurring. Comparison with the results obtained at 2000 ft/min descent rate, however, permits one to deduce that the same processes are occurring.

Figure 25 presents the results from the simulated descent tests conducted with Jet A fuel. These tests were also initiated from an altitude of 40,000 ft with a one-half fuel tank. The Jet A runs were conducted at 120°F liquid temperature, descent rate of 2000 ft/min, with and without vibration and a descent rate of 8000 ft/min with vibration. The data for Jet A also show a departure from equilibrium but not to as great an extent as the JP4 data. While no obvious explanation has been found,

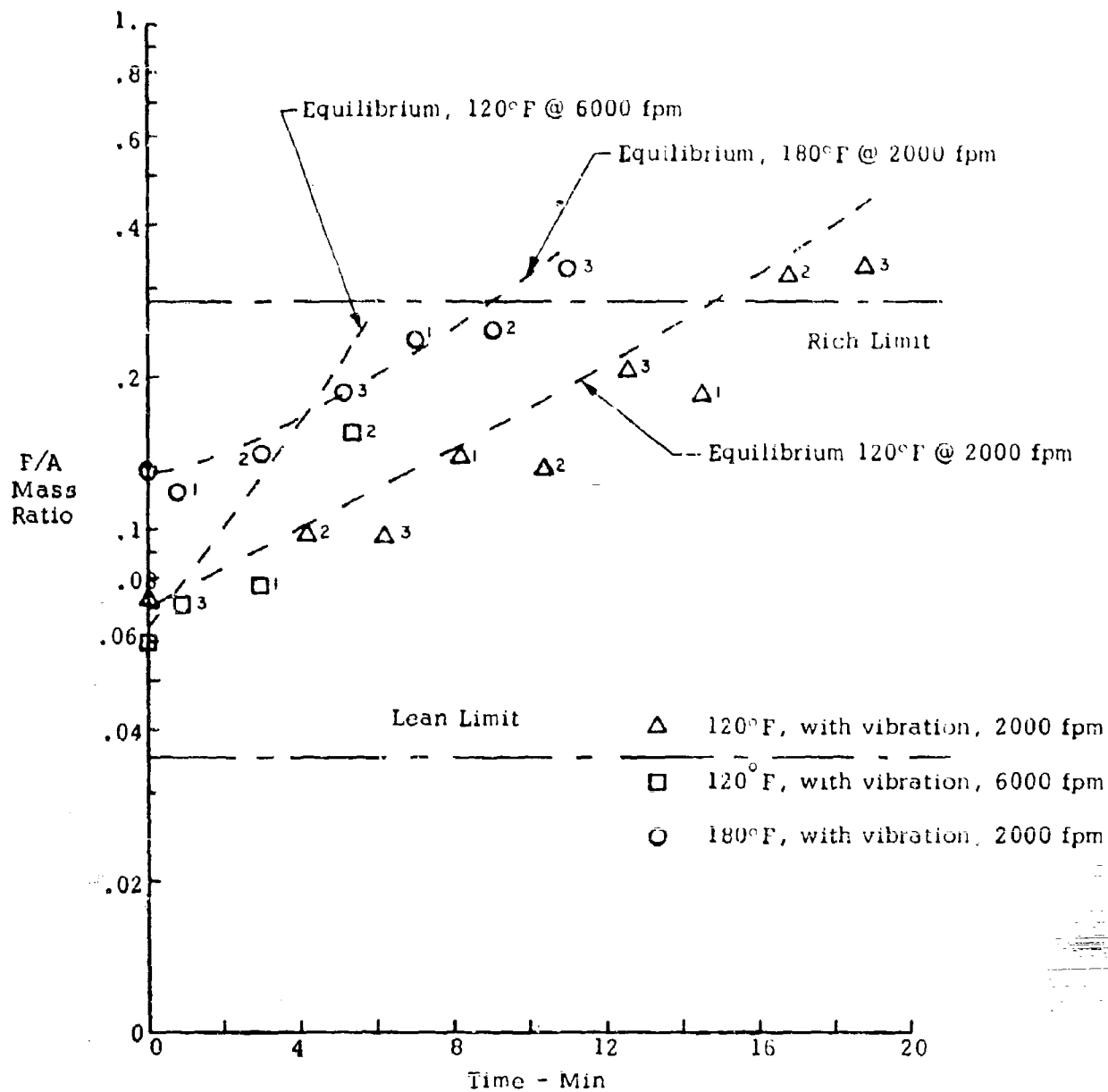


Figure 23. Jet A Ascent Tests to 40,000 ft - 1/2 Full Tank.

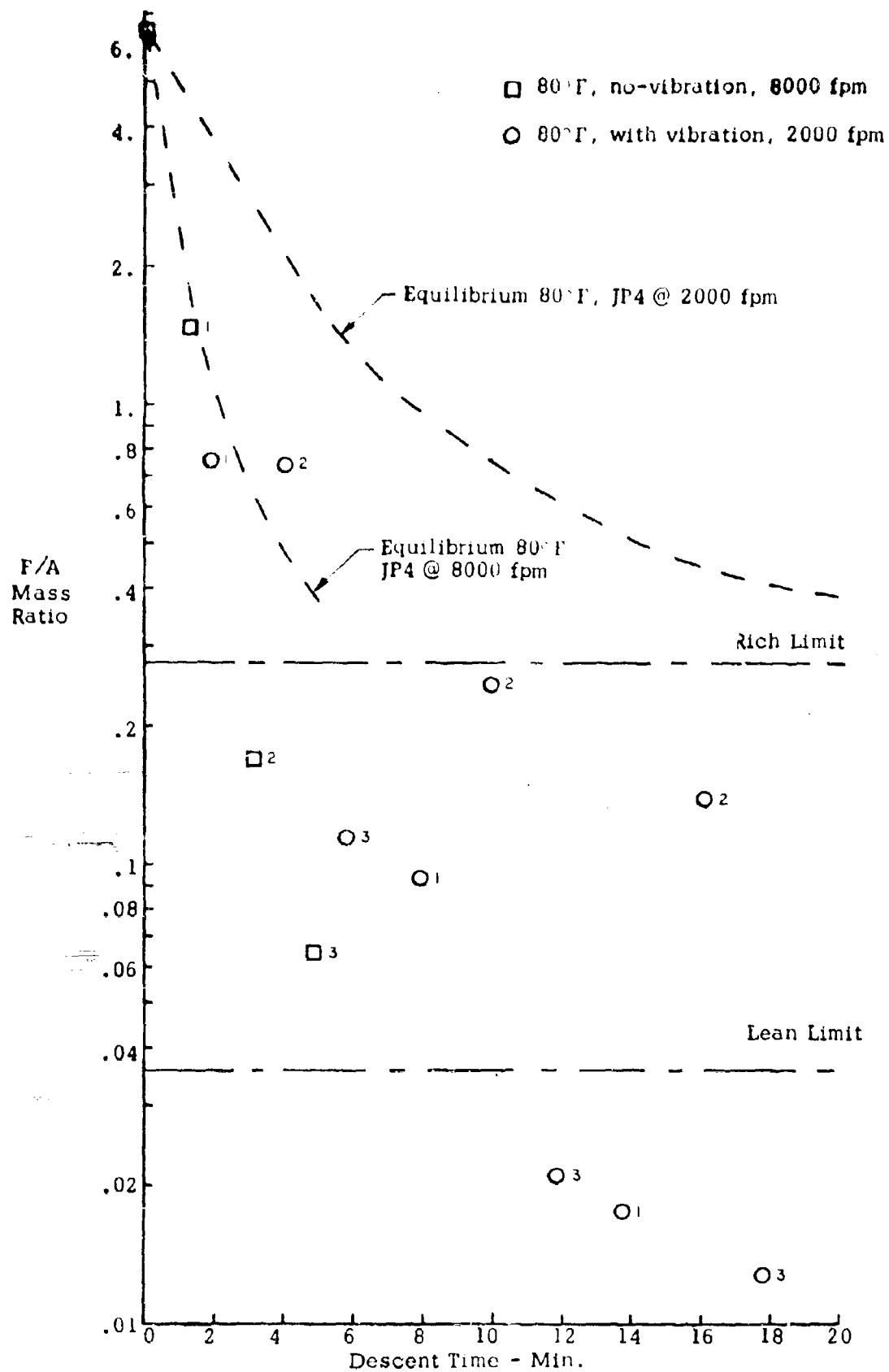


Figure 24. JP4 Descent Tests from 40,000 ft - 1/2 Full Tank.

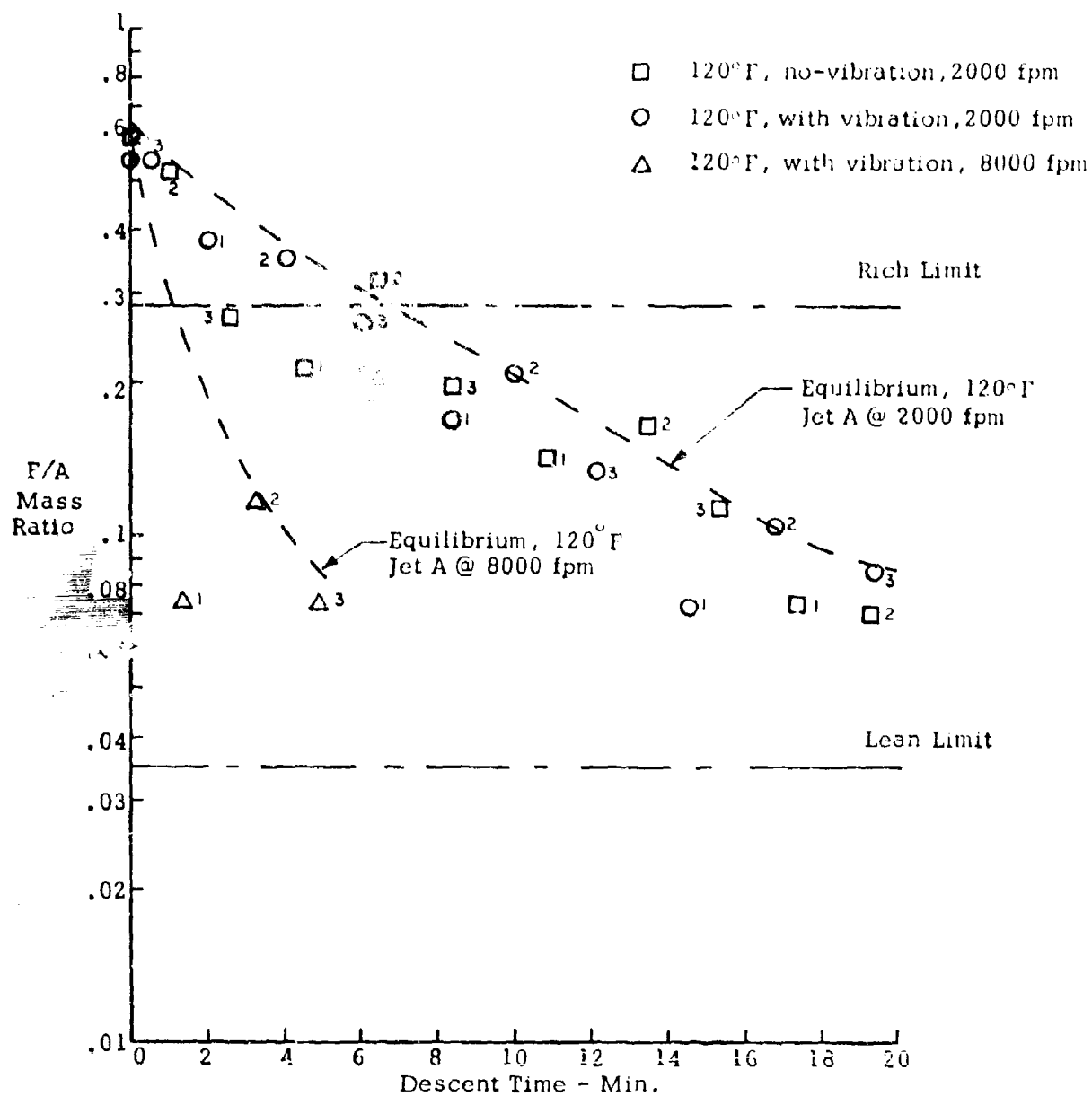


Figure 25. Jet A Descent Runs from 40,000 ft - 1/2 Full Tank.

the ullage in the case of Jet A contains an order of magnitude less vapor than for JP4 even at equilibrium so that the nonequilibrium dilution by air may not be as dramatic for Jet A as it is for JP4. As might be expected, sampling Station 1 at the vent inlet departs more from equilibrium than the others and Station 3 shows a larger departure than Station 2 which is essentially at equilibrium.

Level Flight Test Results

Figure 26 presents the results from the level flight tests of JP4 fuel. These tests were run by rapidly decreasing the pressure to the prescribed altitude, thereby causing a nonequilibrium mixture. At the time the desired altitude was reached very little evaporation had occurred. Fuel withdrawal at .94 gal/min was then initiated for a total of 20 minutes. As the total tank volume is approximately 110 gallons and the tests were run initially with 50 gallons, 20 gallons of fuel withdrawal over this period represents a 1/3 increase in ullage volume at constant pressure. By starting the fuel withdrawal after a rapid rise in altitude we may examine the competing effects of fuel evaporation and fuel loss. Fuel withdrawal is expanding the ullage space intending to reduce the fuel concentration as air is admitted to maintain pressure. Fuel evaporation is attempting to return the fuel partial pressure in the ullage to that corresponding to the vapor pressure of the fuel at the test temperature. The trend over time of either increasing or decreasing fuel/air ratio then indicates the predominance of one effect over the other.

The tests shown in Figure 26 were both done at 20,000 ft altitude and 80°F liquid temperature. The difference between the two was in whether or not the tank was vibrated. Also plotted in the figure is the equilibrium fuel/air ratio corresponding to the vapor pressure of the fuel at 20,000 ft. It is seen that in the case with no-vibration the general trend is toward increasing fuel/air ratio approaching equilibrium indicating evaporation is occurring fast enough to overcome the nonequilibrium initial condition and to compensate for fuel withdrawal. The runs with vibration show a general trend towards a level or slightly decreasing fuel/air ratio. This effect may be attributed to air being outgassed from the fuel due to the vibration environment. It may also be noted in the figure that the Probe 1 located at the vent inlet is generally lower in fuel/air composition than Probe 2 or 3. This would be expected as the inlet air required to maintain the constant pressure compensating for fuel liquid withdrawal enters in this region. The general trend in composition within the tank can be seen from these figures but concentration gradients are rather difficult to define. One factor that would tend to confuse the picture is that the pressure control system requires manual operation to maintain the constant altitude. The operator must therefore turn a control valve to admit air and maintain pressure. This results in a "puffing" and could lead to a high degree of stirring within the tank. Also the ullage is rather shallow which would tend to decrease any gradient in a vertical direction. In essence the level flight profile data run for JP4 fuel indicates a fuel/air gradient axially toward the vent but does not seem to indicate any trends with distance away from the fuel surface.

Figure 27 is shown with test results from level flight with fuel withdrawal using Jet A fuel. All runs were conducted at 40,000 ft altitude. Two runs were conducted at 120°F fuel temperature, with and without vibration and a third test was conducted at 80°F fuel with vibration. The general trend of the data for the two runs conducted at 120°F fuel is the same as that shown

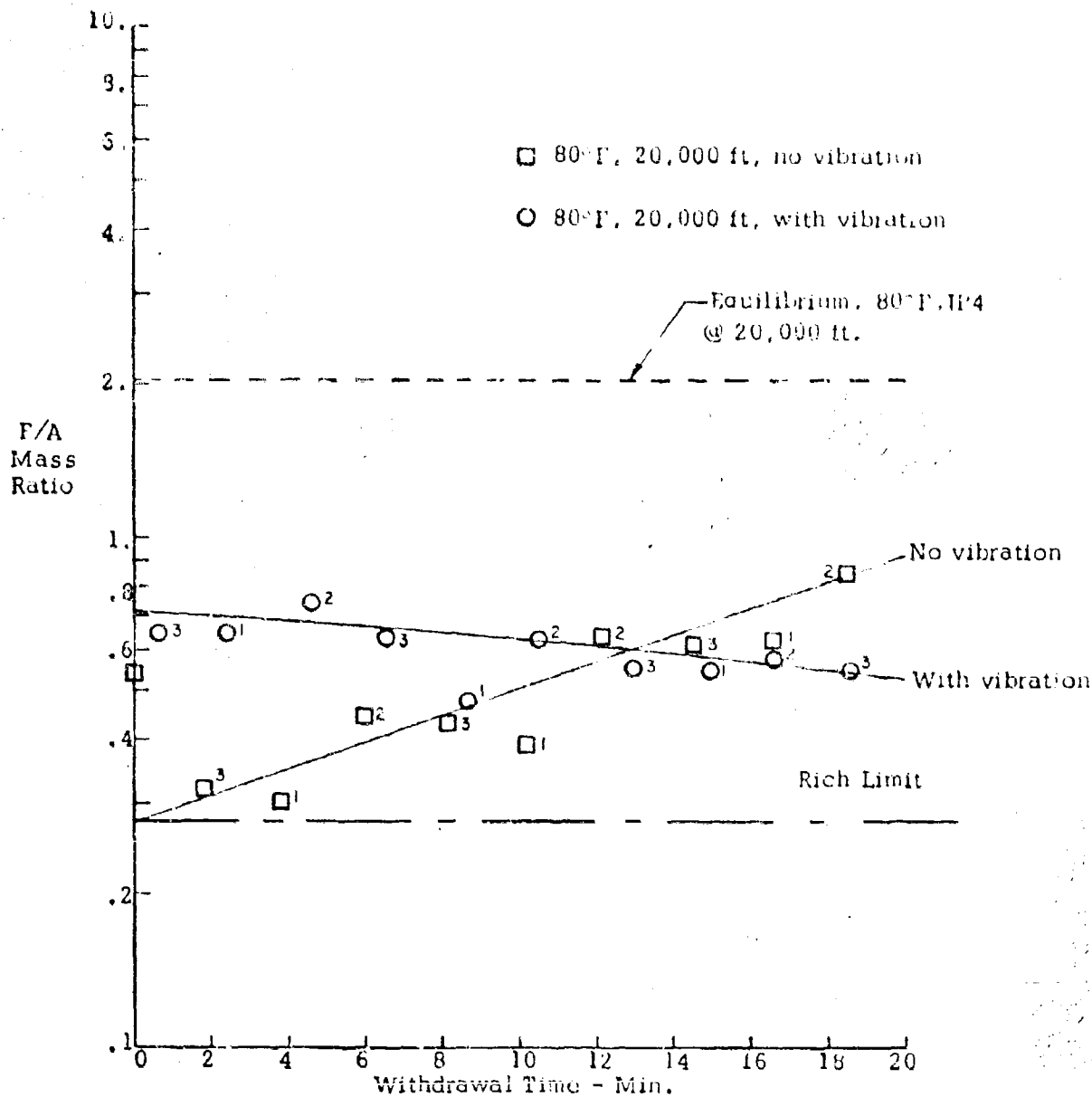


Figure 26. JP4 Runs - Level Flight With Fuel Withdrawal.

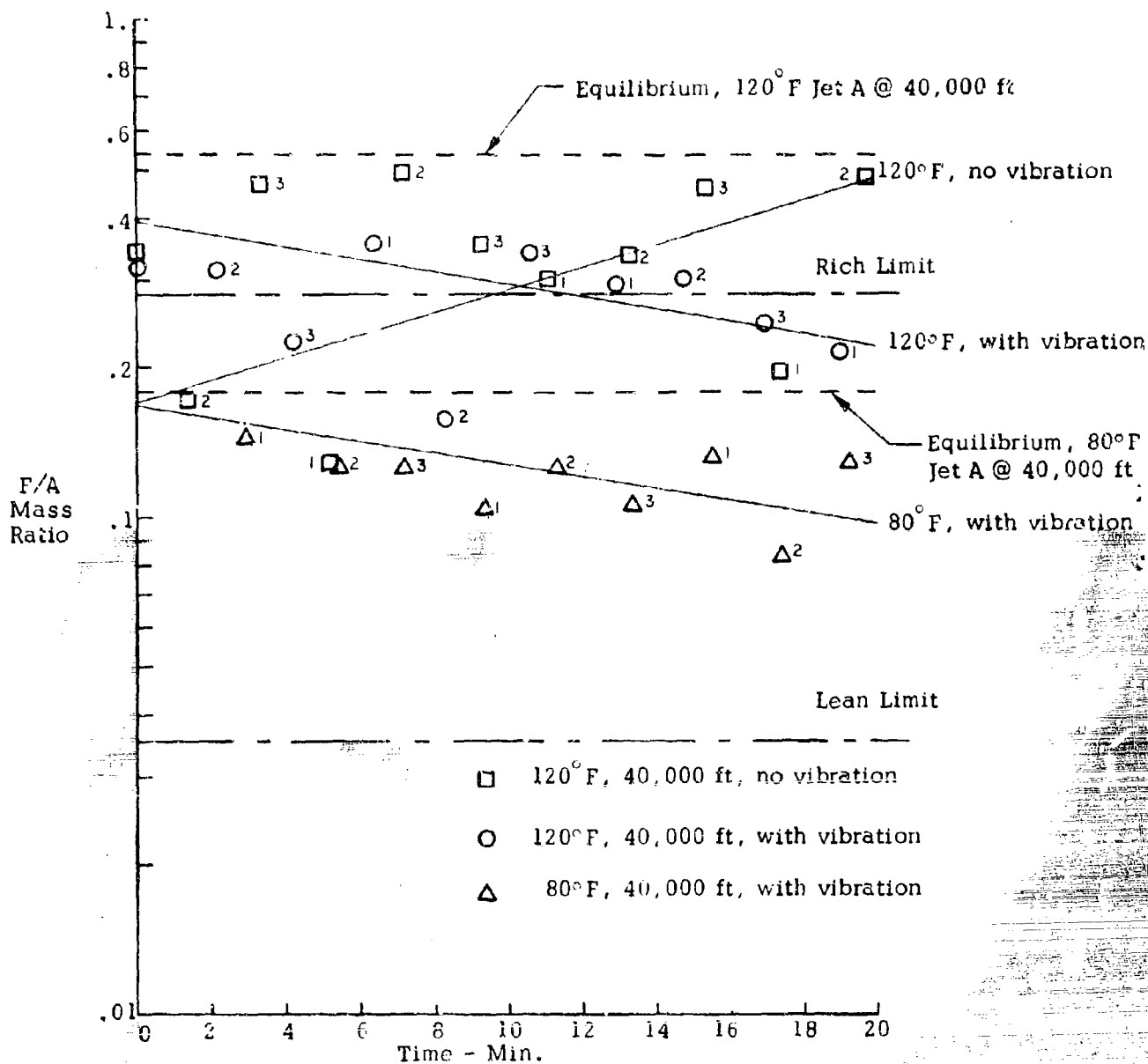


Figure 27. Jet A Runs Level Flight with Fuel Withdrawal.

for JP4 at 80°F, that is the run without vibration tended to increase the fuel/air ratio indicating evaporation occurring more rapidly than air admission due to venting and in the other case with vibration the fuel/air ratio tended to remain level or slightly decrease. Again this effect could be attributed to air evolved from the liquid fuel due to vibration. Also in the same figure is shown the test at 80°F with vibration. The general trend here is for fuel/air ratio to decrease during the run. This effect has been consistently noted throughout the entire level flight test series. In essence it appears that in the absence of vibration, fuel evaporation is sufficient to overcome the amount of air being admitted into the tank to maintain constant pressure. With vibration, however, an additional air component due to air evolution from solution contributes to the amount of air being added into the ullage thereby tending to decrease the fuel/air ratio. Also in these runs it may be noted that Probe 1 generally tends to be lower mixture composition than Probe 2 and 3. Again this is to be expected as Probe 1 is mounted within the inlet of the vent air.

2. COMPARISON BETWEEN EXPERIMENTAL AND ANALYTICAL RESULTS.

To demonstrate the salient features of the Well-Stirred Computer Model and its capability to predict mixture ratio transients, a series of runs was made to provide a comparison between experimental and analytical fuel/air mixture ratios. The runs were selected to simulate the test conditions for the experimental ascent tests made with JP4. Three sets of conditions were tested, these being:

- 120°F fuel, ascent rate 6000 fpm, with vibration
- 80°F fuel, ascent rate 2000 fpm, with vibration
- 80°F fuel, ascent rate 2000 fpm, no vibration

The comparison between measured and calculated values is presented in Figure 28 and is felt to be quite good. Some additional discussion is necessary however.

After the fuel properties, tank geometry, fill ratio, and temperature (wall and liquid) were input to the program, it was necessary to calibrate or "tune" the program as far as evaporation rate was concerned. This was done using the experimental data for the 120°F fuel run. The characteristic length for mass transfer (δ) used in calculating the mass transfer coefficient was varied until this data was matched. The value resulting was .01 ft which represents a reasonable size for a mass transfer boundary layer. Once this value was "fixed," it was used for the remaining runs.

The data from the run at 80°F with no vibration correlated well as seen by the figure when the same evaporation length (δ) was used. No air outgassing was included in this run ($K=0$) as no vibration occurred. This amounts to assuming little or no air outgassing during ascent without vibration.

For the third run (80°F with vibration) an outgassing coefficient of 500 hr⁻¹ was employed. Experimental data presented in Ref. 5 was used to obtain this constant. Extrapolation to 10 cps was required, however.

These data allow a great variation in selection of an outgassing/solution coefficient and this value could easily be double that used. The data do show, however, a several order of magnitude increase in this coefficient from zero to 6 cps frequency, thereby providing support for the zero outgassing used in the case of no vibration.

The comparison between experimental and calculated mixture ratio histories for the 80°F/no vibration case is also shown in Figure 28. Here the agreement is not quite as good as the others. This is due, no doubt, to the large possibilities of variations in the outgassing coefficient. Also the Bunsen coefficient, that determines the initial amount of air dissolved in the fuel was selected from the literature as 0.16. Large excursions in this factor are also possible.

These results although rather limited in scope do demonstrate the capabilities of the computer model to predict F/A composition histories. The existence of evaporative lag was demonstrated analytically and compared with the experiment. The influence of air outgassing was also demonstrated and correctly predicted trends of the influence of inflight vibration. Several constants used as input to the program were "fixed" for this particular tank configuration and vibration levels.

3. AUTOIGNITION CHARACTERISTICS.

Several supersonic aircraft flight profiles were examined for a tendency of Jet A and JP-7 fuel to auto-ignite, that is by cool flame or by normal ignition and/or transition from cool flame to normal ignition. In Figure 29 is shown the basic temperatures associated with the flight of the supersonic transport at Mach 2.7. This information was gathered from various sources in the literature including the FAA, Boeing Aircraft Company, and Wright-Patterson Air Force Base. The quantities required to characterize a particular flight profile are the transient liquid and skin temperatures as well as the history of the vent inlet air. Altitude time profile is also required. These are shown schematically in the figure. Examination shows that there appears to be two distinct regimes even at Mach 2.7 which required testing. These are the wing tank or fuselage tank. For a wing tank the skin temperature at the fuel/air mixture is generally higher than that of a fuselage tank. Also the liquid temperature is generally higher. With these particular fuels a cursory examination concluded that the mixture ratio within the fuel tank would be well on the fuel-rich side. It was felt that the fuselage tank profiles, although lower in temperature, would be closer to that of a stoichiometric mixture and therefore required further study. Values for the various temperatures and altitude histories shown in Figure 29 were extrapolated from flight conditions of Mach 3.0 and Mach 2.4; that is, they were extrapolated to higher and lower Mach numbers to obtain a wider variation for the test series. The profiles calculated for both outboard (wing) and inboard (fuselage) tanks are also shown in the following two figures(30,31). Initial testing using full flight profiles indicated no tendency toward ignition as monitored by the photomultiplier light detector. Testing of the entire flight profiles(32) was continued into the 2.7 and 2.4 range and a wide range of variables examined.

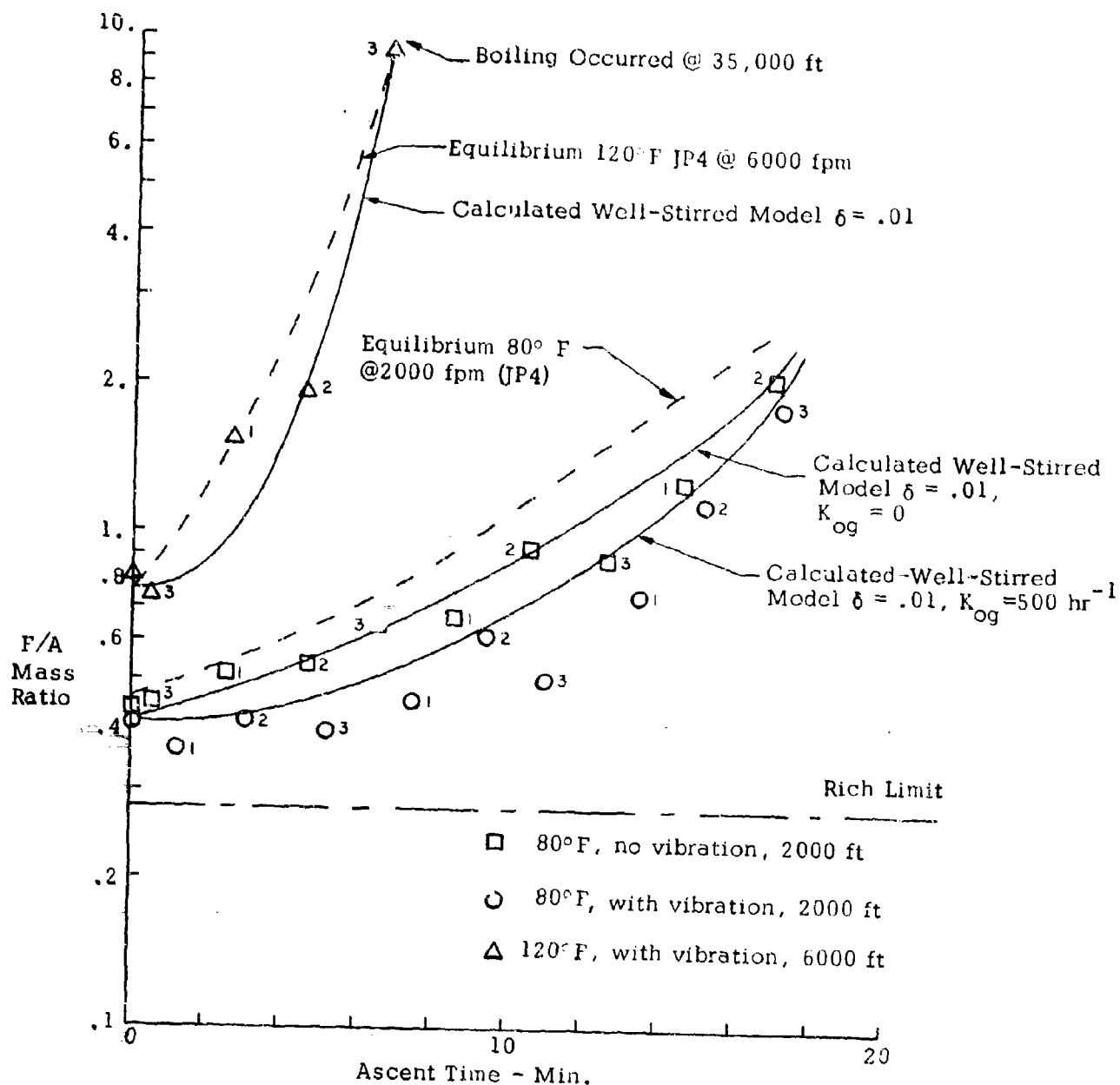


Figure 28 JP4 Ascent Tests to 40,000 ft - 1/2 Full Tank
Comparison Between Experimental and Calculated Results.

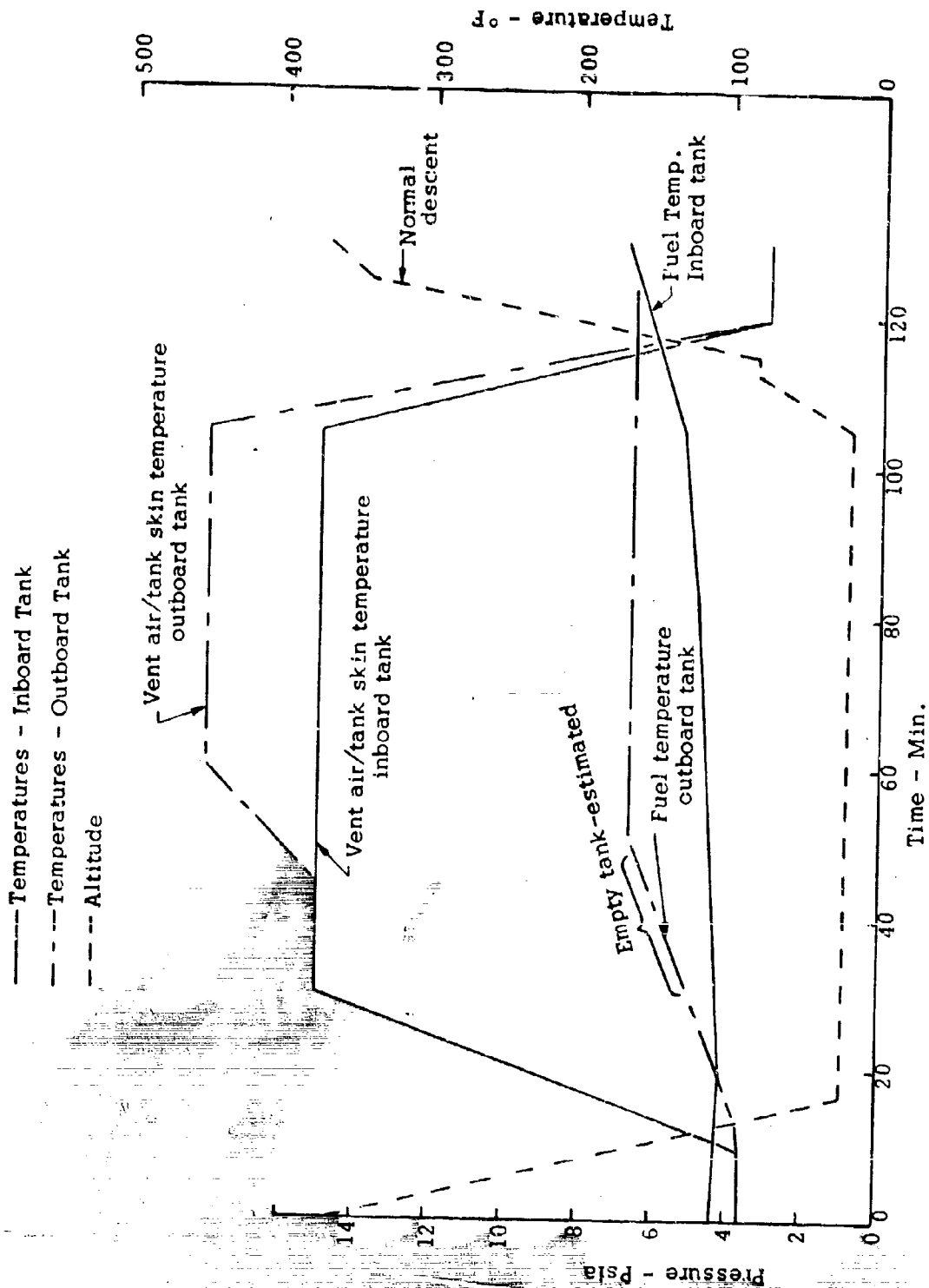


Figure 29. Mach 2.7 Flight Profile - Test Parameters.

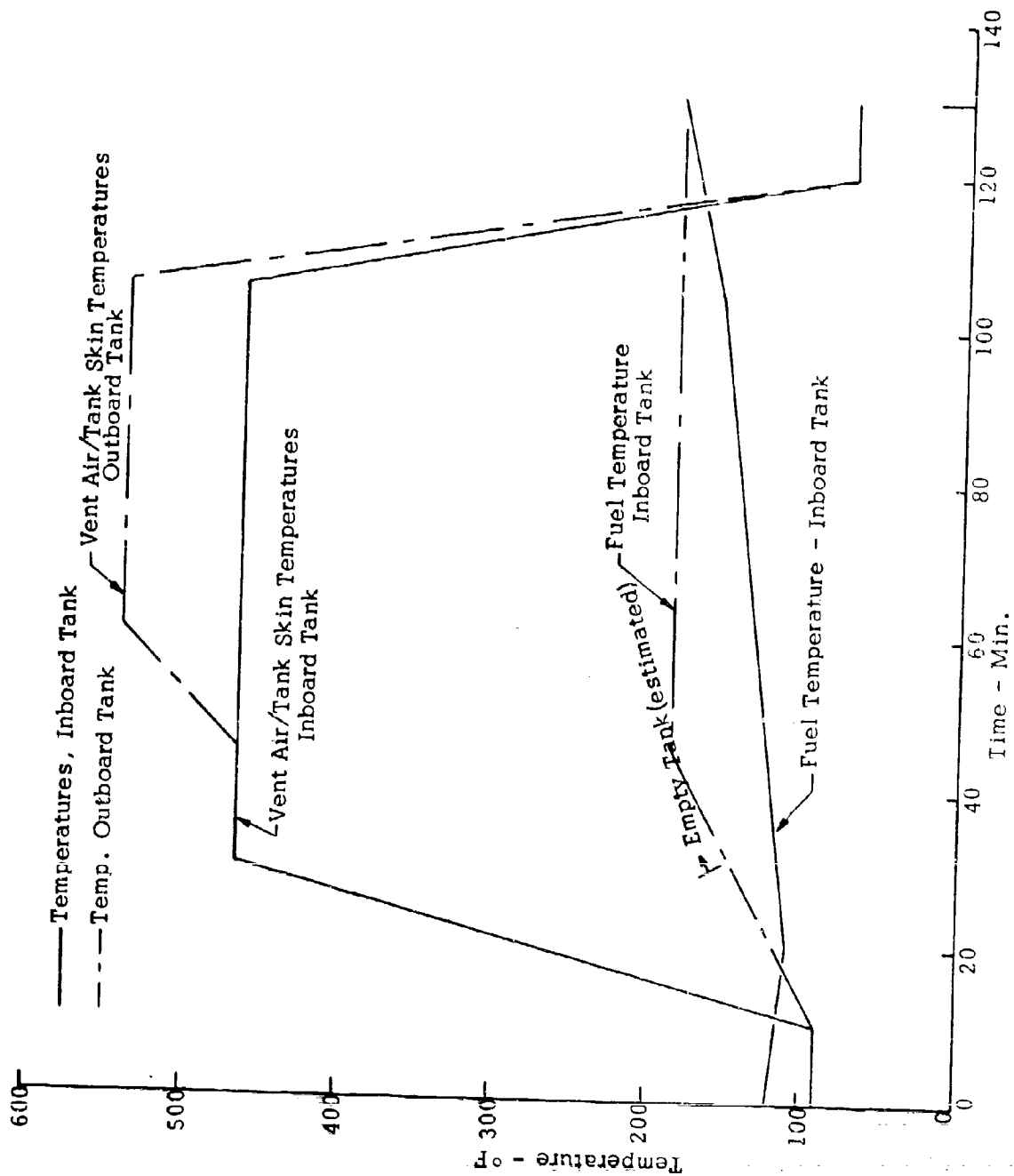


Figure 30. Mach 3.0 Flight Profile (Altitude Same as Mach 2.7)
(Temperatures extrapolated to M=3.0 are estimated)

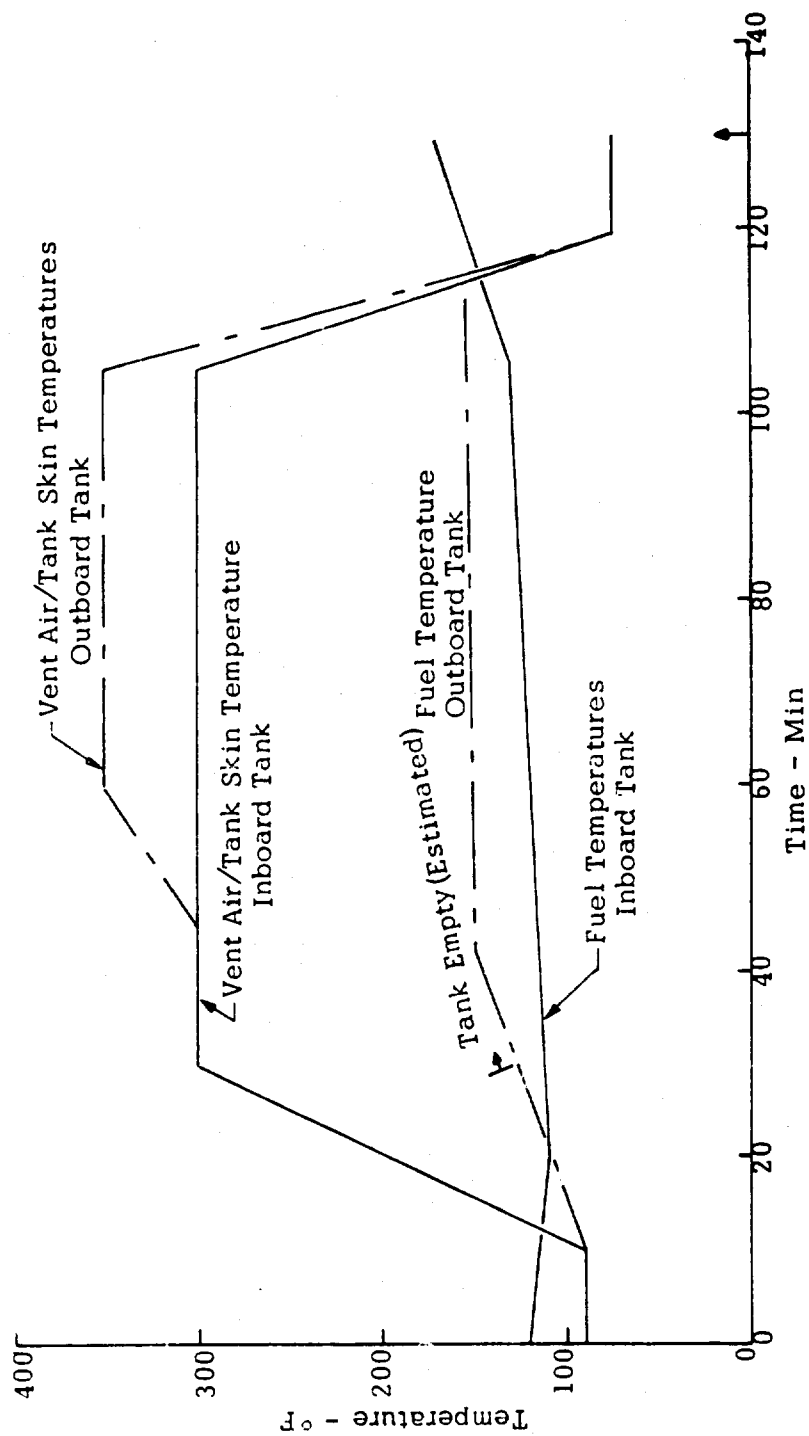


Figure 31. Mach 2.4 Flight Profile (Altitude same as Mach 2.7)
 Temperatures extrapolated to $M=2.4$ are estimated.

Jet A	Mach 2.7			Mach 3.0 Evaluation of Independent Variables	Mach 2.4 Evalu. @ Wors Case Condition
	Evaluation of Independent Variables	Worst Descent Conditions	Worst Descent/ Inboard Tank		
Mach 2.7 (Base profile)	XXXXXXXX	XXXXXXXXX	XXXXXX	XXXXXXXXXX	
Mach 3.0		(none found)			XXXXXX
Mach 2.4					
<u>Flight & Tank Variables</u>					
Emergency Descent @ t ₁	■	0000000	00000	■ 0000	000
Emergency Descent @ t ₂	■			■	0
Emergency Descent @ t ₃	■			■	
Inboard Tank	■			■	
Fill Ratio, 1/3	■	0	0000	■	0
Fill Ratio, 2/3	■	0		■	

Note: Entire matrix repeated using JP-7

Completed (No Luminous Reaction) ■

Completed (Reaction Measured) ●

Figure 32. Flight Profile Test Results - No Ignition.

A series was also run wherein only the descent portion of the flight profile was examined. As a basic autoignition hazard appears higher during this portion of the flight, a series of controlled tests employing Jet A and JP-7 fuel were run using only descent variables that were varied between tests. The parameters investigated include descent rate, liquid temperature, initial skin temperature, and skin temperature cooling rate. Tests were run employing both Jet A and JP-4 fuels. All tests were initiated from 65,000 ft altitude. Approximately one-half hour was allowed for thermal stabilization prior to initiating the descent. Figure 33 shows the results of the descent tests. Shown in the figure are those runs where ignitions were and were not indicated. It would seem that in all runs where the wall temperature was cooled and was not held artificially at the cruise value but was decreased linearly to atmospheric temperature over the time of descent, no ignition was noted. Only in those tests where the wall temperature was held constant during the descent was an ignition noted.

A portion of this study was directed toward determining whether a major difference existed between ignition data obtained in the relatively large tank used to simulate a full scale system compared to experiments conducted in laboratory scale apparatus. A great deal of experimental work has been conducted in containers of relatively small volume compared with an aircraft fuel tank. It is of interest to determine whether such data are applicable to real systems. In order to obtain a crude answer to this question some of the ignition data obtained in this investigation were compared with the data of References 3 and 7.

Some comparison of the two systems is in order. The small, laboratory reactor has a volume of 1.5 ft³ while the large tank simulator has a volume of 15.7 ft³. The small tank was filled with vapor-air mixture essentially at the same temperature as the tank wall. The large tank is partially filled with liquid fuel at a temperature considerably colder (250 to 440°F) than the tank wall. Both temperature and concentration gradients may exist in the large tank while the atmosphere in the small tank is quite uniform.

The following effects might be expected due to these differences.

- 1) The large tank has a larger volume to surface ratio than the small tank so that heat transfer to the walls and free radical quenching should be reduced. These effects could lead to lower ignition temperatures in the large tank.
- 2) The presence of liquid fuel in the large tank, however, introduces a relatively cold surface as one part of the vapor space. The presence of the cold surface tends to cause an increase in the required hot wall temperature for ignition (Ref. 3).
- 3) The presence of gradients in fuel concentration and temperature could cause changes in ignition temperature which are difficult to generalize since the nature of the gradients would determine the direction and magnitude of the effects.

JP7 DESCENT TESTS (With and Without Skin Cooling During Descent)

	Mach 2.7, T _s = 450° F			Mach 2.8, T _s = 500° F			Mach 3.0, T _s = 540° F		
	No Cooling	With Cooling		No Cooling	With Cooling		No Cooling	With Cooling	
Descent Rate (kfp/m)	3 5	3 5 7.5		3 5	3 5 7.5		3 5	3 5 7.5	
Liquid Temperature 100° F		O			O			O	
Liquid Temperature 165° F		O			O O O		X X X	O O O	
Liquid Temperature 200° F		O			O X X		X X X	O O O	

O = no reaction measured, X = luminous reaction noted, blank space = no test

JET A DESCENT TESTS (Constant Skin Temperature)

	Mach 2.7 T _s = 450° F Constant			Mach 2.8 T _s = 500° F Constant			Mach 3.0 T _s = 450° F Constant		
	5	7.5	10	5	7.5	10	5	7.5	10
Descent Rate (kfp/m)									
Liquid Temperature 100° F		O O O			O O		X X X		
Liquid Temperature 165° F		O O O			O O		X X X		
Liquid Temperature 200° F		O O			O X		X		

O = no reaction measured, X = luminous reaction noted, blank space = no test

Figure 33. Autoignition Descent Tests - Tabular Results.

The data for Jet A fuel in Ref. 3 provides a basis for comparison. Figure 11 from that report is reproduced as Figure 34 and is compared with the data of Fig. 33. One would not expect ignition for skin temperature at 450°F or below. Although a small portion of the ignition curve drops below 450°F at sea level, the fuel concentration would have fallen to 2.8 or below during the descent and the cool air drawn in during descent from 65,000 feet would affect ignition even if the tank skin were kept at 450°F.

At 500°F a fairly wide range of fuel concentrations are ignitable at altitudes below 65,000 feet. This temperature, or possibly the range between 450-500 represents a departure from little ignition potential to a large ignition potential. The data in the large tank showed ignition at 500°F for the 200°F liquid temperature. One might have expected ignition at 165°F (fuel concentration range 18.7 to 1.0 volume percent from 65,000 ft to sea level) but ignition for 100°F liquid fuel would not be expected since the concentration range, 3.6 to 1.0, is almost completely outside the flammable range. This is more easily verified in Reference 7 where 1% fuel seems to be a lean limit.

Ignition at 540°F for all cases is also very consistent with the data of Reference 3. It thus appears that within about 25°F the small and large tank are in agreement. It also appears that ignition is a little more difficult in the large tank as compared with the small tank probably due to the large area of relatively cool liquid fuel.

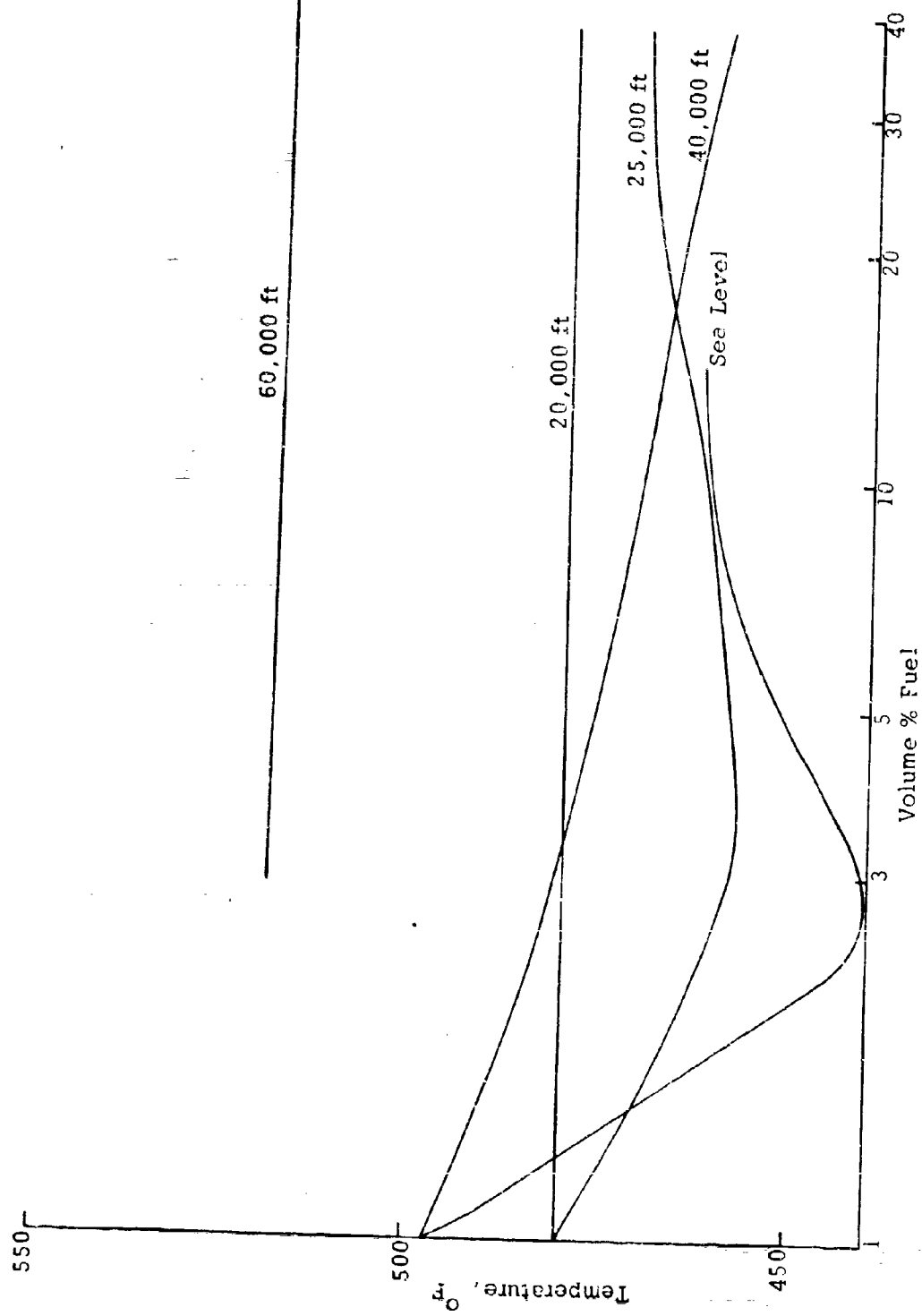


Figure 34. Lower Ignition Limits for TFA/Air Mixtures at Various Simulated Altitudes.

SECTION VI

CONCLUSIONS AND RECOMMENDATIONS

Based on the results of this work, several important observations have been made.

1. For tank configurations where the ratio of ullage volume to liquid surface area is small (ullage/area $< .75$ ft) uniform fuel/air mixture was found to exist within the ullage volume during ascent and cruise portion of the flight profile. However, large fuel/air concentration gradients were observed during the descent portion of the flight profile with mainly air near the vent inlet. For tank configuration where the ratio of ullage volume to liquid surface area is greater than 1.5, fuel/air gradients were observed even during level flight.
2. Experimental results and computer calculations have shown that evaporative lag and air outgassing can cause fuel/air mixture ratios in the ullage to be different from equilibrium values, especially during ascent. Ullage vapor mixture initially fuel-rich may become combustible during ascent due to high air offgassing in high vibration environments. Tanks initially fuel lean can become combustible during ascent at high liquid temperatures that causes high fuel evaporation. Nonequilibrium mixtures were found to exist in most aircraft for ascent rates as low as 2000 fpm.
3. During level flight with fuel withdrawal following a rapid ascent, air outgassing may dominate over evaporation and result in a decrease in F/A ratio with time. In the absence of vibration air offgassing is significantly lower. F/A ratio increases as evaporation dominates over venting to replace withdrawn fuel.
4. During descent even in shallow tanks such as used in this study, large concentration gradients exist in the region of the vent. It appears that there exists a region of vent air control and a well-stirred highly turbulent region away from the vent. This remains to be completely established over wide tank/vent geometry and descent conditions.
5. No ignitions were noted during flight simulations at realistic SST flight conditions. Only at nonrealistic flight conditions such as constant wall temperature during descent could "cool flames" be generated. These ignitions were controlled by wall temperature conditions and were strongly sensitive to values of wall temperature.
6. Two separate and complementary computer models have been developed to predict fuel/air ratios within the ullage volume. Based on the excellent agreement between calculated results and experimental measurements, the models can be fruitfully used in the future to predict fuel tank fire and explosion hazards.

RECOMMENDATIONS

1. The analytical models have been proven to be valid based on the comparison of calculated results using these models and the experimental data. These models should be further refined by improving the occurrence of the parametric variables used in the model and to include the effect of misting and condensation.
2. Further experimental data should be generated to improve the model for the effects of skin temperature and tanks of other geometries.
3. Offgassing of dissolved air in the liquid fuel was found to play a very significant role. Well controlled experimental studies should be carried out to determine the rate of air offgassing as a function of vibration level, initial liquid temperature, rate of pressure decrease, and type of fuel.
4. Because of the high volatility of liquid JP-4 fuel, significant temperature gradients might exist within the liquid fuel close to the surface. This can significantly change the evaporation rate. Experimental studies should be conducted to verify such phenomena.
5. Misting should be studied on an experimental basis to determine flame propagation limits for mists of various sizes and concentrations. Fuel ratios and vibration levels must then be related to the formation of a particular misting condition.
6. Velocity fields within tanks during descent should be studied experimentally and analytically to determine the portion of the tank considered as well stirred. Solutions of the mixing problem can then be superimposed on the well-stirred solution, thereby eliminating the necessity of knowing the velocity at all points within the tank as is presently required in the distributed model.

REFERENCES

1. T. C. Kosvic, N. L. Helgeson, B. P. Breen, "Flight Vibration and Environmental Effects on Formation of Combustible Mixtures within Aircraft Fuel Tanks, Final Report USAAVLABS Rept. 70-43 Contract DAAJ02-69-C-0063, Sept. 1970.
2. Nestor "Investigation of Turbine Fuel Flammability within Aircraft Fuel Tanks," AD 669-001, July 1967.
3. N. L. Helgeson, "Supersonic Aircraft Fuel Tank Fire Hazard Investigation," Final Rept. F33615-67-C-1553, WPAFB, Sept. 1968.
4. E. R. G. Eckert and Robert M. Drake, Jr. Heat and Mass Transfer McGraw-Hill, New York, 1959.
5. WPAFB - "Solution and Evolution of Gases and Vapors in Aircraft Fuels," Coordinating Research Council, Inc. Tech.Rept. 59-193, April 1959.
6. Lockheed, Thermal Analyzer Computer Program for the Solution of General Heat Transfer Problems, Contract No. 9-3349, July 1965.
7. H. D. Fisher and H. G. Weiss, Investigation of Supersonic Aircraft Fuel Tank Fire and Explosion Hazards, Tech. Rept. AFAPL TR-66-105, Air Force Aero Propulsion Laboratory, Wright-Patterson Air Force Base, Ohio, Sept. 1966.
8. H. C. Barnett, et al., "Properties of Aircraft Fuels," August 1956, NACA-TN-3276.

APPENDIX A

EXTENSION OF LEAN FLAMMABILITY LIMIT BY MISTS

Nester (Ref. 1) has indicated an extension of the normal flammability limits of aircraft fuels in the fuel lean direction as a result of dynamic simulated flight conditions. This extension has generally been attributed to the existence of a vibration generated two phase mixture (mist) existing within the tank. This liquid phase component may be pictured (for high vibration environments) as superimposed on the normal mixture ratio that would exist at that particular flight condition. The liquid droplets are generated as a result of liquid surface waves caused by aircraft motion (slosh and vibration).

During the ascent portion of a flight of a flight profile, the ullage gas (fuel/air mixture) cools due to expansion. This expansion is not adiabatic as heat is entering from the tank walls and liquid surface. Also air and fuel vapors are entering the ullage due to outgassing and evaporation. This cooling though, if occurring at a sufficiently high rate (high ascent rate) can occur more rapidly than heat may be added from the walls and the "dew point" or condensation temperature of the mixture may be reached. In the absence of vibration the ullage mixture may remain in a supersaturated condition. In the presence of vibration, the minute fuel particles generated by surface waves provide nucleation sites for condensation to occur. In this condition the F/A ratio in the gas phase (between liquid particles) suddenly decreases although the total F/A ratio, including liquid drops, remains the same. The liquid drops existing in the gas phase are then composed of those expelled from the liquid due to vibration and those condensed from the gas phase. In high vibration environments, the first dominate while the latter dominate in low vibration/high ascent environments. Likewise in the first case the gas phase F/A is unchanged while in the second it is decreased.

To define the extension of the lean flammability limit under controlled conditions, a test series, under the direction of Capt. Ott, at WPAFB was conducted (Ref. 2). In these tests a tank of fuel conditioned to a prescribed temperature was sloshed for a period sufficient for the establishment of an equilibrium within the ullage. An ignition source was introduced and the pressure rise recorded. For these conditions the assumption may be made that the gas phase is at equilibrium mixture conditions, i.e., fuel partial pressure equals vapor pressure and an additional liquid component due to mechanical vibration added.

Calculations were made to define the amount of liquid existing as droplets within the gas phase. The Dynamic Science Chemical Equilibrium Computer Program was used. This program calculates the final pressure caused by the combustion of a mixture of known composition and density, i.e., prescribed enthalpy (H) and density (ρ). The total chemical enthalpy of the mixture is calculated from a mass weighted average (at the F/A ratio) of the enthalpy of the fuel and air. The density is calculated at the known initial conditions. The logic of the calculation was to determine the pressure resulting from combustion of only the gas phase mixture and compare these results to the measured. The density was then increased by an arbitrary amount until the measured pressure equalled the calculated. The increase

in density required to match the measured pressure rise is then the amount of liquid existing within the ullage.

Figures A-1 and A-2 present the test results of pressure rise in JP8 mixtures at 1 atm pressure and 10 psia pressure for various liquid temperatures. Table A-1 presents in tabular form the calculation of gas phase density for several temperature conditions at each of the two total pressures. Fuel vapor pressures were determined from data presented in the report (Ref. 2). Results of the equilibrium combustion program calculated using the gas phase densities are also shown on the figures. The agreement with measured pressure rise is quite good with no additional density component due to liquid.

These results indicate that mist acts only as a flame propagation medium and the amount of mass contained in the ullage in liquid form (mist) is negligible. The calculations are subject to errors due to heat loss to the walls during combustion and some variability in fuel properties (vapor pressure), however, the general conclusions are felt to be valid. Mists may then be treated in the vulnerability model as an extension of the lean flammability limit. The degree that various mist concentrations extend this lean limit remain to be defined.

References

1. Nestor "Investigation of Turbine Fuel Flammability within Aircraft Fuel Tanks," AD 669-001, July 1967.
2. Botteri, B. P., et al, "Evaluation of JP-8 Versus JP-4 Fuel for Enhancement of Aircraft Combat Survivability," APFH-TM-70-34, June 1970.

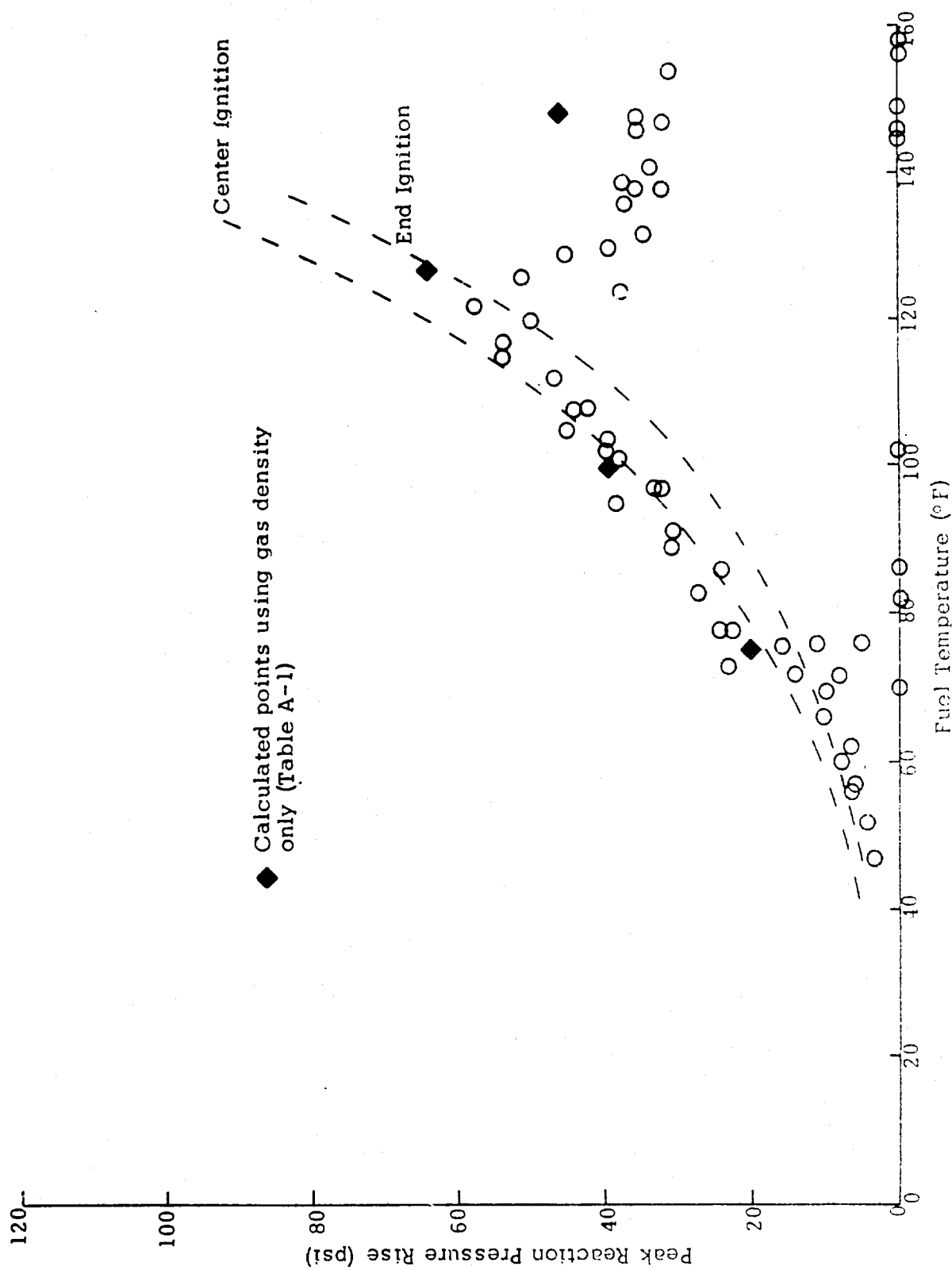


Figure A-1. Extended Lean Flammability for JP-8 Fuel Sloshing at 17.5 cpm and under 10 Psia Initial Ullage Pressure.

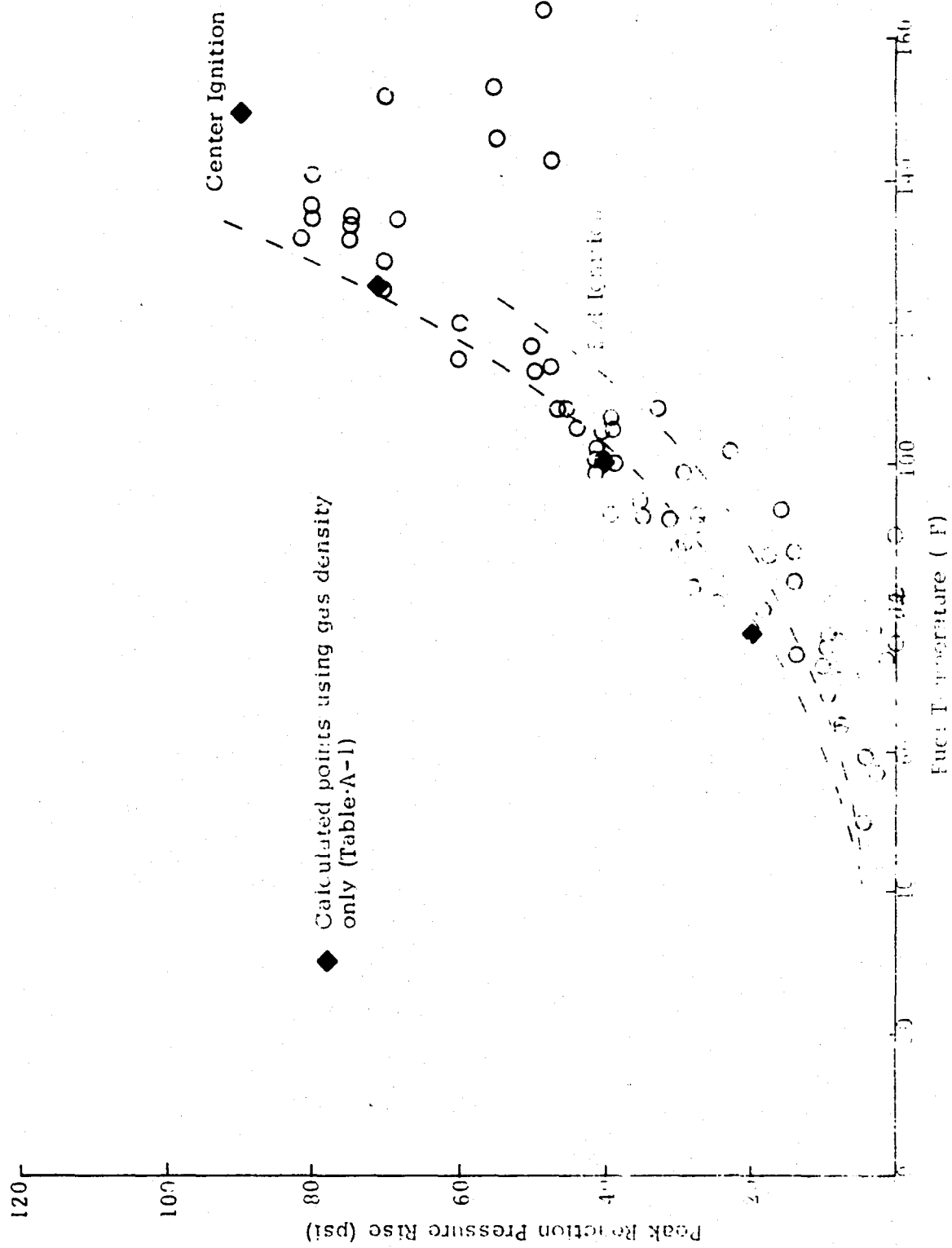


Figure A-2. Extended Lean Flammability for JP-8 Fuel Sloshing at 17.5 cpm and Under one Atmosphere Initial Ullage Pressure

TABLE A-I

JP8 MIST IGNITION CALCULATIONS

Liquid Temp. $T_l, ^\circ R$	Vapor Pres. P_v, psi	Total Pres. P_t, psi	Air Pres. P_a, psi	Av. Mole. Wt. \bar{M}	Air Fuel Ratio, A/F	Density ρ
535	.028	15.0	14.972	29.08	102.9	4.4×10^{-5}
560	.061	15.0	14.939	29.49	47.3	4.26×10^{-5}
585	.123	15.0	14.877	29.99	23.38	4.15×10^{-5}
610	.234	15.0	14.766	30.88	12.19	4.0×10^{-5}
<u>10 psi Total Pressure</u>						
535	.028	10.0	9.972	29.33	68.85	2.95×10^{-5}
560	.061	10.0	9.939	29.74	31.5	2.866×10^{-5}
585	.123	10.0	9.877	30.48	15.52	2.812×10^{-5}
610	.234	10.0	9.766	31.8	8.068	2.816×10^{-5}

Molecular Weight of Air $M_A = 29$

Molecular Weight of Fuel $M_F = 150$